HAMMER AND ROLLER MILLING OF YELLOW SPLIT PEA

A Dissertation
Submitted to the Graduate Faculty
of the
North Dakota State University
of Agriculture and Applied Science

By

Amber Christine Kaiser

In Partial Fulfillment of the Requirements
for the Degree of
DOCTOR OF PHILOSOPHY

Major Program:
Cereal Science

February 2019

Fargo, North Dakota

North Dakota State University
Graduate School

Title

HAMMER AND ROLLER MILLING OF YELLOW SPLIT PEA

By

Amber Christine Kaiser

The Supervisory Committee certifies that this ***disquisition*** complies with North Dakota State University's regulations and meets the accepted standards for the degree of

DOCTOR OF PHILOSOPHY

SUPERVISORY COMMITTEE:

Dr. Clifford Hall, III
Chair

Dr. Frank Manthey

Dr. Bingcan Chen

Dr. Julie Garden-Robinson

Approved:

04/12/2019
Date

Dr. Richard Horsley
Department Chair/Program Coordinator

ABSTRACT

Blending nutrient-rich pulses into cereal-based convenience foods could benefit consumers and the cereal and pulse industries but first requires appropriate milling of raw pulses, for which there is no standardized method. Roller milling is the standard method for wheat flour production, but hammer milling is simpler and more cost-effective. Literature documenting pulse flour quality from either system is limited. The goals of this research were to evaluate (1) the effects of hammer mill setup and seed moisture on quality and flowability and (2) the differences between hammer- and roller-milled quality for yellow split pea. For (1), yellow split pea samples at 9 and 11 % moisture were hammer-milled at two rotor speeds (34 and 102 m/s) and with nine mill screen apertures (0.84 to 9.53 mm) and physicochemical properties and flow properties on 6 surfaces were evaluated. For (2), yellow split pea at 11 % moisture was hammer-milled at 102 m/s through a 0.84 mm screen or roller-milled using a two-pass setup, then sieved through a 150 µm screen and evaluated for physicochemical and functional quality. Hammer mill settings had no practical impact on proximate composition, small impact on damaged starch content, and considerable impact on particle size distribution, pasting properties, and flowability. Particle size parameters impacted color, bulk density, pasting properties, and flowability. Flowability was highest on aluminum and lowest on high-density polyethylene. Hammer milling at 102 m/s rotor speed with 0.84 mm screen aperture produced particle sizes closest to that of flour (D10, D50, and D90 of 12, 98, and 348 µm, respectively). Small differences were observed in the D10, starch damage, moisture, peak and final viscosities, and oil binding capacities of hammer- and roller-milled split pea flours. Data from this research supported the viability of hammer milling to produce split pea flour and provided systematic data to support milling, product development, conveying, and storage operations involving split pea and other pulses.

ACKNOWLEDGEMENTS

I would like to acknowledge many people for their assistance and support. First, I am grateful to my advisor, Dr. Clifford Hall, III, for the opportunity to pursue graduate studies and for unflagging patience throughout various iterations of my research. I have thoroughly enjoyed working in the independent yet supportive environment of his research group. I am also grateful to my other graduate committee members: Dr. Frank Manthey, Dr. Bingcan Chen, and Dr. Julie Garden-Robinson. Their patient guidance and desire for my success have been deeply appreciated.

My thanks are also due to all who provided technical assistance: to Natsuki Barber, for considerable involvement in the initial idea, experimental design, and sample milling; to Mary Niehaus, for kind assistance with many laboratory questions; and to Rilie Morgan, for invaluable milling advice. Deepest thanks to the Northern Crops Institute (Fargo, ND) for the use of milling and laboratory equipment and to the Northern Pulse Growers Association (Bismarck, ND) and U.S. Dry Pea and Lentil Council (Moscow, ID) for financial support of this research. To my fellow graduate students in Cereal Science, thank you for your kind friendship and support. It has been an honor and pleasure to work and study among you.

I am grateful to all those without whom I would never have begun this challenge. To Dr. Lillian Were, professor at Chapman University, I will always be grateful for teaching me how to think and write as a scientist. To my professors from The Master's University—Dr. Joseph Francis, Dr. Ross Anderson, and Dr. Taylor Jones—I am thankful for excellent foundational instruction and unfailing confidence in me, and to Dr. Dennis Englin, I am particularly grateful for continual support and wise advice.

To my family and friends who have supported and loved me during the most stressful times, words will ever fail to express my gratitude. To Kippen, Lisa, Charity, and Nate Jacobson, thank you for hospitality and encouragement at an important time. To the Kaiser family, thank you for supporting the decision to begin this program and for constant interest and confidence in my success. To Paul and Molly Choi and Joseph and Aubrea Jacobson, thank you for your faithful friendship, without which this venture would have been difficult indeed. To my siblings, Whitney Morton and Dallas Hoekstra, thank you for inspiring and encouraging me in your own ways and reminding me who I am. And to my parents, Richard and Amanda Hoekstra, I cannot say how much your love and complete support in all I have done has meant.

Finally, to my husband Brian, thank you for allowing me to prove that your patience is inexhaustible. Your constant love, companionship, and faith in me has kept me going through it all and is more than I could have ever asked.

DEDICATION

I dedicate this work to my two fathers:

To my earthly father, Richard Hoekstra, after whose faith, wisdom, inquisitiveness, and passion I have always tried to pattern my life. This work would never have been accomplished or even attempted without your love for, support of, and confidence in me. You are my hero forever.

To my heavenly Father, whose approval I desire above anything else. Life, mental ability, and the delight and satisfaction of learning are gifts from You, and my gratitude for all You have given me is endless.

TABLE OF CONTENTS

LIST OF TABLES

LIST OF FIGURES

FORMAT OF DISSERTATION

This dissertation has an overall abstract, introduction, and literature review. The literature cited in the overall introduction and literature review is given at the end of each section. The dissertation is written as three separate papers, each with an abstract, introduction, materials and methods, results and discussion, conclusion, and literature cited. Following the three papers is an overall conclusion and recommendations for future research. Due to the format of the dissertation, there may be redundancy in some places.

GENERAL INTRODUCTION

Pulses such as field pea (*Pisum sativum* L.) are rich sources of nutrients currently associated with health benefits, including protein, dietary fiber, and antioxidants (Dahl, Foster & Tyler, 2012; Hall, Hillen & Garden-Robinson, 2017). The addition of pulse ingredients can provide in-demand nutrient claims, such as increased protein, fiber, and phytonutrient contents, to processed cereal products. Such application can benefit consumers by increasing the availability of more healthful convenience foods, the cereal industry by conferring a healthier image on cereal-based products, and the pulse industry by increasing value-added applications of pulses.

Milling is necessary for such applications of pulses. Milling permits miscibility and fractionation and induces chemical changes to milled material (primarily starch damage) that can be important for functionality (Thakur, Scanlon, Tyler, Milani & Paliwal, 2019). While milling methods are well-developed for cereals, standardization in pulse milling is absent and research is still limited (Posner & Hibbs, 2005). Lack of standardization can result in inconsistent quality among milled pulse products, which undermines confidence and complicates development and scale up for new product formulators. Detailed information on the physical, chemical, and functional properties of milled pulses under a variety of milling conditions is necessary to support the development of milling and quality standards for pulse flours.

Hammer milling and roller milling are two common methods of size reduction. The former is rapid, simple to perform, and relatively cost-effective, while the latter provides a very controlled milling process and is the standard for wheat milling. Previous evaluation of the quality of hammer-milled pulses has been mostly limited to a narrow range of mill parameters (Indira & Bhattacharya, 2006; Maaroufi, Melcion, De Mondredon, Giboulot, Guibert & Le

Guen, 2000; Maskus, Bourre, Fraser, Sarkar & Malcolmson, 2016; Singh, Hung, Corredig, Phillips, Chinnan & McWatters, 2005). Currently available comparisons of the quality of hammer-milled pulse flours to those produced with other milling methods have not been designed to permit comparisons of the effect of mill type apart from particle size differences (Maskus et al., 2016). Evaluation of the bulk flow properties of pulse flours produced by any milling technique is also largely absent in the literature.

Research Objectives

The goal of this research was to address the knowledge gaps in pulse milling outlined above by completing the following objectives:

- Quantify the effects of seed moisture, rotor speed, and screen aperture size on the quality of hammer-milled yellow split pea.
- Provide foundational data on the flowability of milled yellow split pea at a variety of particle sizes and on multiple common food contact surfaces.
- Isolate and evaluate the effect of mill selection (hammer and roller mills) on the quality of milled yellow split pea

The initial hypotheses were, first, that mill parameters would have an important effect on milled split pea physicochemical quality and bulk flow properties, and second, that the effect of mill selection would be less dramatic than previously reported when all milling methods were designed to produce comparable particle size distributions.

References

Dahl, W. J., Foster, L. M., & Tyler, R. T. (2012). Review of the health benefits of peas (Pisum sativum L.). *British Journal of Nutrition*, **108**:S3-S10. https://doi.org/10.1017/S0007114512000852

Hall, C., Hillen, C., & Garden-Robinson, J. (2017). Composition, nutritional value, and health benefits of pulses. *Cereal Chemistry*, **94**:11-31. https://doi.org/10.1094/CCHEM-03-16-0069-FI

Indira, T. N., & Bhattacharya, S. (2006). Grinding characteristics of some legumes. *Journal of Food Engineering*, **76**, 113–118. https://doi.org/10.1016/j.jfoodeng.2005.04.040

Maaroufi, C., Melcion, J. P., De Monredon, F., Giboulot, B., Guibert, D., & Le Guen, M. P. (2000). Fractionation of pea flour with pilot scale sieving. I. Physical and chemical characteristics of pea seed fractions. *Animal Feed Science and Technology*, **85**(1–2), 61–78. https://doi.org/10.1016/S0377-8401(00)00127-9

Maskus, H., Bourre, L., Fraser, S., Sarkar, A., & Malcolmson, L. (2016). Effects of grinding method on the compositional, physical and functional properties of whole and split yellow pea flour. *Cereal Foods World*, **61**:59-64. https://doi.org/10.1094/CFW-61-2-0059

Posner, E. S., & Hibbs, A. N. (2005). *Wheat Flour Milling*. St. Paul, Minnesota, USA: American Association of Cereal Chemists, Inc. https://doi.org/10.1016/B978-1-891127-55-7.50012-4

Singh, A., Hung, Y.-C., Corredig, M., Phillips, R. D., Chinnan, M. S., & McWatters, K. H. (2005). Effect of milling method on selected physical and functional properties of cowpea (*Vigna unguiculata*) paste. *International Journal of Food Science and Technology*, **40**, 525–536. https://doi.org/10.1111/j.1365-2621.2005.00964.x

Thakur, S., Scanlon, M. G., Tyler, R. T., Milani, A., & Paliwal, J. (2019). A comprehensive review of pulse flour characteristics from a wheat flour miller's perspective. *Comprehensive Reviews in Food Science and Food Safety*, in press.

LITERATURE REVIEW

Classification and Nomenclature

Pea (*Pisum sativum* L.) is a cool-season annual vine belonging to the legume family (*Fabaceae*). Pea may be classified either as field/dry pea (*P. sativum ssp. arvense*), which has a smooth seed surface, or as garden pea (*P. sativum ssp. hortense*), which has an irregular seed surface (U.S. Dry Pea & Lentil Council, 2016). The latter class of pea is higher in sucrose and is often harvested before maturity for human consumption as fresh or frozen seeds or pods, while the former class is higher in starch and is harvested at maturity for use as animal feed or for human consumption in whole, split, or ground form (Pavek, 2012). Split pea designates whole pea that has undergone a milling operation to remove the hull and separate the cotyledons. Ground pea or pea flour refers to whole or split pea that has undergone a size reduction process beyond cotyledon separation. Field pea may be further classified by color as either green or yellow (U.S. Dry Pea & Lentil Council, 2016) (Figures 1 and 2). Yellow field pea has a brighter color than green field pea (annual mean CIE L* value of 57-71 for yellow versus 52-66 for green pea for American crop years 2012-2017) with more red and yellow coloring (annual mean Hunter a and b values of 5 to 7 and 14 to 22, respectively, for yellow pea versus (-4) to (-1) and 9 to 15, respectively, for green pea for American crop years 2012-2017) (U.S. Dry Pea & Lentil Council, 2017).

Production and Consumption

The United States is an important participant in the global field pea market. It has been among the top five field pea producers in the last five years along with Canada, Russia, China, and India. Additional major dry pea producing areas have included parts of Europe (primarily France and Ukraine), Australia, and Ethiopia (FAO, 2017a). The United States has also been one

of the top three exporters of field pea for the last decade, along with Canada, Russia, France, and Ukraine (FAO, 2017b). Major importers during this period have included the United States as well as India, China, Bangladesh, Spain, Pakistan, Belgium, Italy, and the United Kingdom.

Figure 1. Whole (left) and split (right) green pea (http://northerngate.ca/agricultural-products/peas/)

Figure 2. Whole (left) and split (right) yellow pea (http://northerngate.ca/agricultural-products/peas/)

Within the United States, field pea has been produced predominantly in the Midwest (North Dakota, Montana, Minnesota, and South Dakota) and the Pacific Northwest (Washington, Idaho, and Oregon) (U.S. Department of Commerce, 2010). North Dakota has been a leader in field pea production during the last decade, providing on average over 40 % of the annual national production (roughly 322,000 metric tons per year) (NASS, 2017). Domestic consumption of dry pea and lentil has been on the rise recently. Average annual per capita consumption was 0.24 kg during the 1980s, 0.29 kg during the 1990s, and 0.36 kg during the 2000s (ERS, 2010).

Physical Seed Characteristics

Field pea seeds are round and of intermediate size compared to other pulses. The 1000 seed weight for American-grown yellow pea is 206-224 g, which is between that of lentil (~45 g) and chickpea (~400 g) (U.S. Dry Pea & Lentil Council, 2017). Field pea seeds are composed of an outer seed coat (~10 % of seed weight) surrounding a pair of cotyledons (~89 % of seed weight) and an attached embryonic axis (~1 % of seed weight) (Chibbar, Ambigaipalan & Hoover, 2010). The seed coat, also called the hull or testa, is about 90 % dietary fiber (primarily cellulose with some xylans and pectin), 5 % protein, 3 % ash, and 2 % starch (Dalgetty & Baik, 2003). The remainder of the seed is primarily starch (~48 %) and protein (~28 %) with a moderate amount of dietary fiber (~14 %) and small amounts of inorganic material (~3 %) and lipids (~1 %) (Dalgetty & Baik, 2003; Tosh & Yada, 2010).

In split pea, the hull has been removed and only the separated cotyledons and attached embryo remain. Within the cotyledon, microstructure is not homogeneous. The outer portion of the cotyledon (roughly ¼ of the total cotyledon by weight) is composed of tightly-packed cells while the inner portion contains more loosely-packed cells with larger intercellular spaces

(Figure 3) (Otto, Baik & Czuchajowska, 1997). The differences in cell packing within the cotyledon result in differences in fracture behavior. The inner portion of the cotyledon tends to fracture more readily than the outer, tightly packed area, resulting in smaller particles of inner cotyledon material and larger particles of outer cotyledon material following a single roller mill pass (Figure 4). Because of these differences in microstructure, a roller milling process consisting of three break and three reduction stands results in inner cotyledon flour from the break rolls and the first reduction roll and outer cotyledon flour from the second and third reduction rolls (Otto et al., 1997). The composition of the inner and outer cotyledon fractions is also not homogeneous. Outer cotyledon tends to be higher in dietary fiber and protein and lower in starch than inner cotyledon material.

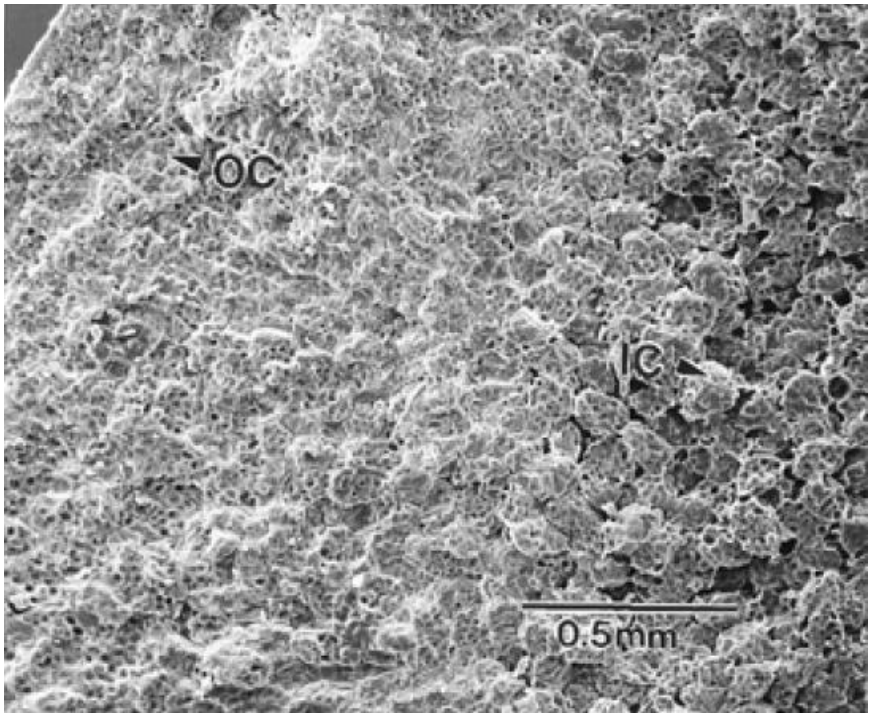

Figure 3. SEM image of vertical cross section of field pea showing structural differences between outer (OC) and inner (IC) cotyledon (Adapted from Otto et al., 1997)

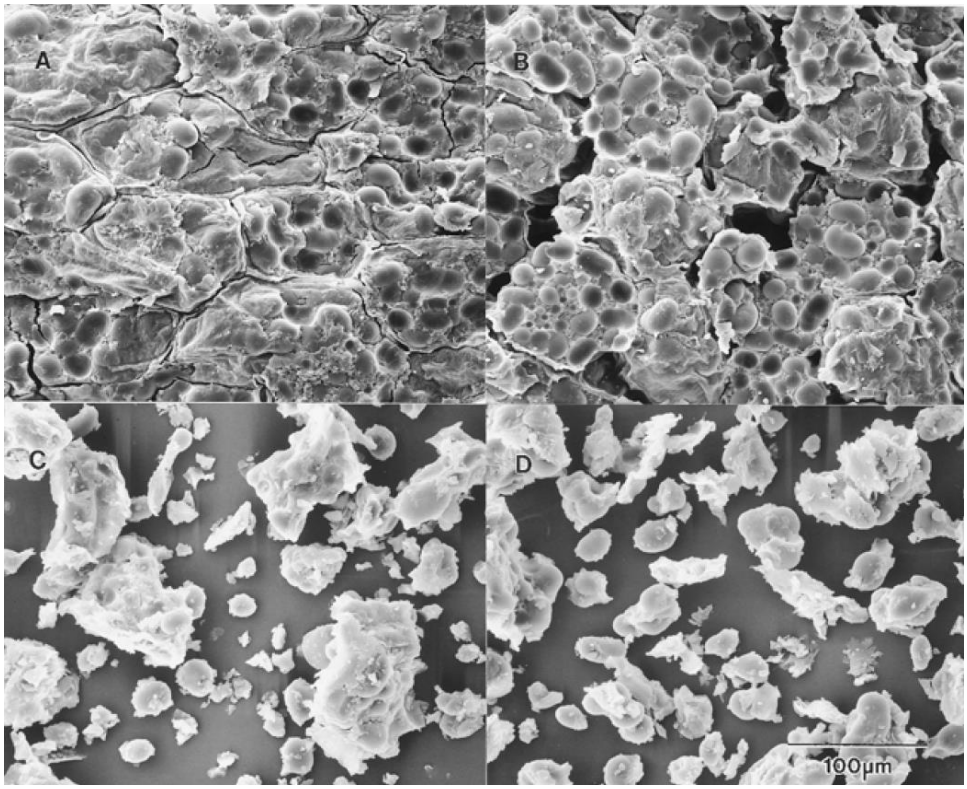

Figure 4. SEM image of the cross section of the outer (A) and inner (B) cotyledon of field pea and of flour particles from the outer (C) and inner (D) cotyledon (Adapted from Otto et al., 1997)

Chemical Composition and Nutritional Value

Carbohydrate

Field pea seed is 55-72 % carbohydrate, the main component of which is starch (Hall, Hillen & Garden-Robinson, 2017). The U.S. pulse quality survey reports annual mean American-grown field pea starch content at 42-52 % (U.S. Dry Pea & Lentil Council, 2017). Other sources have reported North American field pea starch content at 29.1-49.5 % (Hoover & Ratnayake, 2002; Raghunathan, Hoover, Waduge, Liu & Warkentin, 2017; Wang, Hatcher & Gawalko, 2008). The range in starch content may be affected by differences in genetic makeup and growing conditions, though the former may have a greater effect than the latter on seed composition (Hood-Niefer, Warkentin, Chibbar, Vandenberg & Tyler, 2011; Lam, Karaca, Tyler & Nickerson, 2018). Pea starch granules are usually ellipsoidal or round with a smooth or

slightly cracked surface (Figure 5) and a mean diameter of ~28 µm (Raghunathan et al., 2017), though granule size can vary with lengths from 2-50 µm and widths from 2-35 µm (Hoover, Hughes, Chung & Liu, 2010; Hoover & Ratnayake, 2002; Ratnayake, Hoover, Shahidi, Perera & Jane, 2001; Simsek, Tulbek, Yao & Schatz, 2009; Zhou, Hoover & Liu, 2004).

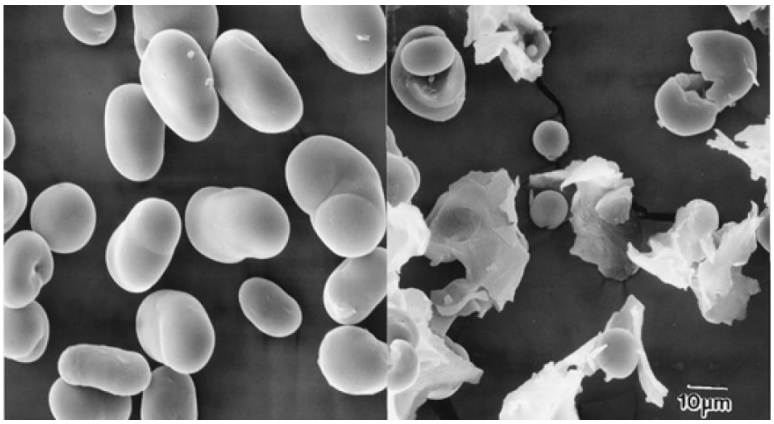

Figure 5. SEM images of field pea starch granules in prime (left) and tailings (right) fractions (Adapted from Otto et al., 1997)

In terms of molecular composition, field pea starch is 22-43 % amylose, which is higher than the 18-33 % that is typical of most native starches (Biliaderis, Grant & Vose, 1979; Delcour & Hoseney, 2010; Hoover & Ratnayake, 2002; Raghunathan et al., 2017; Zhou et al., 2004). The amylose from pea starch has a degree of polymerization (DP) of 1300-1400 (Biliaderis, Grant & Vose, 1981; Ratnayake et al., 2001). The remaining 57-78 % of pea starch is amylopectin, the structure of which is frequently characterized by determining the molecular weight of branch chains and limit dextrins following debranching. Following such a procedure, the average branch chain length of pea starch amylopectin is 22.9-24.2 glucose units (Ratnayake et al., 2001). Since amylopectin chain length is not homogeneous, it is common to divide branch chains into multiple populations. However, without standardized end points for these chain length intervals, it is difficult to compare the chain length distribution from multiple studies (Biliaderies et al., 1979; Biliaderis et al., 1981; Chung, Liu, Donner, Hoover, Warkentin & Vandenberg, 2008;

Raghunathan et al., 2017; Simsek et al., 2009). The range of the chain length distribution in pea starch amylopectin is < 6 up to 65 glucose units (Raghunathan et al., 2017).

The ratio and individual structure of amylose and amylopectin affect the crystallinity of a starch granule which is a key feature to starch functionality. Pea starch granule crystallinity has been reported over a wide range of 7.8-36.8 % (Hoover & Ratnayake, 2002; Raghunathan et al., 2017; Ratnayake et al., 2001; Simsek et al., 2009; Zhou et al., 2004). The lower end of this range is below that of typical cereal or tuber starches and other pulse starches. Regular (31.5 %) and waxy (39.5 %) corn starches, regular (28.9 %) and waxy (37.7 %) wheat starches, potato starch (26 %), sweet potato starch (50.7 %), and chickpea starch (21.1-27.4 %) all have a higher degree of crystallinity than that most commonly reported for field pea starch (Li & Zhu, 2017; Sun, Li, Dai, Ji & Xiong, 2014; Xu, Sismour, Narina, Dean, Bhardwaj & Li, 2013; Yu et al., 2015; Zhou et al., 2015). Kidney bean, black gram, and pigeon pea starches also contain a larger crystalline region than field pea starch (Singh, Nakaura, Inouchi & Nishinari, 2008). Crystallinity generally decreases as amylose content increases (Zhou et al., 2015) and as amylopectin branching increases (Biliaderis et al., 1981). Therefore, the low crystallinity of field pea starch may be due in part to the combination of highly-branched amylopectin and high amylose content. Like other legume starches, field pea starch exhibits a C-type X-ray diffraction pattern (Delcour & Hoseney, 2010). The C-type pattern indicates the presence of both A-type (less hydrated) and B-type (more hydrated) crystals. The A-type crystals tend to be located on the periphery of the starch granule and are more resistant to swelling and disruption than the B-type crystals in the interior of the granule. Therefore, starches with a greater ratio of B-type to A-type crystals will tend to have a lower gelatinization temperature than those with a lower ratio of B-type to A-type

crystals. Field pea starch B-type crystal polymorph content has been reported at 27.1-55.5 % (Raghunathan et al., 2017; Zhou et al., 2004).

Field pea contains other carbohydrates in addition to starch, namely soluble sugars and non-starch polysaccharides (NSPs). Soluble sugar content ranges from 5-7 % (Berrios, Morales, Camara & Sanchez-Mata, 2010; Brummer, Kagiani & Tosh, 2015). The main soluble sugars in field pea include sucrose, galactose, raffinose, stachyose, and verbascose at individual levels of 0.5 to 2.5 g/100g. Smaller amounts of ribose, fructose, glucose, maltose, and melibiose are also present. The NSP content is roughly equivalent to dietary fiber content in field pea (waxes and lignin, if present, also contribute to dietary fiber), which is 11-20 % (Dalgetty & Baik, 2003; Stoughton-Ens, Hatcher, Wang & Warketin, 2010; Tosh & Yada, 2010; Wang et al., 2008). The NSP composition of field pea hull is predominantly insoluble cellulose with smaller amounts of soluble pectins, xylans, and xylogalacturonans (Chibbar et al., 2010; Dalgetty & Baik, 2003). In the cotyledon, cellulose is present in much smaller quantities while the soluble arabinose-substituted pectins, xylans, and xyloglucans predominate (Brummer et al., 2015; Dalgetty & Baik, 2003). The size and shape of these soluble NSPs is relevant to both health benefits and functionality. Soluble NSPs from yellow pea are polydisperse with a weight average molecular weight of 478,000 ±38,000 g/mol, and number average molecular weight of 50,000 ±5,000 g/mol, and a polydispersity index of 9.6 (Brummer et al., 2015).

Protein

The annual mean protein content of American-grown field pea is 20-25 %, according to the U.S. pulse quality survey (U.S. Dry Pea & Lentil Council, 2017). Other sources list protein content of North American field pea at 15.7-28.6 % (Boye et al., 2010; Chakraborty, Sosulski & Bose, 1979; Ma, Boye & Hu, 2017; Park, Kim & Baik, 2010). As with starch content, pea seed

protein content is affected by both genetic and environmental factors (Hood-Niefer et al., 2011; Lam et al., 2018).

Plant proteins are typically divided into classes based on solubility, with albumins being the water-soluble protein fraction, globulins dilute salt soluble, prolamins alcohol soluble, and glutelins soluble in dilute acid or base (Delcour & Hoseney, 2010). In grain legumes, 70-80 % of the crude protein consists of globulins, which act as storage proteins in the whole seed. Grain legume globulins can be further divided into 7S and 11S fractions, which are also called vicilin and legumin, respectively. Legumin is a hexamer with a molecular weight of 300-400 kDa that is relatively high in glutamic acid, leucine, alanine, and valine (Lam et al., 2018). Vicilin is a trimer with a molecular weight of 150-170 kDa that shares 70-80 % similarity in amino acid profile to legumin but tends to be lower in sulphur-containing amino acids. A third protein designated convicilin is present in the 7S fraction as a monomer (70 kDa), a homotrimer (210 kDa), or a heterotrimer with vicilin. Convicilin is higher in sulphur-containing amino acids than the other globulin proteins. In field pea, total globulin content has been reported at 7.1 % of the total seed mass, of which 4.1 % was 7S vicilin/convicilin and 3 % was 11S legumins (Rubio, Perez, Ruiz, Guzman, Aranda-Olmedo & Clemente, 2013). In general, vicilin tends to be more abundant than legumin in pea protein, although the legumin/vicilin ratio is dependent upon genetics and is very sensitive to environmental factors during seed development (Lam et al., 2018).

Albumin is the second most abundant class of grain legume protein, making up about 2 % of the total seed mass (Rubio et al., 2013). Grain legume albumins are a heterogeneous class of proteins with a molecular weight range of 5-80 kDa and a variety of *in vivo* functions including enzymes, enzyme inhibitors, and lectins (Lam et al., 2018). Prolamins and glutelins can also be found in grain legume proteins in small amounts.

The amino acid profile of legumes differs from that of cereals in that legumes are relatively rich in the essential amino acid lysine. A comparison of the essential amino acid contents of field pea with that of diploid wheat, for example, reveals that field pea protein possesses almost three times the lysine content of wheat, along with equivalent contents of most of the remaining essential amino acids phenylalanine, tyrosine, leucine, valine, and histidine (tryptophan content not determined in diploid wheat and cysteine/methionine slightly lower in field pea) (Figure 6). In a study on the protein quality of cooked pulses, the sulfur amino acids were limiting for green pea while tryptophan was limiting for yellow pea (Nosworthy, Neufeld, Frohlich, Young, Malcolmson & House, 2017). Protein quality, expressed in protein digestibility corrected amino acid scores (PDCAAS), was calculated based on amino acid profile as well as true protein digestibility (TPD), which reflects the bioavailability of the protein. TPD of yellow and green pea were similar, however, PDCAAS was higher for yellow than for green pea. The Protein Rating is a combined expression of amino acid quality, protein digestibility, and protein content per serving. Despite having a lower protein content than green pea, yellow pea had a higher Protein Rating, indicating that the differences in amino acid profile between the two market classes could be important *in vivo*. Despite these differences between yellow and green pea, PDCAAS was sufficient for both to be considered quality protein sources for noninfant and infant foods in the US (based on PDCAAS > 0.4). The high protein quality and high lysine and total protein contents of field pea are motivating factors for the fortification of cereal-based products with pulse flours.

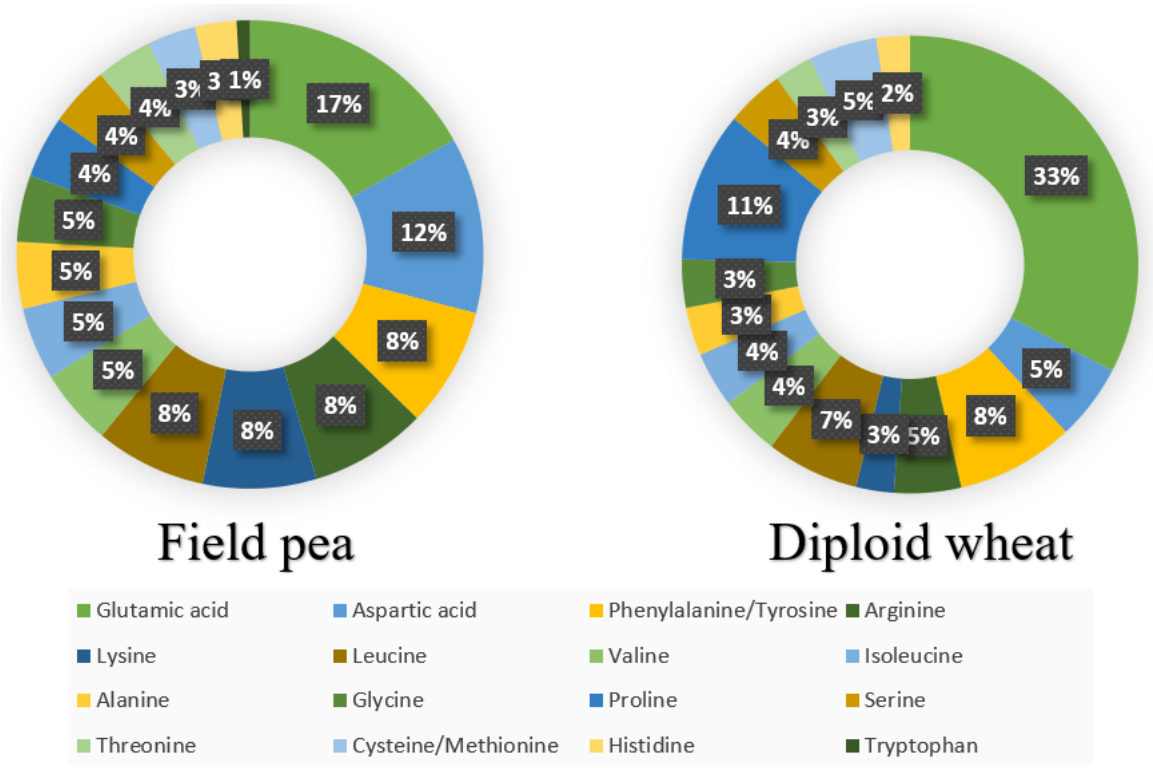

Figure 6. Comparison of the amino acid profiles of field pea and diploid wheat (data from Hall et al., 2017 and Acquistucci, D'Egidio & Vallega, 1995)

Lipid

Lipids make up a very small fraction of the field pea seed. American-grown field pea lipid content was 0.9-3.3 % in the 2017 U.S. pulse quality survey (U.S. Dry Pea & Lentil Council, 2017). North American-grown field pea lipid content has been quantified by other researchers at 1.5-2.0 % (Boye et al., 2010; Solis, Patel, Orsat, Singh & Lefsrud, 2013), while lipid content of field pea grown worldwide ranges from 1-4 % (Alonso, Grant, Dewey & Marzo, 2000; Ryan, Galvin, O'Connor, Maguire & O'Brien, 2007; Yoshida, Tomiyama, Saiki & Mizushina, 2007a; Yoshida, Tomiyama, Tanaka & Mizushina, 2007b). Most of the lipids in field pea are phospholipids (52-61 %) and triacylglycerols (31-40 %) with small amounts of diacylglycerols (2-4 %), free fatty acids (1.3-2.7 %), steryl esters (0.8-2.4 %) and hydrocarbons (0.5-0.9 %) (Yoshida et al. 2007b). The fatty acid profile of pea oil is dominated by linoleic (46-

54 %) and oleic (15-31 %) acids with smaller quantities of linolenic (9-11 %), palmitic (7-13 %), and stearic (2-3 %) acids and trace amounts of lignoceric, gadoleic, arachidic, and erucic acids (El-Saied, Amer & Gabran, 1981; Ryan et al., 2007; Solis et al., 2013).

Minor constituents

Important minor constituents of field pea include essential minerals and trace elements, volatile compounds, and bioactive substances. While present in field pea in much smaller quantities than the macronutrients discussed above, these minor constituents can play a major role in nutritional and sensory quality. The average mineral content of American-grown yellow field pea was 630, 8, 50, 1,116, 10, 2,424, 6,918, and 31 mg/kg for calcium, copper, iron, magnesium, manganese, phosphorus, potassium, and zinc, respectively, and 216 µg/kg for selenium in the U.S. pulse quality survey of 2017 (U.S. Dry Pea & Lentil Council, 2017). Average mineral content of Canadian field pea has been reported at 5.8, 53.6, 1,171, 12.7, 2.7, 10,376, and 30.5 mg/kg for copper, iron, magnesium, manganese, nickel, potassium, and zinc, respectively, and at 469 µg/kg for selenium (Ray, Bett, Tar'an, Vandenberg, Thavarajah & Warkentin, 2014). Another Canadian study reported mineral contents of 821, 6.4, 51.5, 1,230, 11.7, 1.6, 3,320, 9,832, and 35.6 mg/kg for calcium, copper, iron, magnesium, manganese, nickel, phosphorus, potassium, and zinc, respectively, and 331 µg/kg for selenium (Gawalko, Garrett, Warkentin, Wang & Richter, 2009). This study also evaluated levels of toxic trace elements in field pea and found all measured values to be below the maximum residue levels (MRLs) set out by the Codex Alimentarius. Mean cadmium content was 23 µg/kg while mean arsenic, lead, and mercury contents were all below limits of quantification. Mineral content tends to vary more widely than other proximate components of field pea and is strongly affected by the mineral availability of the soil during seed development.

Field pea is also a dietary source of vitamins. The folate content of field pea is of interest because of the importance of this vitamin to certain human life stages and because it is a limiting nutrient in refined cereal grains. Folate content ranges from 25.0-64.8 µg/100g for green pea and from 23.7-55.6 µg/100g for yellow pea, levels which are comparable to the 44 µg/100g given for whole-grain wheat flour by the USDA national nutrient database for standard reference (Han & Tyler, 2003). Additionally, field pea is a dietary source of carotenoids, primarily luteins with small amounts of β-carotene, zeaxanthin, and violaxanthin (Ashokkumar, Diapari, Jha, Tar'an, Arganosa & Warkentin, 2015; Marles, Warkentin & Bett, 2012; Padhi, Liu, Hernandez, Tsao & Ramdath, 2017). Although none of these β-carotenes have previtamin A activity in humans, there are other health benefits associated with their consumption such as antioxidant activity and skin and eye maintenance (Ashokkumar et al., 2015). Field pea carotenoid content ranges from 5.3-24.5 µg/g for luteins and 5.4-28.2 µg/g for total carotenoids in green and yellow market classes (Ashokkumar et al., 2015; Padhi et al., 2017), with similar levels (5-25 µg/g) sequestered in hull tissue as were observed in the whole seed (Marles et al., 2012). Total carotenoid and β-carotene contents are both higher in green than in yellow varieties.

Volatile compounds in field pea are responsible for a large portion of field pea aroma and flavor. These compounds include alcohols, aldehydes, ketones, aromatic compounds, terpenes, and sulphur- and nitrogen-containing compounds, and may be either native to the pea seed or developed during processing and storage (Ma, Boye, Azarnia & Simpson, 2016; Roland, Pouvreau, Curran, van de Velde, & de Kok, 2017). When a product is meant to smell and taste of pea, many of these compounds are not objectionable. However, for many products in which pea-derived ingredients are used, flavor descriptors such as green, beany, pea, earthy, and hay-like are undesirable (Malcolmson, Frohlich, Boux, Bellido, Boye, & Warkentin, 2014). Multiple

approaches have been tried for reducing or removing these characteristic pea flavors including soaking, thermal treatment, germination, fermentation, enzyme treatment, and solvent extraction. Solvent extraction and fermentation techniques have both been applied successfully to flavor modification in field pea (Hillen, 2016; Schindler, Zelena, Krings, Bez, Eisner & Berger, 2012).

Finally, field pea contains a wide variety of other bioactive substances including phenolic compounds, oligosaccharides, saponins, phytate, enzyme inhibitors, and lectins (Hall et al., 2017; Patterson, Curran & Der, 2017). These compounds are also called antinutrients in some places in the literature due to their disruptive effects on parts of human digestion. However, subsequent research has indicated some of these compounds might be beneficial to human health in the right context (Dahl, Foster & Tyler, 2012; Singh, Singh, Kaur & Singh, 2017a; Singh, Singh, Singh & Kaur, 2017b). Because of these conflicting views on the bioactive compounds in field pea, some research has focused on reducing bioactive content through breeding and processing while other research has focused on leveraging the proposed health benefits of these substances.

Functionality of Milled Pea

Starch

Starch is a carbohydrate with many applications in food systems, particularly as related to texture and rheology. Pulse starches are functionally unique in providing resistance to shear-thinning, rapid retrogradation, and high gel elasticity, and are nutritionally unique in possessing a low glycemic index and high resistant starch content (Ambigaipalan, Hoover, Donner & Liu, 2013; Ambigaipalan et al., 2011; Hoover et al., 2010). The functional properties of a given starch are caused by starch molecule structure and resultant structure of the starch granule. Functionality assessment can be divided into properties related to starch gelatinization

(irreversible starch granule swelling in the presence of water and heat) and those related to starch retrogradation (interaction among amylose and amylopectin following gelatinization).

Starch gelatinization is generally evaluated with differential scanning calorimetry (DSC) or viscometry. DSC can provide the temperature range over which starch undergoes gelatinization. Gelatinization onset and conclusion temperatures for pea starch range from 59.1 to 64 °C and 72 to 88 °C, respectively (Chung et al., 2008; Hood-Niefer et al., 2011; Raghunathan et al., 2017; Simsek et al., 2009; Zhou et al., 2004). Most sources report a gelatinization conclusion temperature at the lower end of this range, which is comparable to that of maize, sorghum, or rice starch, and higher than that of wheat, barley, oat, and rye starch (Delcour & Hoseney, 2010). The most common viscometric analysis method uses a rapid viscoanalyzer (RVA) to treat a starch slurry to a standardized sequence of time, temperature, and shear conditions. The pasting curve obtained from such analysis provides the time and temperature at which viscosity begins to increase due to granule swelling (pasting time and temperature), the maximum viscosity obtained in the hot slurry due to granule swelling (peak viscosity), the decrease in viscosity as continued heat and shear cause starch granules to break down (breakdown viscosity), and the maximum viscosity obtained upon cooling the slurry as the leached amylose molecules crystallize (final viscosity) (Figure 7). The pasting profile of isolated field pea starch is characterized by a pasting temperature of 69.6-74.9 °C and peak, breakdown, and final viscosities of 1,100-4,663, 20-2,397, and 1,900-6,026 cP (Chung et al., 2008; Hood-Niefer et al., 2011; Raghunathan et al., 2017). U.S. whole milled field pea had annual mean pasting time and temperature ranges of 5-6 min and 76-78 °C (U.S. Dry Pea & Lentil Council, 2017). Furthermore, mean peak, breakdown, and final viscosities of whole pea flour were 1,476-1,752, 72-240, and 2,544-3,012 cP, respectively. Pea starch has a lower breakdown viscosity

than cereal starches such as wheat and corn, indicating granules are more resistant to collapse and have a lower rate of amylose leaching. Low breakdown viscosity indicates pea starch is resistant to shear thinning, making it suitable in applications in which viscosity retention is needed, such as in a product that must be extensively mixed or pumped.

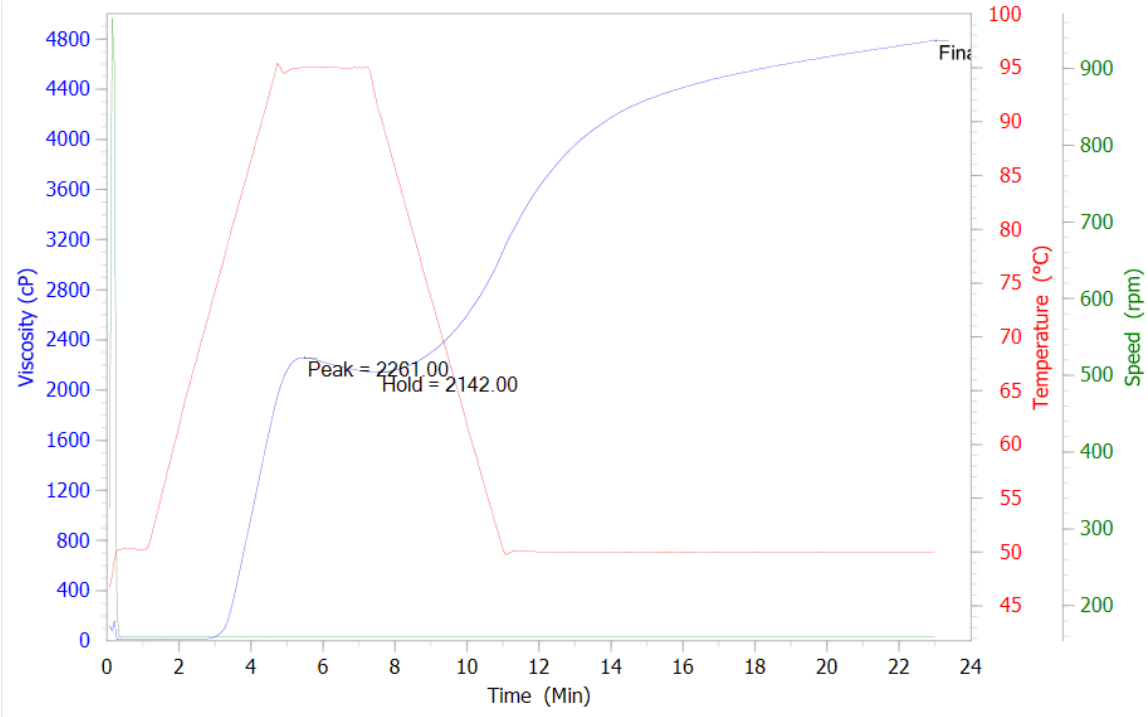

Figure 7. Example RVA output for a sample of yellow pea flour

Retrogradation in pulse starches is not as well understood as gelatinization. The lack of understanding is partly due to the variability in the methods used (Hoover et al., 2010). Available methods include measuring syneresis after a selected number of freezing and thawing cycles, measurement of turbidity and texture, DSC, X-ray diffraction, and nuclear magnetic resonance (NMR). Since not all these methods evaluate the same crystallization process of starch molecules, it is very important to use results from the same method when comparing starches, even when only a relative rather than an absolute analysis is desired (Ambigaipalan et al., 2013). The most commonly-used method of evaluating starch retrogradation in pulses is measuring

syneresis. However, there is no standard for the number and duration of freeze/thaw cycles, the speed and length of centrifugation, or the method of quantifying water loss. Standardized methods for starch retrogradation are needed to allow for further understanding and comparison of the retrogradation characteristics of pulse starches.

Fiber

As mentioned in a previous section, field pea is 11-20 % dietary fiber. The insoluble component of pea fiber is mostly cellulose while the soluble component is rich in pectin (Brummer et al., 2015). Pea fiber is already widely used in fiber fortification of processed foods. Pea hull fiber, which is mostly insoluble, is commonly added to cereal-based processed foods to increase dietary fiber (Tosh & Yada, 2010). Due its low viscosity, the soluble fiber from pea cotyledons would be suited to fortification of non-viscous products such as fortified beverages (Brummer et al., 2015; Dalgetty & Baik, 2003). In addition to fiber fortification, pea fiber has potential to serve functional roles in foods including fat and water binding (Dalgetty & Baik, 2003; Wang & Toews, 2011). Pea cotyledon fiber performed the best among 10 commercial fat-binding ingredients in retaining fat in ground beef during heating (Anderson & Berry, 2001). Pea cotyledon fiber was also used successfully as a water binder in low-fat ground beef (Anderson and Berry, 2000). This promising initial research indicates that the use of pea flour or fiber as a water or fat binder should be the focus of additional research and attention. Use of pea flour as a binder and/or extender may also increase as deodorization technologies improve, allowing the use of pea flour as a functional ingredient in the absence of native pea odor and flavor.

Protein

Field pea protein functionality modes include solubility, water and oil binding, emulsifying, foaming, and gelation. Although pea protein may not be the superlative in all these

properties, it is a popular choice in food formulation as a plant-based protein with low allergenicity (versus wheat or soy), high nutritional value, and low cost (Lam et al., 2018). Protein solubility, also sometimes called protein dispersibility, refers to how easily a protein can be suspended in solution, with the solvent usually being water or a buffer. Solubility is affected by how readily protein molecules interact with solvent molecules. This is controlled by both intrinsic factors (particle surface charge and polarity) and extrinsic factors (pH, salt concentration, and temperature). Pea protein intrinsic factors can differ somewhat because extraction protocol can affect how much hydrophobic portions of the proteins are exposed to the solvent (Taherian, Mondor, Labranche, Drolet, Ippersiel & Lamarche, 2011). However, solubility differences among pea cultivars and extraction methods are not as drastic as those that occur under different external conditions, particularly under varying pH. The pH of a solution affects the charge of ionizable groups within a protein, directly affecting protein surface charge and the extent of electrostatic repulsion among protein molecules. Solubility is low (2-4 %) at the pI (pH 5) of pea protein (Shevkani, Singh, Kaur & Rana, 2015) and increases as the pH increases or decreases. The addition of salts or polysaccharides can modify protein-protein and solvent-protein interactions and has shown promise in increasing the solubility of pulse proteins (Braudo, Plashchnia, & Schwenke, 2001).

The water binding capacity of a protein is affected by protein matrix structure (particularly pore size) and the number of hydrophilic amino acids present (Lam et al., 2018). As with solubility, water binding capacity is lowest at the pI of a protein. Water binding capacity values for pea protein isolate range from 1.9-4.0 g/g (Fuhrmeister & Meuser, 2003; Stone, Avramenko, Warkentin & Nickerson, 2015). Oil binding capacity, on the other hand, is enhanced in the presence of hydrophobic amino acids and can be heavily affected by pea variety and

method of protein isolation (Lam et al., 2018). Oil binding capacity of pea protein isolate falls in the range of 0.87-5.3 g/g, depending upon extraction methods (Fuhrmeister & Meuser, 2003; Stone, Karalash, Tyler, Warkentin & Nickerson, 2015).

Emulsions are unstable dispersions or suspensions of immiscible liquids (Lam et al., 2018). Agitation is used to disperse droplets of one liquid in the continuous phase of the other. Emulsions can be stabilized by the addition of protein, which can form a physical barrier around the droplets of the dispersed phase, preventing structural changes of the droplets. Emulsifying activity or capacity quantifies the surface area of dispersed phase that can be stabilized per gram of protein and emulsifying stability measures the stability of the protein layer surrounding the droplets over time. Emulsifying properties tend to be greater for proteins that can rapidly unfold and form a layer around dispersed droplets and that possess sufficient charged/hydrophilic groups to interact with surrounding solvent and provide electrostatic repulsion of other coated droplets (Boye, Zare & Pletch, 2010). Emulsifying properties of pea protein are affected by extraction method and by the ratio of globulin proteins (vicilin to legumin) (Dagorn-Scaviner, Gueguen & Lefebvre, 1987; Liang & Tang, 2013). Partial hydrolysis can improve the emulsifying activity of pea protein, but negatively impacts emulsion stability (Tsoukala, Papalamprou, Mari, Doxatakis & Braudo, 2006).

Foams are dispersions of gas bubbles in a liquid or solid (Lam et al., 2018), though foam stability is mostly an issue for dispersions involving gas-liquid interfaces rather than gas-solid interfaces. Foams can be stabilized by proteins that are able to migrate to the gas-liquid interface and form layers along the interface that reduce the surface tension of the liquid. Foaming capacity quantifies the interfacial area over which a protein can stabilize a foam, while foaming stability measures foam stabilization over time and when exposed to stress. In contrast to good

emulsifying agents, good foaming agents are hydrophobic with low electrostatic repulsion to form stable layers that relieve surface tension. The pH of a solution can be used to modify surface charge of proteins and enhance foam stability; however, in the case of pea protein, solubility limitations when charge is minimized (near pI) tend to prevent pH modification from being beneficial to foam stability (Aluko, Mofolasayo & Watts, 2009). Stability of foams containing pea protein can be enhanced by the addition of small amounts of salts (Taherian, Mondor, Labranche, Drolet, Ippersiel & Lamarche, 2011).

Protein gels are three-dimensional networks of protein molecules within which is trapped water and other components of the food system. The mechanism of gelation involves initial protein denaturation followed by aggregation of unfolded proteins into an interconnected matrix. Protein gelation can be induced by heating, change in pH or salt concentration, and exposure to high pressure, shear, or certain solvents (Lam et al., 2018). Gelation induction methods can greatly affect the gelation capacity and texture of a protein gel. Gelation capacity is often expressed as the least gelling concentration (LGC), which is the lowest protein concentration required to form a self-supporting gel (Boye et al., 2010). The LGC of pea protein isolates is similar to that of soy protein isolates (Fernandez-Quintela, Macarulla, Del Barrio & Martinez, 1997). Vicilin-rich pea protein fractions tend to have higher gelling properties than legumin-rich fractions (Mession, Chihi, Sok & Saurel, 2015).

Pulse Milling

Pulse milling serves a three-fold purpose of reducing particle size, facilitating separation of seed components, and inducing structural and chemical changes to seed components (Scanlon, Thakur, Tyler, Milani, Der & Paliwal, 2018). Milling characteristics of pulses are dictated by the combination of seed characteristics (grain size, hardness, and moisture), post-harvest storage,

and pre-milling treatments. These factors are discussed in the following sections along with a review of field pea milling methods and applications of pea flour.

Seed properties

Seed properties most relevant to milling include size, shape, hardness, and moisture content. Whole field peas are approximately round with a sphericity (ratio of the surface area of a sphere of the same volume to the surface area of the seed) of 0.84 and a diameter of 5.6-7.8 mm (Vishwakarma, Shivhare, Gupta, Yadav, Jaiswal & Prasad, 2018; Yalcin, Ozarslan & Akbas, 2007). Uniformity in these seed properties promotes higher milled product quality, particularly in roller milling in which an appropriate roll gap must be selected based on seed dimensions. Roller milling protocols must consider variation in seed dimensions, which is greater for pulse seeds than for grain kernels (Scanlon et al., 2018). Pulse seed size variability is due to differences within a plant (due to indeterminate maturity of pulse plants) as well as to differences among varieties and growing conditions (Harden & Wood, 2017; Wood, Edmund & Harden, 2008). The U.S. grading system has standards for seed color, defective and small seeds, and foreign material, but does not require seed size variability to be quantified (FGIS 2009). Therefore, incoming material should be evaluated for seed size variability prior to milling and intermittent roll gap adjustment or a pre-milling sizing step might be required to maintain appropriate roller mill settings (Harden & Wood, 2017).

Seed hardness refers to the combination of seed density and strength of association between starch and protein in the endosperm or cotyledon that results in resistance to size reduction forces. Standardized methods for wheat hardness are available (AACC International, 1999), but there are currently no standardized methods for pulse hardness. Hardness of grains and pulses has been quantified by texture analysis as the amount of cutting (Dijkink &

Langelaan, 2002a) or compressive force (Pelgrom, Boom & Schutyser, 2015) required for seed fracture or by milling experiments based on the amount of time, energy, or force required to achieve a certain degree of milling (Kongseree & Juliano, 1972; Miller, Afework, Hughes & Pomeranz, 1981; Pomeranz, Czuchajowska, Martin & Lai, 1985) or by the particle size distribution produced under fixed milling conditions (Miller, Afework, Pomeranz, Bruinsma & Booth, 1982; Tyler, 1984). The cause of pulse seed hardness is not as well understood as the cause of wheat kernel hardness. The NSP reflected in cell wall material yield has been proposed to take part in seed hardness based on correlation between protein separation efficiency (PSE, reflecting milling efficiency) and both NSP content and seed hardness (determined by particle size index) (Tyler 1984). In low moisture seed, high protein and lipid and low starch contents were associated with decreased seed hardness (measured by texture analysis) (Dijkink & Langelaan, 2002b). Further research is needed to provide more detailed information concerning the mechanism of raw pulse hardness.

Unlike most other seed properties, moisture content can be modified to optimize milling efficiency. Adjusting seed moisture by tempering is a regular practice in the dry milling of wheat and rye since appropriate moisture content optimizes energy requirements and equipment wear by mellowing the endosperm, facilitates separation by plasticizing the bran, and ensures appropriate moisture content for both functionality and shelf stability in the final flour (Delcour & Hoseney, 2010). Endosperm mellowing and bran plasticization are caused by the transition of kernels from glassy to rubbery state due to moisture uptake. However, not all seeds display the same relationship between hardness and moisture content. The hardness of corn kernels does not decrease with increasing moisture content due to highly cross-linked protein structure (Delcour & Hoseney, 2010). At moisture content below 16 %, hardness of mung bean seed increased with

moisture (Erkinbaev, Derksen & Paliwal, 2017), but field pea transitions from glassy to rubbery state above ~13 % moisture, resulting in a decrease in hardness (Pelgrom et al., 2013). Tempering of field pea prior to milling may not be desirable since milling efficiency is lower in rubbery state than in glassy state. This is particularly true when separation of the hull is not a concern, as is the case for decorticated pulses such as split pea.

Pre-milling treatments

Pre-milling treatment goals may include moisture modification, as mentioned above for tempering or drying steps, but additional changes to pulse seeds are sometimes desirable and may be accomplished through a variety of methods. In addition to moisture modification, heat can cause structural modification of protein, starch, and flavor compounds and formation of colored products (Ahmed, Taher, Mulla, Al-Hazza & Luciano, 2016; Ma, Boye & Hu, 2017; Pelgrom et al., 2013). Heat can also modify cotyledon microstructure, facilitating size reduction and the separation of protein and starch post-milling (Pelgrom et al. 2013).

Seed treatments have also been employed to modify pulse flavor and nutritional properties. Germination of pea and other pulses resulted in increased protein and fiber contents and antioxidant activity and decreased phytic acid, trypsin inhibitor, and galactooligosaccharide contents (Bellaio, Kappeler, Zamprogna-Rosenfeld & Jacobs, 2013; Camacho, Sierra, Campos, Guzman & Marcus, 1992; Dominguez-Arispuro, Cuevas-Rodriguez, Milan-Carrillo, Leon-Lopez, Gutierrez-Dorado & Reyes-Moreno, 2018). Germination treatment has also facilitated hull removal and splitting of some pulses and resulted in a sweeter flavor and changes in cooking properties (Bellaio, Kappeler, Zamprogna-Rosenfeld & Jacobs, 2013).

Additionally, seed treatments are sometimes used to control pest infestation in pulse shipments. Microwave treatment has been used to reduce pulse beetle populations in selected

pulses (Singh, Singh & Kotwaliwale, 2012). Treatments of up to 700 W, resulting in temperature of up to 80 °C, had no impact on cotyledon yield from a dehulling procedure or on cooking time.

Milling and pea flour applications

Milling equipment can be classified into two general categories of impact mills and attrition mills. The former results in size reduction through compression forces generated by the collision of material particles with moving and/or stationary mill components and with other particles. A hammer mill (Figure 8) is a type of impact mill that uses rapidly rotating blades within a milling chamber to reduce material particle size via impact against the blades, milling chamber walls, and other seed particles. Particles are retained until small enough to pass through screen apertures at the chamber base. Roller mills are a common example of an attrition mill that accomplishes size reduction through a combination of shear and compression. Roller mills are the standard equipment for wheat milling. An experimental version of the standardized roller milling process using a laboratory-scale Buhler mill (Figure 9) is laid out in AACC approved method 26-21.02. This experimental procedure involves the use of 6 sets of rolls and sieves, a bran sifter, and a final sieve box. Most commonly, flour from all three break rolls and the first two reduction rolls is combined and then blended with the third reduction roll and bran flour fractions at a rate that depends on the moisture and ash content of the individual mill streams (Izydorczyk & Kletke, 2016). This process is well adapted to the goals of wheat milling, which are size reduction to certain particle size specifications and separation of endosperm and bran. However, differences in the structure and composition of grain legumes may result in different goals during milling and different methods of achieving those goals.

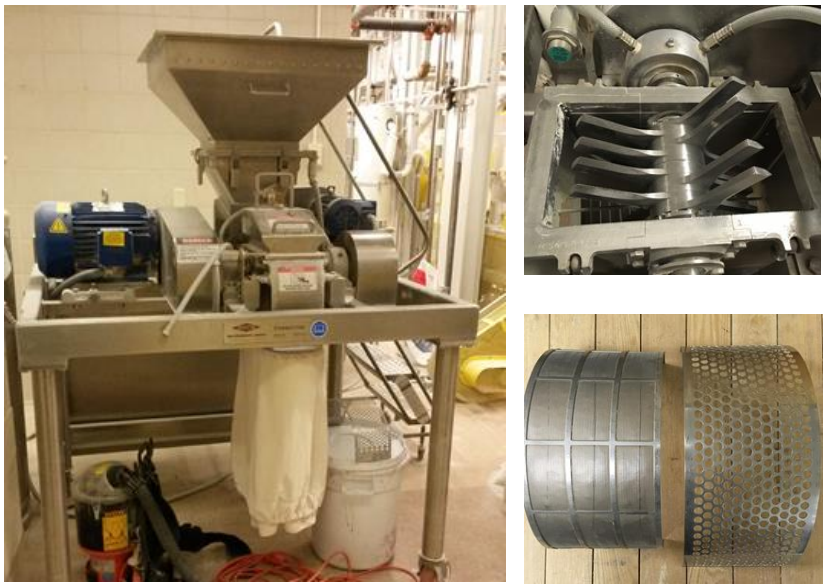

Figure 8. Hammer mill (Fitzpatrick model DASO6) (left), milling chamber (top right), and mill screens (bottom right)

Figure 9. Laboratory-scale Buhler mill (model MLU-202)

Field pea milling research has explored pin and impact milling with air classification for fractionation purposes (Pelgrom, Boom & Schutyser, 2015), hammer and roller milling to investigate protein quality (Le Gall, Gueguen, Seve & Quillien, 2005), and milling split and whole pea with multiple methods (stone, hammer, roller, and pin) (Maskus, Bourre, Fraser, Sarkar & Malcolmson, 2016). Comparing field pea milling studies, and pulse milling studies in general, is made difficult by the variety of milling equipment used, variety of milled fractions obtained (whole pulse, dehulled pulse, and starch, fiber, or protein isolates), and lack of a standard definition of pulse flour in terms of granulation (Gomez, Doyague & de la Hera, 2012; Kerr, Ward, McWatters & Resurreccion, 2000; Mohammed, Ahmed & Senge, 2014; Scanlon et al., 2018). Lack of systematic design of milling experiments and complete, standardized description of milling conditions also complicates comparison among and within milling methods.

Lack of a standardized definition of granulation for whole and fractionated pulse flours also complicates the evaluation of flour application studies (Scanlon et al., 2018). Mixed results of cereal-based product fortification with pulse ingredients can be partly attributed to differences in milling method and resulting particle size distribution. The greatest challenges faced in pulse flour fortification of cereal products tend to be maintaining structural quality of the original product. Pulse-fortified breads tend to have reduced loaf volume and expansion and increased chewiness, and pulse fortified extruded products tend to be harder (Sozer, Holopainen-Mantila & Poutanen, 2017). Additionally, flavor properties can be affected by pulse fortification, especially if the original pulse material possesses strong flavors as is the case in field pea.

References

AACC International. *Approved Methods of Analysis*, 11th Ed. Method 26-21.02. Experimental milling—Buhler method for hard wheat. Approved November 3, 1999. Method 39-70.02. Near-Infrared reflectance method for hardness determination in wheat. Approved November 3, 1999. Method 55-30.01. Particle size index for wheat hardness. Approved November 3, 1999. Method 55-31.01. Single-kernel characterization system for wheat kernel texture. Approved November 3, 1999. Available online only. St Paul, MN: AACC International, Inc.

Acquistucci, R., D'Egidio, M. G., & Vallega, V. (1995). Amino acid composition of selected strains of diploid wheat, *Triticum monococcum* L. *Cereal Chemistry*, **72**:213-216.

Ahmed, J., Taher, A., Mulla, M. Z., Al-Hazza, A., & Luciano, G. (2016). Effect of sieve particle size on functional, thermal, rheological and pasting properties of Indian and Turkish lentil flour. *Journal of Food Engineering*, **186**:34-41. https://doi.org/10.1016/j.jfoodeng.2016.04.008

Alonso, R., Grant, G., Dewey, P., & Marzo, F. 2000. Nutritional assessment in vitro and in vivo of raw and extruded peas (*Pisum sativum* L.). *Journal of Agricultural and Food Chemistry*, **48**:2286-2290. https://doi.org/10.1021/jf000095o

Aluko, R.E., Mofolasayo, O.A., & Watts, B.M. (2009). Emulsifying and foaming properties of commercial yellow pea (Pisum sativum L.) seed flours. *Journal of Agricultural and Food Chemistry*, **57**:9793–9800. https://doi.org/10.1021/jf902199x

Ambigaipalan, P., Hoover, R., Donner, E., & Liu, Q. (2013). Retrogradation characteristics of pulse starches. *Food Research International*, **54**:203-212. http://dx.doi.org/10.1016/j.foodres.2013.06.012

Ambigaipalan, P., Hoover, R., Donner, E., Liu, Q., Jaiswal, S., Chibbar, R., Nantanga, K. K. M., & Seetharaman, K. (2011). Structure of faba bean, black bean and pinto bean starches at different levels of granule organization and their physicochemical properties. *Food Research International*, **44**:2962-2974. https://doi.org/10.1016/j.foodres.2011.07.006

Anderson, E. T., & Berry, B. W. (2001). Identification of nonmeat ingredients for increasing fat holding capacity during heating of ground beef. *Journal of Food Quality*, **24**:291–299. https://doi.org/10.1111/j.1745-4557.2001.tb00610.x

Anderson, E. T., & Berry, B. W. (2000). Sensory, shear, and cooking properties of lower-fat beef patties made with inner pea fiber. *Journal of Food Science*, **65:**805–810. https://doi.org/10.1111/j.1365-2621.2000.tb13591.x

Ashokkumar, K., Diapari, M., Jha, A. B., Tar'an, B., Arganosa, G., & Warkentin, T. D. (2015). Genetic diversity of nutritionally important carotenoids in 94 pea and 121 chickpea accessions. *Journal of Food Composition and Analysis*, **43**:49-60. http://dx.doi.org/10.1016/j.jfca.2015.04.014

Bellaio, S., Kappeler, S., Zamprogna-Rosenfeld, E., & Jacobs, M. (2013). Partially germinated ingredients for naturally healthy and tasty products. *Cereal Foods World*, **58**:55-59. http://dx.doi.org/10.1094/CFW-58-2-0055

Berrios, J. De J., Morales, P., Camara, M., & Sanchez-Mata, M. C. (2010). Carbohydrate composition of raw and extruded pulse flours. *Food Research International*, **43**:531-536. https://doi.org/10.1016/j.foodres.2009.09.035

Biliaderis, C. G., Grant, D. R., & Vose, J. R. (1979). Molecular weight distributions of legume starches by gel chromatography. *Cereal Chemistry*, **56**:475-480.

Biliaderis, C. G., Grant, D. R., & Vose, J. R. (1981). Structural characterization of legume starches. I. Studies on amylose, amylopectin, and beta-limit dextrins. *Cereal Chemistry*, **58**:496-502.

Boye, J. I., Aksay, S., Roufik, S., Ribereau, S., Mondor, M., Farnworth, E., & Rajamohamed, S. H. (2010). Comparison of the functional properties of pea, chickpea and lentil protein concentrates processed using ultrafiltration and isoelectric precipitation techniques. *Food Research International*, **43**:537-546. https://doi.org/10.1016/j.foodres.2009.07.021

Boye, J., Zare, F., & Pletch, A. (2010). Pulse proteins: processing, characterization, functional properties and applications in food and feed. *Food Research International*, **43**:414-431. https://doi.org/10.1016/j.foodres.2009.09.003

Braudo, E. E., Plashchina, I. G., & Schwenke, K. D. (2001). Plant protein interactions with polysaccharides and their influence on legume protein functionality. *Nahrung/Food*, **45**:382–384. https://doi.org/10.1002/1521-3803(20011001)45:6<382::AID-FOOD382>3.0.CO;2-W

Brummer, Y., Kaviani, M., & Tosh, S. M. (2015). Structural and functional characteristics of dietary fibre in beans, lentils, peas and chickpeas. *Food Research International*, **67**:117-125. https://doi.org/10.1016/j.foodres.2014.11.009

Camacho, L., Sierra, C., Campos, R. R., Guzman, E. C., & Marcus, D. W. (1992). Cambios nutricionales inducidos por la germinacion de leguminosas de consume habitual en Chile. *Archivos Latino Americanos de Nutricion*, **42**:283-290.

Chakraborty, P., Sosulski, F., & Bose, A. (1979). Ultracentrifugation of salt-soluble proteins in ten legume species. *Journal of the Science of Food and Agriculture*, **30**:766-771.

Chibbar, R. N., Ambigaipalan, P., & Hoover, R. (2010). Molecular diversity in pulse seed starch and complex carbohydrates and its role in human nutrition and health. *Cereal Chemistry*, **87**:342-352. https://doi.org/10.1094/CCHEM-87-4-0342

Chung, H. -J., Liu, Q., Donner, E., Hoover, R., Warkentin, T. D., & Vandenberg, B. (2008). Composition, molecular structure, properties, and in vitro digestibility of starches from newly released Canadian pulse cultivars. *Cereal Chemistry*, **85**:471-479. https://doi.org/10.1094/CCHEM-85-4-0471

Dagorn-Scaviner, C., Gueguen, J., & Lefebvre, J. (1987). Emulsifying properties of pea globulins as related to their absorption behaviours. *Journal of Food Science*, **52**:335–341. https://doi.org/10.1111/j.1365-2621.1987.tb06607.x

Dahl, W. J., Foster, L. M., & Tyler, R. T. (2012). Review of the health benefits of peas (*Pisum sativum* L.). *British Journal of Nutrition*, **108**:S3-S10. https://doi.org/10.1017/S0007114512000852

Dalgetty, D. D., & Baik, B. B. (2003). Isolation and characterization of cotyledon fibers from peas, lentils, and chickpeas. *Cereal Chemistry*, **80**:310-315. https://doi.org/10.1094/CCHEM.2003.80.3.310

Delcour, J. A., & Hoseney, R. C. (2010). *Principles of Cereal Science and Technology*, 3rd ed. St Paul, MN: AACC International, Inc. https://doi.org/10.1094/9781891127632

Dijkink, B. H., & Langelaan, H. C. (2002a). Milling properties of peas in relation to texture analysis. Part I. Effect of moisture content. *Journal of Food Engineering*, **51**:99-104.

Dijkink, B. H., & Langelaan, H. C. (2002b). Milling properties of peas in relation to texture analysis. Part II. Effect of pea genotype. *Journal of Food Engineering*, **51**:105-111.

Dominguez-Arispuro, D. M., Cuevas-Rodriguez, E. O., Milan-Carrillo, J., Leon-Lopez, L., Gutierrez-Dorado, R., & Reyes-Moreno, C. (2018). Optimal germination condition impacts on the antioxidant activity and phenolic acids profile in pigmented desi chickpea (*Cicer arietinum* L.) seeds. *Journal of Food Science and Technology*, **55:**638-647**.** https://doi.org/10.1007/s13197-017-2973-1

El-Saied, H. M., Amer, M. M. A., & Gabran, A. (1981). Unsaponifiable matter and fatty acid composition of pea oil. *Zeitschrift für Ernährungswissenschaft*, **20**:132-138.

Erkinbaev, C., Derksen, K., & Paliwal, J. (2017). Assessment of mung bean quality through single kernel characterization. *Food and Bioprocess Technology*, **10**:2156-2164. https://doi.org/10.1007/s11947-017-1977-1

ERS (Economic Research Service of the United States Department of Agriculture). (2010). Data products: Vegetables and pulses data, by commodity—dry peas. Retrieved on 02/25/2019 from https://www.ers.usda.gov/data-products/vegetables-and-pulses-data/by-commodity.aspx

FAO (Food and Agriculture Organization of the United Nations). (2017a). Production: crops. Retrieved on 02/25/2019 from http://www.fao.org/faostat/en/#data/QC

FAO (Food and Agriculture Organization of the United Nations). (2017b). Trade: crops and livestock products. Retrieved on 02/25/2019 from http://www.fao.org/faostat/en/#data/TP

Fernandez-Quintela, A., Macarulla, M. T., Del Barrio, A. S., & Martinez, J. A. (1997). Composition and functional properties of protein isolates obtained from commercial legumes grown in northern Spain. *Plant Foods for Human Nutrition*, **51**:331–342. https://doi.org/10.1023/A:1007936930354

FGIS. (2009). *United States Standards for Split Peas*. Washington, DC: USDA.

Fuhrmeister, H., & Meuser, F. (2003). Impact of processing on functional properties of protein products from wrinkled peas. *Journal of Food Engineering*, **56**:119–129. https://doi.org/10.1016/S0260-8774(02)00241-8

Gawalko, E., Garrett, R. G., Warkentin, T., Wang, N., & Richter, A. (2009). Trace elements in Canadian field peas: a grain safety assurance perspective. *Food Additives and Contaminants*, **26**:1002-1012. https://doi.org/10.1080/02652030902894389

Gomez, M., Doyague, M. J., & de la Hera, E. (2012). Addition of pin-milled pea flour and air-classified fractions in layer and sponge cakes. *LWT – Food Science and Technology*, **46**:142-147. https://doi.org/10.1016/j.lwt.2011.10.014

Hall, C., Hillen, C., & Garden-Robinson, J. (2017). Composition, nutritional value, and health benefits of pulses. *Cereal Chemistry*, **94**:11-31. https://doi.org/10.1094/CCHEM-03-16-0069-FI

Han, J. -Y., & Tyler, R. T. (2003). Determination of folate concentrations in pulses by a microbiological method employing trienzyme extraction. *Journal of Agricultural and Food Chemistry*, **51**:5315-5318. https://doi.org/10.1021/jf0211027

Harden, S., & Wood, J. A. (2017). A single parameter for within-sample uniformity of seed size in grain, with an emphasis on pulses. *Cereal Chemistry*, **93**:430-436. http://dx.doi.org/10.1094/CCHEM-04-16-0121-R

Hillen, C. E. (2016). *Sensory and quality attributes of deodorized pea flour used in gluten-free food products*. Master's thesis. Fargo, ND: North Dakota State University.

Hood-Niefer, S. D., Warkentin, T. D., Chibbar, R. N., Vandenberg, A., & Tyler, R. T. (2011). Effect of genotype and environment on the concentrations of starch and protein in, and the physicochemical properties of starch from, field pea and fababean. *Journal of the Science of Food and Agriculture*, **92**:141-150.

Hoover, R., Hughes, T., Chung, H. J., & Liu, Q. (2010). Composition, molecular structure, properties, and modification of pulse starches: a review. *Food Research International*, **43**:399-413. https://doi.org/10.1016/j.foodres.2009.09.001

Hoover, R., & Ratnayake, W. S. (2002). Starch characteristics of black bean, chick pea, lentil, navy bean and pinto bean cultivars grown in Canada. *Food Chemistry*, **78**:489-498. https://doi.org/10.1016/S0308-8146(02)00163-2

Izydorczyk, M., & Kletke, J. 2016. Milling for quality evaluation of new wheat lines. *Canadian Grain Commission*, Grain Research Laboratory technical report. Available from: https://www.grainscanada.gc.ca/research-recherche/izydorczyk/cwmgrl-lrgmbc/cwmgrl-lrgmbc-en.htm

Kerr, W. L., Ward, C. D. W, McWatters, K. H., & Resurreccion, A. V. A. (2000). Effect of milling and particle size on functionality and physicochemical properties of cowpea flour. *Cereal Chemistry*, **77**:213-219.

Kongseree, N., & Juliano, B. O. (1972). Physicochemical properties of rice grain and starch from lines differing in amylose content and gelatinization temperature. *Journal of Agricultural and Food Chemistry*, **20**:714-718.

Lam, A. C. Y., Karaca, A. C., Tyler, R. T., & Nickerson, M. T. (2018). Pea protein isolates: structure, extraction, and functionality. *Food Reviews International*, **34**:126-147. http://dx.doi.org/10.1080/87559129.2016.1242135

Le Gall, M., Gueguen, J., Seve, J., & Quillien, L. (2005). Effects of grinding and thermal treatments on hydrolysis susceptibility of pea proteins (Pisum sativum L.) *Journal of Agricultural and Food Chemistry*, **53**:3057-3064. https://doi.org/10.1021/jf040314w

Li, D., & Zhu, F. (2017). Physicochemical properties of kiwifruit starch. *Food Chemistry*, **220**:129-136. https://doi.org/10.1016/j.foodchem.2016.09.192

Liang, H.-N., & Tang, C.-H. (2013). pH-dependent emulsifying properties of pea [Pisum sativum (L.)] proteins. *Food Hydrocolloids*, **33**:309–319. https://doi.org/10.1016/j.foodhyd.2013.04.005

Ma, Z., Boye, J. I., Azarnia, S., & Simpson, B. K. (2016). Volatile flavor profile of Saskatchewan grown pulses as affected by different thermal processing treatments. *International Jounral of Food Properties*, **19**:2251-2271. https://doi.org/10.1080/10942912.2015.1121494

Ma, Z., Boye, J. I., & Hu, X. (2017). *In vitro* digestibility, protein composition and techno-functional properties of Saskatchewan grown yellow field peas (*Pisum sativum* L.) as affected by processing. *Food Research International*, **92**:64-78. https://doi.org/10.1016/j.foodres.2016.12.012

Malcolmson, L., Frohlich, P. Boux, G., Bellido, A. -S., Boye, J., & Warkentin, T. D. (2014). Aroma and flavor properties of Saskatchewan grown field peas (*Pisum sativum* L.). *Canadian Journal of Plant Science*, **94**:1419-1426. https://doi.org/10.4141/CJPS-2014-120

Marles, M. A. S., Warkentin, T. D., & Bett, K. E. (2012). Genotypic abundance of carotenoids and polyphenolics in the hull of field pea (*Pisum sativum* L.). *Journal of the Science of Food and Agriculture*, **93**:463-470. https://doi.org/10.1002/jsfa.5782

Maskus, H., Bourre, L., Fraser, S., Sarkar, A., & Malcolmson, L. (2016). Effects of grinding method on the compositional, physical and functional properties of whole and split yellow pea flour. *Cereal Foods World*, **61**:59-64. https://doi.org/10.1094/CFW-61-2-0059

Mession, J., Chihi, M.L., Sok, N., & Saurel, R. (2015). Effect of globular pea proteins fractionation on their heat-induced aggregation and acid cold-set gelation. *Food Hydrocolloids*, **46**:233−243. https://doi.org/10.1016/j.foodhyd.2014.11.025

Miller, B. S., Afework, W., Hughes, J. W., & Pomeranz, Y. (1981). Wheat hardness: time to grind wheat with the Brabender automatic microhardness tester. *Journal of Food Science*, **46**:1863-1865. https://doi.org/10.1111/j.1365-2621.1981.tb04505.x

Miller, B. S., Afework, S., Pomeranz, Y., Bruinsma, B. L., & Booth, G. (1982). Measuring the hardness of wheat. *Cereal Foods World*, **27**:61-64.

Mohammed, I., Ahmed, A. R., & Senge, A. B. (2014). Effect of chickpea flour on wheat pasting properties and bread making quality. *Journal of Food Science and Technology*, **51**:1902-1910. https://doi.org/10.1007/s13197-012-0733-9

NASS (National Agricultural Statistics Service of the United States Department of Agriculture). (2017). Quick Stats. Retrieved on 02/25/2019 from https://quickstats.nass.usda.gov/

NASS (National Agricultural Statistics Service of the United States Department of Agriculture). (2016). Crop production 2015 summary. Retrieved on 02/25/2019 from https://www.usda.gov/nass/PUBS/TODAYRPT/cropan16.pdf

Nosworthy, M. G., Neufeld, J., Frohlich, P., Young, G., Malcolmson, L., & House, J. D. (2017). Determination of the protein quality of cooked Canadian pulses. *Food Science and Nutrition*, **5**:896-903. https://doi.org/10.1002/fsn3.473

Otto, T., Baik, B. K., & Czuchajowska, Z. (1997). Microstructure of seeds, flours, and starches of legumes. *Cereal Chemistry*, **74**:445-451.

Padhi, E. M. T., Liu, R., Hernandez, M., Tsao, R., & Ramdath, D. D. (2017). Total polyphenol content, carotenoid, tocopherol and fatty acid composition of commonly consumed Canadian pulses and their contribution to antioxidant activity. *Journal of Functional Foods*, **38**:602-611. http://dx.doi.org/10.1016/j.jff.2016.11.006

Park, S. J., Kim, T. W., & Baik, B. K. (2010). Relationship between proportion and composition of albumins, and *in vitro* protein digestibility of raw and cooked pea seeds (*Pisum sativum* L.). *Journal of the Science of Food and Agriculture*, **90**:1719-1725. https://doi.org/10.1002/jsfa.4007

Patterson, C. A., Curran, J., & Der, T. (2017). Effect of processing on antinutrient compounds in pulses. *Cereal Chemistry*, **94**:2-10. http://dx.doi.org/10.1094/CCHEM-05-16-0144-FI

Pavek, P. L. S. (2012). *Plant guide for pea* (*Pisum sativum* L.). Pullman, WA: USDA-Natural Resources Conservation Service.

Pelgrom, P. J. M., Boom, R. M., & Schutyser, M. A. I. (2015). Method development to increase protein enrichment during dry fractionation of starch-rich legumes. *Food and Bioprocess Technology*, **8**:1495-1502. https://doi.org/10.1007/s11947-015-1513-0

Pelgrom, P. J. M., Schutyser, M. A. I., & Boom, R. M. (2013). Thermomechanical morphology of peas and its relation to fracture behavior. *Food and Bioprocess Technology*, **6**:3317-3325. https://doi.org/10.1007/s11947-012-1031-2

Pomeranz, Y., Czuchajowska, Z., Martin, C. R., & Lai, F. S. (1985). Determination of corn hardness by the stenvert hardness tester. *Cereal Chemistry*, **62**:108-112.

Raghunathan, R., Hoover, R., Waduge, R., Liu, Q., & Warkentin, T. D. (2017). Impact of molecular structure on the physicochemical properties of starches isolated from different field pea (*Pisum sativum* L.) cultivars grown in Saskatchewan, Canada. *Food Chemistry*, **221**:1514-1521. http://dx.doi.org/10.1016/j.foodchem.2016.10.142

Ratnayake, W. S., Hoover, R., Shahidi, F., Perera, C., & Jane, J. (2001). Composition, molecular structure, and physicochemical properties of starches from four field pea (*Pisum sativum* L.) cultivars. *Food Chemistry*, **74**:189-202. https://doi.org/10.1016/S0308-8146(01)00124-8

Ray, H., Bett, K., Tar'an, B., Vandenberg, A., Thavarajah, D., & Warkentin, T. (2014). Mineral micronutrient content of cultivars of field pea, chickpea, common bean, and lentil grown in Saskatchewan, Canada. *Crop Science*, **54**:1698-1708. https://doi.org/10.2135/cropsci2013.08.0568

Roland, W. S. U., Pouvreau, L., Curran, J., van de Velde, F., & de Kok, P. M. T. (2017). Flavor aspects of pulse ingredients. *Cereal Chemistry*, **94**:58-65. https://doi.org/10.1094/CCHEM-06-16-0161-FI

Rubio, L. A., Perez, A., Ruiz, R., Guzman, M. A., Aranda-Olmedo, I., & Clemente, A. (2013). Characterization of pea (*Pisum sativum*) seed protein fractions. *Journal of the Science of Food and Agriculture*, **94**:280-287. https://doi.org/10.1002/jsfa.6250

Ryan, E., Galvin, K., O'Connor, T. P., Maguire, A. R., & O'Brien, N. M. (2007). Phytosterol, Squalene, Tocopherol Content and Fatty Acid Profile of Selected Seeds, Grains, and Legumes. *Plant Foods for Human Nutrition*, **62**:85-91. https://doi.org/10.1007/s11130-007-0046-8

Scanlon, M. G., Thakur, S., Tyler, R. T., Milani, A., Der, T., & Paliwal, J. (2018). The critical role of milling in pulse ingredient functionality. *Cereal Foods World*, **63**:201-206. http://dx.doi.org/10.1094/CCHEM-04-16-0121-R

Schindler, S., Zelena, K., Krings, U., Bez, J., Eisner, P., & Berger, R. G. (2012). Improvement of the aroma of pea (*Pisum sativum*) protein extracts by lactic acid fermentation. *Food Biotechnology*, **26**:58-74. https://doi.org/10.1080/08905436.2011.645939

Shevkani, K., Singh, N., Kaur, A., & Rana, J.C. (2015). Structural and functional characterization of kidney bean and field pea protein isolates: A comparative study. *Food Hydrocolloids*, **43**:679–689. https://doi.org/10.1016/j.foodhyd.2014.07.024

Simsek, S., Tulbek, M. C., Yao, Y., & Schatz, B. (2009). Starch characteristics of dry peas (*Pisum sativum* L.) grown in the USA. *Food Chemistry*, **115**:832-838. https://doi.org/10.1016/j.foodchem.2008.12.093

Singh, N., Nakaura, Y., Inouchi, N., & Nishinari, K. (2008). Structure and viscoelastic properties of starches separated from different legumes. *Starch/Starke*, **60**:349-357. https://doi.org/10.1002/star.200800689

Singh, B., Singh, J. P., Kaur, A., & Singh, N. (2017a). Phenolic composition and antioxidant potential of grain legume seeds: a review. *Food Research International*, **101**:1-16. http://dx.doi.org/10.1016/j.foodres.2017.09.026

Singh, R., Singh, K. K., & Kotwaliwale, N. (2012). Study on disinfestation of pulses using microwave technique. *Journal of Food Science and Technology*, **49**:505-509. https://doi.org/10.1007/s13197-011-0296-1

Singh, B., Singh, J. P., Singh, N., & Kaur, A. (2017b). Saponins in pulses and their health promoting activities: a review. *Food Chemistry*, **233**:540-549. http://dx.doi.org/10.1016/j.foodchem.2017.04.161

Solis, M. I. V., Patel, A., Orsat, V., Singh, J., & Lefsrud, M. (2013). Fatty acid profiling of the seed oils of some varieties of field peas (*Pisum sativum*) by RP-LC/ESI-MS/MS: Towards the development of an oilseed pea. *Food Chemistry*, **139**:986-993. https://doi.org/10.1016/j.foodchem.2012.12.052

Sozer, N., Holopainen-Mantila, U., & Poutanen, K. (2017). Traditional and new food uses of pulses. *Cereal Chemistry*, **94**:66-73. http://dx.doi.org/10.1094/CCHEM-04-16-0082-FI

Stone, A.K., Avramenko, N.A., Warkentin, T.D., & Nickerson, M.T. (2015). Functional properties of protein isolates from different pea cultivars. *Food Science and Biotechnology*, **24**:827–833. https://doi.org/10.1007/s10068-015-0107-y

Stone, A.K., Karalash, A., Tyler, R.T., Warkentin, T.D., & Nickerson, M.T. (2015). Functional attributes of pea protein isolates prepared using different extraction methods and cultivars. *Food Research International*, **76**:31–38. https://doi.org/10.1016/j.foodres.2014.11.017

Stoughton-Ens, M. D., Hatcher, D. W., Wang, N., & Warkentin, T. D. (2010). Influence of genotype and environment on the dietary fiber content of field pea (*Pisum sativum* L.) grown in Canada. *Food Research International*, **43**:547-552. https://doi.org/10.1016/j.foodres.2009.07.011

Sun, Q., Li, G., Dai, L., Ji, N., & Xiong, L. (2014). Green preparation and characterization of waxy maize starch nanoparticles through enzymolysis and recrystallization. *Food Chemistry*, **162**:223-228. http://dx.doi.org/10.1016/j.foodchem.2014.04.068

Taherian, A.R., Mondor, M., Labranche, J., Drolet, H., Ippersiel, D., & Lamarche, F. (2011). Comparative study of functional properties of commercial and membrane processed yellow pea protein isolates. *Food Research International*, **44**:2505–2514. https://doi.org/10.1016/j.foodres.2011.01.030

Thakur, S., Scanlon, M. G., Tyler, R. T., Milani, A., & Paliwal, J. (2019). A comprehensive review of pulse flour characteristics from a wheat flour miller's perspective. *Comprehensive Reviews in Food Science and Food Safety*, in press.

Tosh, S. M., & Yada, S. (2010). Dietary fibres in pulse seeds and fractions: characterization, functional attributes, and applications. *Food Research International*, **43**:450-460. https://doi.org/10.1016/j.foodres.2009.09.005

Tsoukala, A., Papalamprou, E., Mari, E., Doxatakis, G., & Braudo, E.E. (2006). Absorption at the air-water interface and emulsification properties of grain legume protein derivatives from pea and broad bean. *Colloids and Surfactants B*, **53**:203–208. https://doi.org/10.1016/j.colsurfb.2006.08.019

Tyler, R. T. (1984). Impact milling quality of grain legumes. *Journal of Food Science*, **49**:925-930. https://doi.org/10.1111/j.1365-2621.1984.tb13243.x

U.S. Dry Pea & Lentil Council. (2017). *2017 U.S. Pulse Quality Survey*. Moscow, ID: U.S. Dry Pea and Lentil Council.

U.S. Dry Pea & Lentil Council. (2016). *USA Pulses Technical Manual*. Moscow, ID: U.S. Dry Pea and Lentil Council.

Vishwakarma, R. K., Shivhare, U. S., Gupta, R. K., Yadav, D. N., Jaiswal, A., & Prasad, P. (2018). Status of pulse milling processes and technologies: a review. *Critical Reviews in Food Science and Nutrition*, **58**:1615-1628. https://doi.org/10.1080/10408398.2016.1274956

Wang, N., Hatcher, D. W., & Gawalko, E. J. (2008). Effect of variety and processing on nutrients and certain anti-nutrients in field peas (*Pisum sativum*). *Food Chemistry*, **111**:132-138. https://doi.org/10.1016/j.foodchem.2008.03.047

Wang, N., & Toews, R. (2011). Certain physicochemical and functional properties of fibre fractions from pulses. *Food Research International*, **44**:2515-2523. https://doi.org/10.1016/j.foodres.2011.03.012

Wood, J. A., Edmund, K. J., & Harden, S. (2008). Milling performance in desi-type chickpea (*Cicer arietinum* L.): Effects of genotype, environment and seed size. *Journal of the Science of Food and Agriculture*, **88**:108-115. https://doi.org/10.1002/jsfa.3053/

Xu, Y., Sismour, E. N., Narina, S. S., Dean, D., Bhardwaj, H. L., & Li, Z. (2013). Composition and properties of starches from Virginia-grown kabuli chickpea (*Cicer arietinum* L.) cultivars. *International Journal of Food Science & Technology*, **48**:539-547. https://doi.org/10.1111/j.1365-2621.2012.03217.x

Yalcin, I., Ozarslan, C., & Akbas, T. (2007). Physical properties of pea (*Pisum sativum*) seed. *Journal of Food Engineering*, **79**:731-735. https://doi.org/10.1016/j.jfoodeng.2006.02.039

Yoshida, H., Tomiyama, Y., Saiki, M., & Mizushina, Y. (2007a). Tocopherol Content and Fatty Acid Distribution of Peas (*Pisum sativum* L.). *Journal of the American Oil Chemists' Society*, **84**:1031-1038. https://doi.org/10.1007/s11746-007-1134-5

Yoshida, H., Tomiyama, Y., Tanaka, M., & Mizushina, Y. (2007b). Characteristic profiles of lipid classes, fatty acids and triacylglycerol molecular species of peas (*Pisum sativum* L.). *European Journal of Lipid Science and Technology*, **109**:600-607. https://doi.org/10.1002/ejlt.200600219

Yu, X., Yu, H., Zhang, J., Shao, S., Zhou, L., Xiong, F., & Wang, Z. (2015). Comparison of endosperm starch granule development and physicochemical properties of starches from waxy and non-waxy wheat. *International Journal of Food Properties*, **18**:2409-2421. https://doi.org/10.1080/10942912.2014.980949

Zhou, Y., Hoover, R., & Liu, Q. (2004). Relationship between α-amylase degradation and the structure and physicochemical properties of legume starches. *Carbohydrate Polymers*, **57**:299-317. https://doi.org/10.1016/j.carbpol.2004.05.010

Zhou, W., Yang, J., Hong, Y., Liu, G., Zheng, J., Gu, Z., & Zhang, P. (2015). Impact of amylose content on starch physicochemical properties in transgenic sweet potato. *Carbohydrate Polymers*, **122**:417-427. https://doi.org/10.1016/j.carbpol.2014.11.003

PAPER 1. PHYSICOCHEMICAL PROPERTIES OF HAMMER-MILLED YELLOW SPLIT PEA (*PISUM SATIVUM* L.)[1]

Based on the article of Kaiser, Barber, Manthey & Hall published in Cereal Chemistry online, December 2018 (https://doi.org/10.1002/cche.10127)

Abstract

Incorporating pulse flours into cereal-based foods is of interest due to demand for healthful convenience foods. A hammer mill is a simple and inexpensive machine that can facilitate pulse flour production when processing capacity is limited. The goal of this research was to evaluate relationships among hammer mill parameters, seed moisture, and pea flour quality that are not yet extensively described in the literature. Yellow split pea at 9 and 11 % moisture was hammer-milled at two rotor speeds (34 and 102 m/s) and with nine mill screen apertures (0.84 to 9.53 mm). Although reduction in flour moisture and protein was observed following milling, flour composition differences appeared to be due to the drying process rather than to milling. Median particle size was lowest (98 μm) and peak and final viscosities highest (2,108 and 4,240 cP, respectively) when milling at 102 m/s rotor speed with 0.84 mm screen aperture. Flour particle size was negatively related to bulk density, redness, yellowness, and pasting properties and positively correlated with brightness. Damaged starch ranged from 0.1-1.4 % and was highest at 102 m/s rotor speed and small screen aperture. Results indicated that

[1] The material in this chapter was co-authored by Amber Kaiser, Natsuki Barber, Frank Manthey, and Clifford Hall. Amber Kaiser had primary responsibility for data collection and analysis, was the primary developer of the conclusions advanced here, and drafted and revised all versions of this chapter. Natsuki Barber assisted with sample processing and data collection. Frank Manthey assisted with the experimental design. Clifford Hall served as proofreader.

seed moisture and hammer mill settings are important parameters in particle size reduction of yellow split pea and that particle size is a predictor of flour functional quality.

Introduction

Pulses such as field pea (*Pisum sativum* L.) contain several nutrients that are associated with health benefits, including high protein, low lipid, and high dietary fiber contents, a high amylose-to-amylopectin ratio, and high antioxidant content (Dahl, Foster & Tyler, 2012; Hall, Hillen & Garden-Robinson, 2017). Blending pulse ingredients into cereal-based products has the potential to improve nutritional profile. The amino acid profiles of pulse and cereal protein can complement each other. For example, wheat is relatively low in lysine and high in sulfur-containing amino acids (i.e. methionine and cysteine) while pulses are rich in lysine but tend to be low in methionine and cysteine (Hall et al., 2017).

Milling is a major unit operation in the preparation of field pea for inclusion in most processed foods (Wood, Knights & Choct, 2017). Milling is a particle size reduction process that can increase bioavailability of nutrients and modify functional properties of macromolecules. Mill selection and configuration determine the type (impact, compression, shear, or attrition) and intensity of the forces applied to a material. The applied force determines the properties of the ground product such as particle size, shape, and distribution, and amount of starch damaged during size reduction (Li, Dhital & Hasjim, 2014; Tran, Shelat, Tang, Li, Gilbert & Hasjim, 2011). Heat generation during the milling process is dependent on sample characteristics and mill configuration and can also contribute to some flour properties such as starch damage, protein structural integrity, and lipid quality (Ngamnikom & Songsermpong, 2011; Prabhasankar & Rao, 2001).

Flour properties affected by milling method are important to flour application. The shape and size of flour particles affects the interaction of flour with the environment, impacting blending and surface-active properties such as solubility, emulsifying, and foaming. Flour particle properties also affect the texture of end-use products. Starch damage (i.e. disruption of starch granule structure) and breakdown of amylopectin molecules can impact starch pasting properties (Li et al., 2014) as well as starch digestibility (Ngamnikom & Songsermpong, 2011). Since both particle size and starch damage are important factors affecting flour functionality, milling method must be appropriate to achieve the desired flour quality.

Milling procedure has been well established for some commodities such as wheat. However, excluding fractionation of protein and starch, pulse milling for food application is a relatively new area of research and there are currently no standardized milling procedures for field pea. The hammer mill, a type of impact mill, is a relatively simple size reduction method that requires little operator training and is inexpensive compared to some other milling methods. It uses rapidly rotating blades within a milling chamber to reduce material particle size via impact against the blades, milling chamber walls, and other seed particles. Particles are retained until small enough to pass through screen apertures at the chamber base. Previous comparisons have been made among the quality of whole and split pea flours produced with hammer, disc, pin, stone, and roller mills (Indira & Bhattacharya, 2006; Nguyen, Gidley & Sopade, 2015; Maskus, Bourre, Fraser, Sarkar & Malcolmson, 2016). However, there is limited information available regarding hammer mill parameters for pulse milling.

In addition to the mill type and configuration, moisture of raw materials affects energy input during milling and resultant flour properties. Pelgrom, Shutyser & Boom (2013) reported brittle fracture behavior of glassy pea (below ~13 % moisture) compared to rubbery pea (above

~13 % moisture). Rubbery pea had more elastic fracture behavior than glassy pea, resulting in a higher energy input during size reduction. Furthermore, heat treatment that may accompany the drying process is known to affect not only moisture content and glass transition temperature but also starch properties. Heat treatment changes the microstructure of pulses, especially protein and starch, leading to disentanglement of these two macromolecules (Pelgrom et al., 2013).

Recent pulse milling research has included pin milling and air classification for fractionation purposes (Wu & Nichols, 2005), hammer and roller milling to investigate pea flour protein quality (Le Gall, Gueguen, Seve & Quillien, 2005), and a comparison of milling equipment (stone, hammer, roller, and pin) in the production of split and whole pea flour (Maskus et al., 2016). However, an in-depth exploration of the relationship between hammer mill parameters and split pea flour quality has not yet been reported. Since hammer milling could be a simple and cost-effective method of pea flour production, this investigation was conducted to fill this knowledge gap. The goal of this research was to quantify the effects of rotor speed, screen aperture size, and seed moisture on split pea flour physicochemical properties, with the hypothesis that each of these factors would be important to pea flour quality parameters.

Materials and Methods

Sample preparation and milling

Split yellow pea was obtained from AGT Foods USA (Minot, ND). Upon determination of initial moisture of 11 %, low-moisture split yellow pea was prepared in a custom-made laboratory-scale pasta dryer (Standard Industry, Fargo, ND) using the 12 h pasta drying cycle. Temperature was brought to 56 °C in the first hour, held at 56 °C for 3 h, brought up to 72 °C in 15 min, held at 72 °C for 6 h, then cooled to 30 °C in 2 h. Moisture of 9 % and 11 % represented typical middle and upper moisture values, respectively, of American-grown field pea (based on

6–11 % annual mean moisture from 2012 to 2017) (U.S. Dry Pea & Lentil Council, 2017). Samples (~1 kg) of both 9 and 11 % moisture samples were ground in a hammer mill (Model DASO6, Fitzpatrick, Elmhurst, IL) at a constant feed rate of 2.3 kg/min with 9 screen aperture sizes (round apertures of 0.84, 1.27, 1.65, 2.01, 2.77, 3.96, 4.75, 6.35, and 9.53 mm diameter) and at two hammer rotor speeds (34 and 102 m/s). Flour temperature immediately after milling was measured with an infrared laser thermometer and ranged from 18-27 °C. Milling combinations were completed in triplicate, resulting in a total of 108 samples. A commercially-available sample of raw split pea flour (AGT, Regina, SK, Canada) was also obtained and evaluated along with the hammer-milled sample for comparison.

Pea flour quality analysis

Moisture, protein, and ash contents were determined using AACC International Approved Methods 44-15.02, 46-30.01, and 08-01.01, respectively. A nitrogen conversion factor of 6.25 was used for protein determination. Color was measured with a chroma meter CR-410 (Minolta, Tokyo, Japan) using the granular material attachment to provide sample presentation consistency and was reported in CIE (L*, a*, and b*) color space. Bulk density was obtained using the loose bulk density method described in ASTM D7481-09 (ASTM International, 2009). In this method, 250 mL of flour was added, without tapping or shaking, to a graduated cylinder and the weight recorded. Particle size distribution curves and the D10, D50, and D90 were determined using a Mastersizer 3000 laser particle size analyzer (Malvern, Worcestershire, UK) with a dry powder dispersion unit. Flours produced at screen apertures of 6.350 and 9.525 mm were too coarse for particle size evaluation by this method and were omitted from the analysis. Small and large mean particle sizes were determined by evaluating the mean particle size above and below 67 μm, and small to large particle size ratio was calculated by dividing the volume of

particles below 67 µm by the volume of particles above 67 µm. Pasting properties were determined with a Rapid Visco Analyzer (RVA 4500, Perten Instruments, Springfield, IL) using AACC International Approved Method 61-02.01 with extension of the final hold time for 12 min. Damaged starch was estimated using the Megazyme starch damage assay kit (Megazyme, Inc., Bray, Ireland) following AACC International Approved Method 76-31.01.

Water activity data was collected with the Aqualab vapor sorption analyzer (Decagon Devices, Inc., Pullman, WA). The dynamic dewpoint isotherm (DDI) method was used to generate adsorption and desorption isotherms and to calculate the critical water activity (a_w^{crit}) of treatments milled at all combinations of 9 and 11 % moisture, 34 and 102 m/s rotor speed, and 0.84, 1.27, 1.65, 2.01, and 3.96 mm screen aperture). A a_w range of 0.1 to 0.9 and flow rate of 0.8 ml/min was used to generate desorption and resorption isotherms, and critical water activity was calculated based on resorption data. The assay was run in duplicate on each sample.

Statistical analysis

Milling treatments were randomly assigned to split pea in triplicate. Statistical analysis was performed with SAS 9.3 (SAS Institute, Inc., Cary, NC) (Appendix B). Model selection for flour quality variables was performed among the main effects, interaction effects, and non-linear transformations (reciprocal, square, and natural logarithm) of milling parameters. Due to the presence of multicollinearity among the predictors under consideration, least angle regression was used during model selection (Efron, Hastie, Johnstone & Tibshirani, 2004). Adjusted R^2, Mallow's C_p, and PRESS were used to assess model fits. When fit statistics were close for multiple models, the simplest model was selected. ANCOVA was performed on flour quality variables using the factors selected through model selection. *F*-tests were used to test the significance of each factor and factors with $p < 0.05$ were retained. This same sequence of model

selection and ANCOVA was used to develop models between particle size parameters and flour quality variables. For the critical a_w data, technical replicates were used as treatment replicates and ANOVA was performed using an additive model involving all three milling parameters.

Results and Discussion

Proximate analysis

Flour moisture was significantly related to the main effects of all three milling parameters (Table 1). Although flour moisture was higher when milled at 34 m/s rotor speed with larger screen aperture sizes, most of the flour moisture variation could be attributed to seed moisture (Figure 10). Samples milled at 9 % seed moisture had lower flour moisture (8.8 to 9.4 %) than that of samples milled at 11 % moisture (10.9 to 11.5 %). Previously, seed moisture was the most important factor in determining flour moisture (Khalid, Manthey & Simsek, 2017; Posner & Hibbs 2005). Grain is generally conditioned before milling to optimize flour moisture. The moisture of the commercial control (10.1 %) was within the range of observed sample moisture.

Seed moisture and rotor speed were significant predictors of pea flour protein content (Table 1). Protein content differences due to seed moisture were of greater practical significance than those due to rotor speed (Figure 11). Protein was higher in flours milled at 11 % moisture (24.9 to 25.9 %) than those milled at 9 % moisture (24.2 to 25.3 %) for all but two treatments. Reduction in crude nitrogen content of up to ~5% has been noted previously in pea flours exposed to heat treatments in the range of 100-200 °C for 1-20 min (Ma, Boye & Hu, 2017). The moderate intensity of the heat treatment in this study (72 °C) resulted in comparatively moderate changes in protein of up to ~1 %. Heat-induced loss of nitrogen may be due to formation of nitrogen-containing volatile compounds such as alkylated pyrazines and pyrrole. Protein in all hammer-milled samples (24.2-25.9 %) was higher than that of the commercial sample (18.8 %).

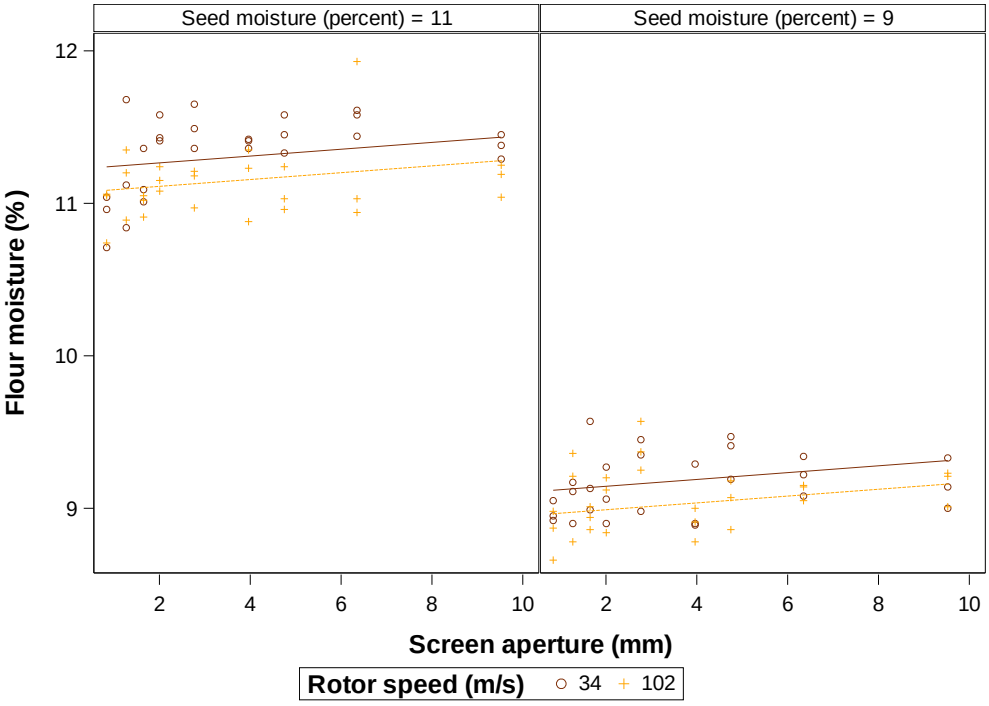

Figure 10. Split pea flour moisture versus hammer milling variables, with data points representing observed values and lines representing model prediction (R^2_{adj} = 0.961)

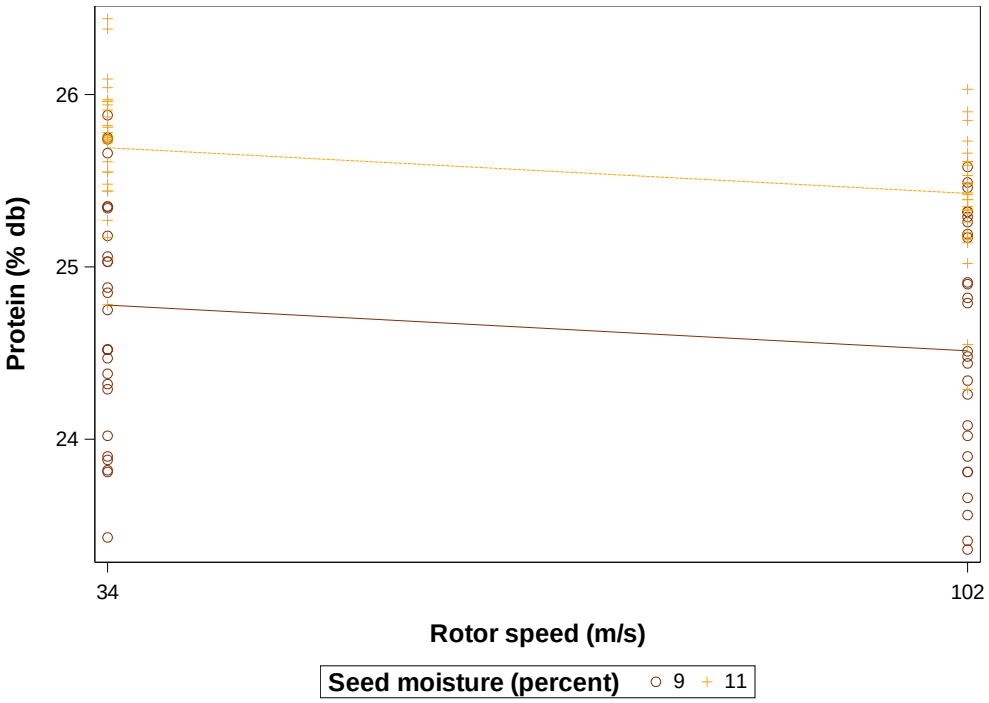

Figure 11. Split pea flour protein content versus hammer milling variables, with data points representing observed values and lines representing model prediction (R^2_{adj} = 0.425)

Table 1. *F*-test *p*-values from models of yellow split pea flour quality variables vs. hammer milling variables

Variable	Main effects			Transformations		Interactions involving rotor speed			Interactions involving seed moisture	
	Moisture	Speed	Screen	1/Screen	Ln(Screen)	Speed* Screen	Speed* 1/Screen	Speed* ln(Screen)	Speed* Moisture	1/Screen* Moisture
Protein	< 0.0001	0.0136								
Moisture	< 0.0001	0.0003	0.0047							
Brightness	< 0.0001	< 0.0001	0.0013	< 0.0001			< 0.0001		0.0032	
Redness	< 0.0001	< 0.0001		< 0.0001			< 0.0001		0.0003	0.0147
Yellowness	0.0097	0.0001		< 0.0001					0.0410	
Bulk density	0.0011	< 0.0001		< 0.0001						
Starch damage	< 0.0001	0.0003		< 0.0001						
Peak viscosity	0.0083	< 0.0001	< 0.0001	< 0.0001		< 0.0001	< 0.0001			
Breakdown viscosity		0.0037		< 0.0001						
Final viscosity		< 0.0001	< 0.0001	< 0.0001		< 0.0001	< 0.0001			
Pasting temperature	0.0012	< 0.0001	< 0.0001			< 0.0001				
D50		< 0.0001	< 0.0001	< 0.0001		0.0053	< 0.0001			
D90		< 0.0001	< 0.0001	< 0.0001			< 0.0001			
Large mean particle size		< 0.0001	< 0.0001	< 0.0001			< 0.0001			
Small:large particle ratio		< 0.0001		< 0.0001						
Small mean particle size	0.0005				< 0.0001					
Ln(D10)		0.2626			< 0.0001			< 0.0001		

Ash content was not related significantly to any of the design factors. Ash was higher in all samples (2.88-3.07 %) than in the commercial sample (2.57 %). It is possible that a sieving process during the production of the commercial sample is responsible for the differing protein and ash contents. Variability in pulse varieties and growing location might also contribute to differences in proximate content (Wang & Daun, 2004).

Particle size distribution

Six variables were used to represent the particle size distribution of milled split pea. The D10, D50, and D90 represent the 10^{th}, 50^{th}, and 90^{th} particle size percentiles by volume. In simple terms, 10 % of the particles in a sample are smaller than the D10, 50 % are smaller than the D50, and 90 % are smaller than the D90. Because particle size distributions were bimodal, the means of the small and large sub-distributions were also considered as predictor variables (Figure 12). The ratio of small particles to large particles in each sample was also considered. As mentioned previously, particle size analysis was not performed on samples produced using the 6.35 and 9.53 mm screen apertures due to equipment limitations.

Modelling the relationship between the D10 and milling parameters was complicated by inconsistent variation across different screen aperture sizes (Figure 13). Modelling with the natural log transformation of the D10 mediated this issue and resulted in a relatively high R^2_{adj}. Both rotor speed and the interaction between rotor speed and the natural log transformed screen aperture were significant predictors of the D10 (Table 1). At 102 m/s rotor speed, D10 did not change much across screen aperture sizes. The intense collisions resulting from 102 m/s rotor speed resulted in the production of a similar volume of small particles regardless of screen size. However, at low rotor speed the D10 increased in an exponential fashion with screen aperture. Because each collision was less intense, a greater number of collisions was required to generate

the same volume of small particles. This larger number of collisions was facilitated at smaller screen apertures. At the smallest screen size of 0.84 mm, the D10 was similar for both rotor speeds (Figure 13).

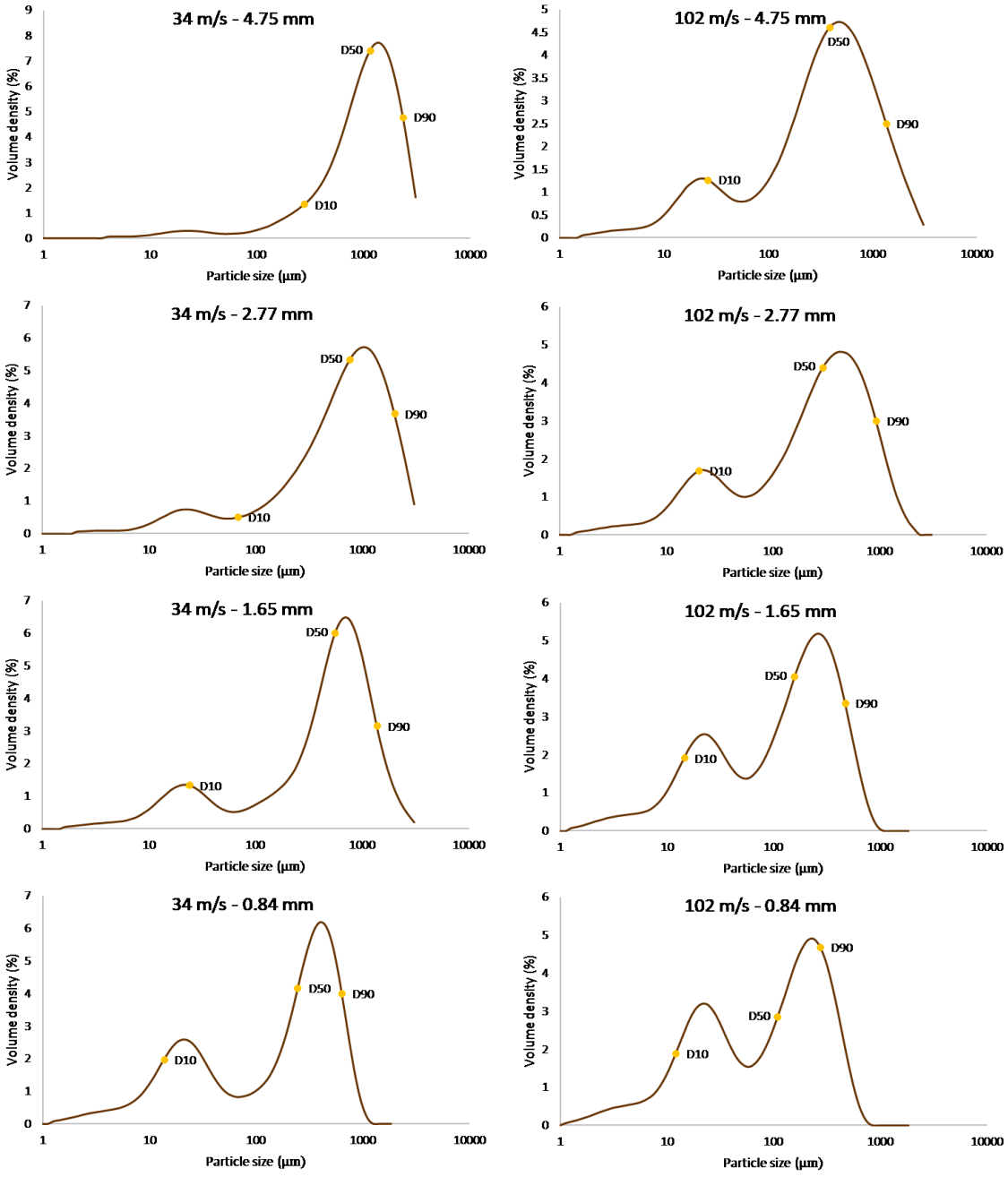

Figure 12. Particle size distributions of yellow split pea flour produced at different hammer mill settings (rotor speed and screen aperture size noted above each chart)

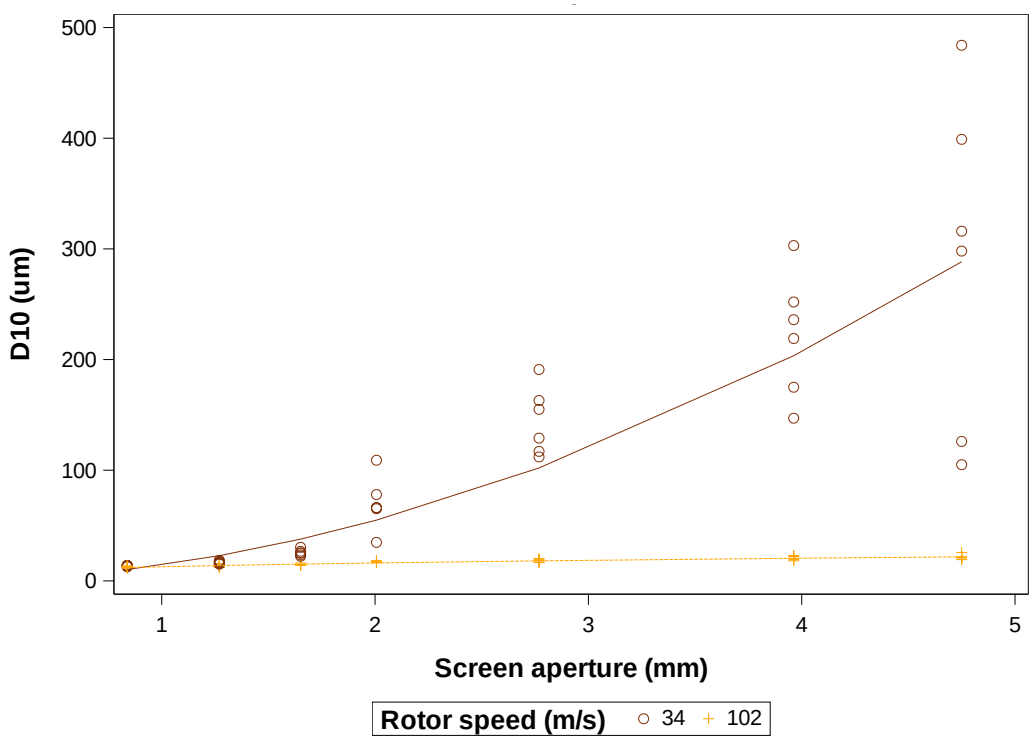

Figure 13. Split pea flour D10 values versus hammer milling variables, with data points representing observed values and lines representing model prediction (R^2_{adj} = 0.928)

The D50 was significantly related to rotor speed, screen aperture, and the reciprocal transformation of screen aperture (Table 1). Interactions between rotor speed and screen aperture and its transformation were also significant. As with the D10, screen aperture had a greater impact on the D50 at low rotor speed (Figure 14). Additionally, the D50 decreased sharply at very low screen apertures, but did not change as drastically between larger screen aperture sizes.

The D90 exhibited a similar relationship with mill parameters to that of the D50 (Figure 15). There was a significant relationship between the D90 and rotor speed, screen aperture, and the reciprocal transformation of screen aperture as well as significant interaction between rotor speed and the transformation of screen aperture (Table 1). The reciprocal relationship between the D90 and screen aperture at low rotor speed may be due partly to screen aperture approaching the size of some intact split peas at apertures of 3.96 mm and greater. U.S. grade #1 split pea can

have up to 3 % of the peas smaller than 3.97 mm (FGIS, 2009). Observed D90 values were very close to the maximum value permitted at a screen aperture of 2.01 mm. At screen apertures smaller than 2.01 mm, the D90 decreased more rapidly as small screen apertures forced the retention and size reduction of large particles within the milling chamber.

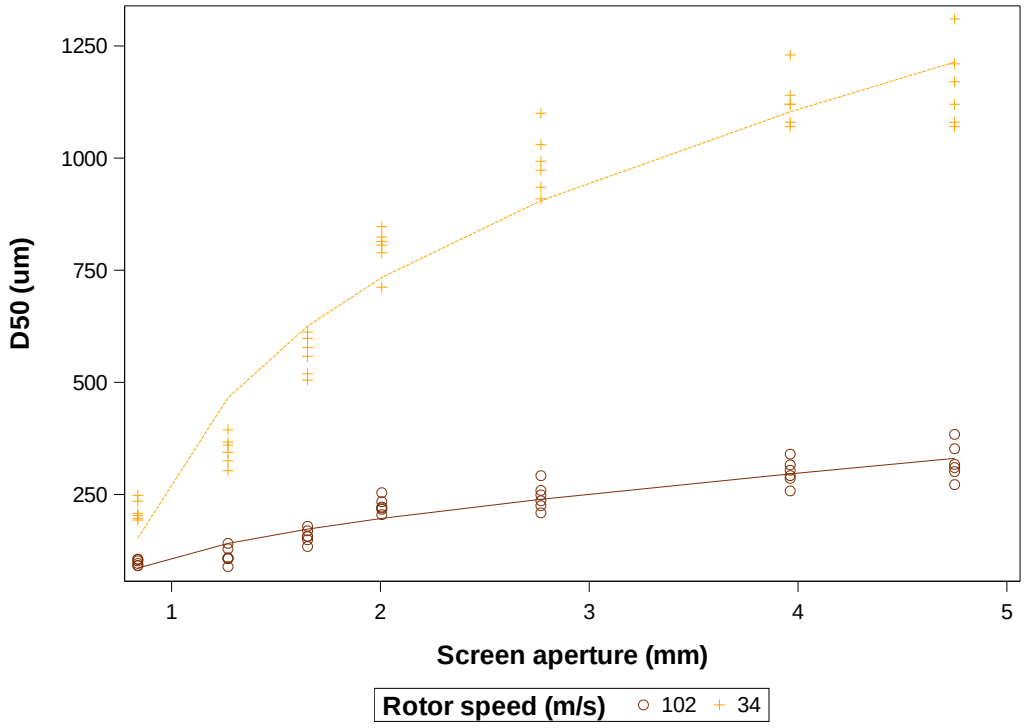

Figure 14. Split pea flour D50 values versus hammer milling variables, with data points representing observed values and lines representing model prediction (R^2_{adj} = 0.967)

Previous studies have reported that the D10, D50, and D90 of hammer-milled yellow split pea were 18, 249, and 559 µm, respectively, with a screen aperture size of 0.60 mm, while a screen aperture size of 1.19 mm resulted in D10, D50, and D90 vales of 256, 726, and 1,323 µm, respectively (Maskus, Bourre & Malcolmson, 2016; Maskus et al., 2016). Rotor speed in these studies was not specified, but the particle size distribution of the sample milled with the 0.60 mm screen aperture was comparable to results in this study at 34 m/s rotor speed and a slightly larger (0.84 mm) screen aperture size (14, 203, and 620 µm, respectively). The particle size distribution of the sample milled with the 1.19 mm screen aperture had a higher center and wider spread than

the results of the current study at 34 m/s and a similar (1.27 mm) screen aperture (16, 324, and 845 µm, respectively). Few studies have involved a variety of hammer mill rotor speeds in the size reduction of whole cereals, but in general higher rotor speeds result in smaller particle sizes (Mugabi, Eskridge & Weller, 2017). The median particle size of the commercial sample (31 µm) was lower and the width of the distribution narrower (D10 of 10 µm to D90 of 132 µm) than any hammer milled samples. Use of sieving or alternative milling equipment such as a pin mill could result in these differences in particle size (Maskus, Bourre & Malcolmson, 2016; Maskus et al., 2016).

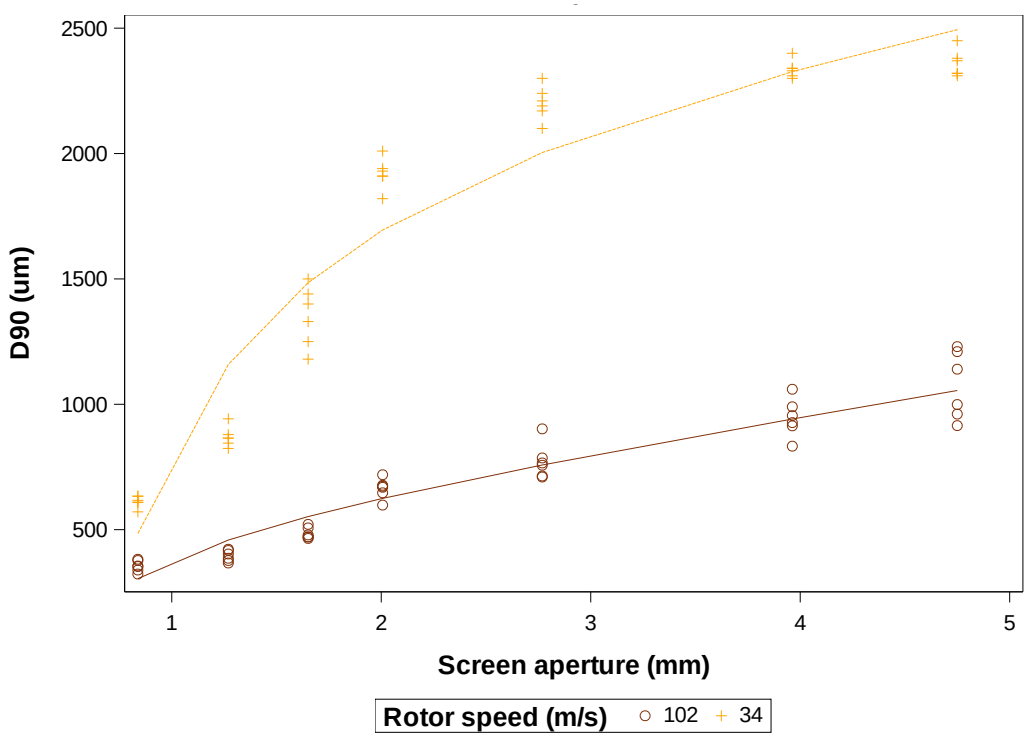

Figure 15. Split pea flour D90 values versus hammer milling variables, with data points representing observed values and lines representing model prediction (R^2_{adj} = 0.957)

Considering the particle size distribution of hammer-milled split pea as the combination of two bell-shaped sub-distributions has not been done extensively in the literature, although the bimodal shape of the hammer-milled particle size distribution has been noted previously (Maskus et al., 2016). From a bimodal perspective, the D10, D50, and D90 were not the best

representations of the distribution since they did not consistently represent the characteristics of these two sub-distributions. For example, when most particles lay within the larger sub-distribution (at mill settings of 34 m/s rotor speed and 4.75 mm screen aperture), the D50 was close to the mean of the larger sub-distribution (Figure 12). However, when particles were split more evenly between the two sub-distributions (at mill settings of 102 m/s rotor speed and 0.84 mm screen aperture), the D90 was much closer to the mean of the large sub-population. Therefore, the effects of milling parameters on the means of the small and large sub-distributions and the ratio of particles in the small sub-distribution to the large sub-distribution were also evaluated.

Small mean particle size was significantly related to seed moisture and the natural log of screen aperture (Table 1). Despite statistically significant differences, small mean particle sizes fell into a very small range (23-30 µm) compared to the range of observed D10 values (12-484 µm) (Figure 16). The similar small mean particle size can be seen in the particle size curves across milling treatments—while the area under the curve changed with milling treatment, the center location remained approximately the same (Figure 12). Mean large particle size, however, was both statistically and practically different across different rotor speeds and screen aperture sizes (Table 1). As with the D50 and D90, mean large particle size was related to the reciprocal of screen aperture, particularly at low rotor speed (Figure 17). Small to large particle ratio was also significantly related to rotor speed and the reciprocal of screen aperture (Table 1). While the D10 exhibited no practical differences across screen aperture at 102 m/s rotor speed (Figure 13), the small to large particle ratio did increase notably at small screen aperture and 102 m/s rotor speed (Figure 18). This result indicated that the volume of small particles did increase at 102 m/s rotor speed and small screen aperture, even though the D10 did not change much.

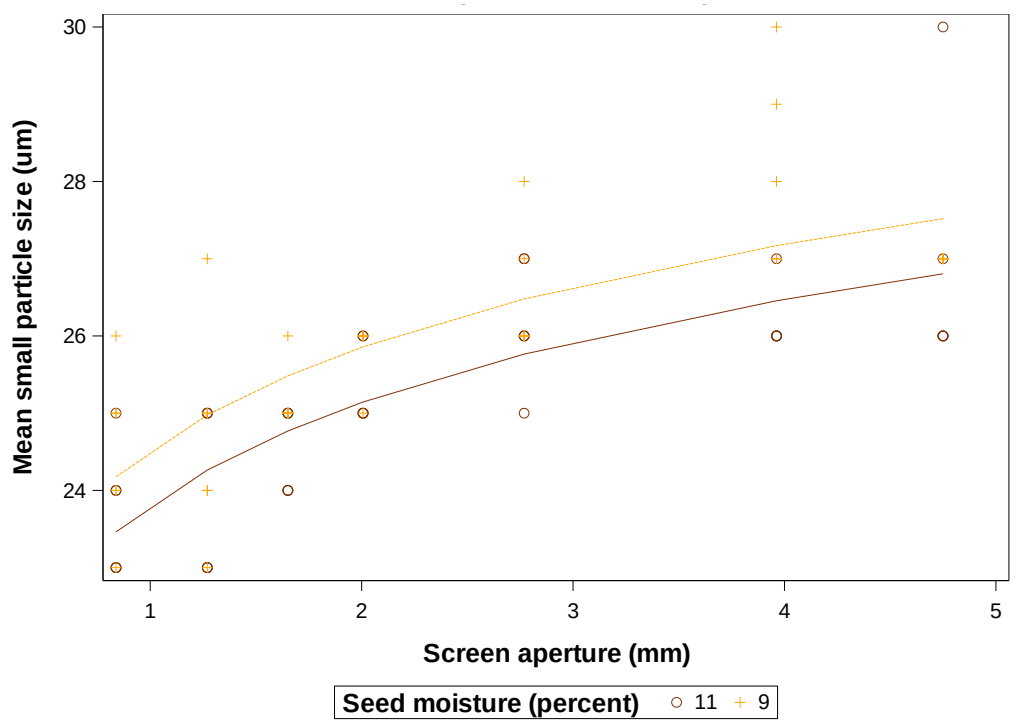

Figure 16. Small mean particle size of split pea flour versus hammer milling variables, with data points representing observed values and lines representing model prediction (R^2_{adj} = 0.619)

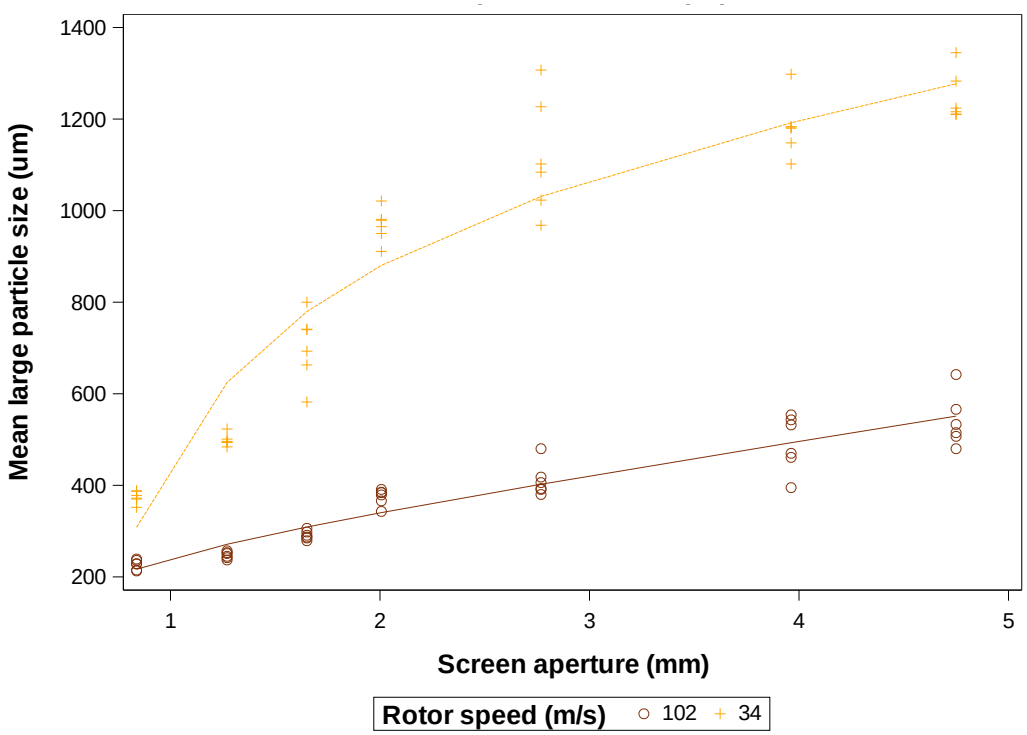

Figure 17. Large mean particle size of split pea flour versus hammer milling variables, with data points representing observed values and lines representing model prediction (R^2_{adj} = 0.953)

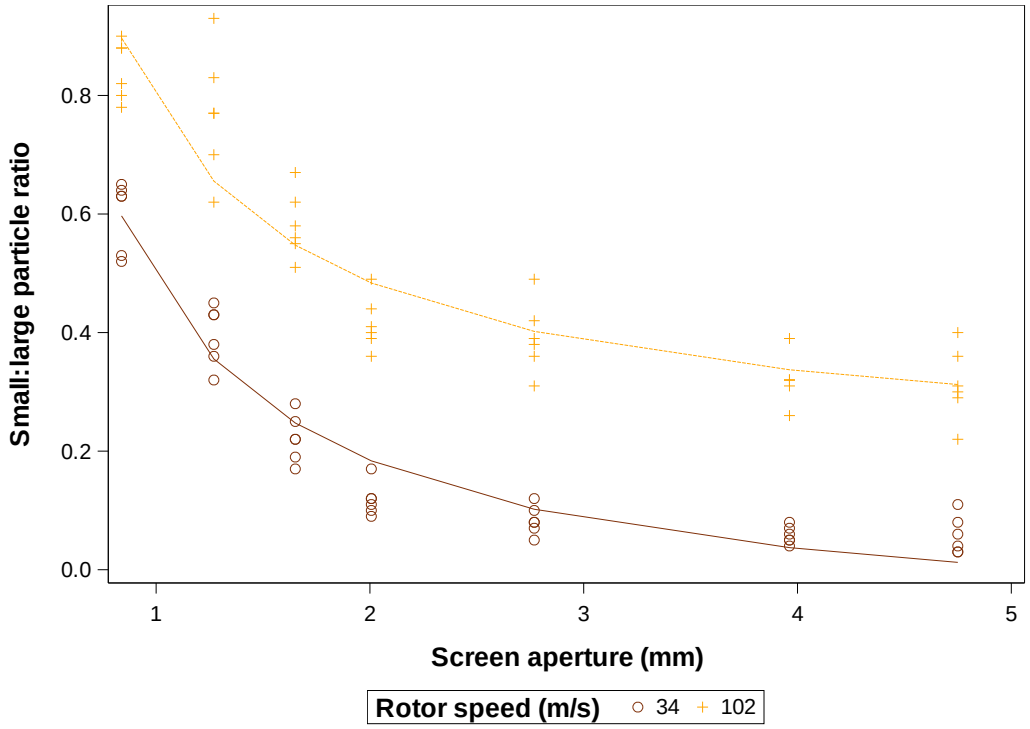

Figure 18. Small to large particle ratio of split pea flour versus hammer milling variables, with data points representing observed values and lines representing model prediction (R^2_{adj} = 0.926)

Bulk density

The bulk density of pea flour ranged from 0.62-0.81 g/cm^3 and was significantly related to seed moisture, rotor speed, and the reciprocal of screen aperture size (Table 1). However, differences in bulk density due to moisture were in the practically small range of 0.02-0.03 g/cm^3 (Figure 19). The relationship between bulk density and milling parameters might have been explained by differences in sample particle size. The model predicting bulk density with only seed moisture and the natural log transformation of the D90 had an R^2_{adj} very close to that of the model predicting bulk density based on milling parameters (Figure 20) (Table 2). This result indicated that the relationship between bulk density and mill parameters could be understood by considering the differences in particles sizes among samples. In the untapped bulk density assessment, flour was poured freely, and uncompacted small particles tended to entrap more air. Samples with larger particle sizes tended to contain large chunks of very compact, un-milled

material (especially at 34 m/s rotor speed) that excluded air and increased bulk density (Figure 21). Larger particles might also have landed with greater force in the cylinder, resulting in tighter packing. Other research suggests that both tapped and untapped bulk densities can exhibit varying relationships with particle size, depending on the commodity. In roasted chickpea and maize flours, bulk density decreased with increasing particle size (Raigar & Mishra 2015; 2017), while in roasted soybean flour, untapped and tapped densities increased with increasing particle size (Raigar & Mishra 2017). The bulk density of the commercial pea sample (0.55 g/cm^3) was lower than any of the hammer-milled samples. Since the particle size of the commercial sample was also smaller than that of the hammer-milled samples, these results confirmed the observation that bulk density of pea flour decreased with reduction in particle size.

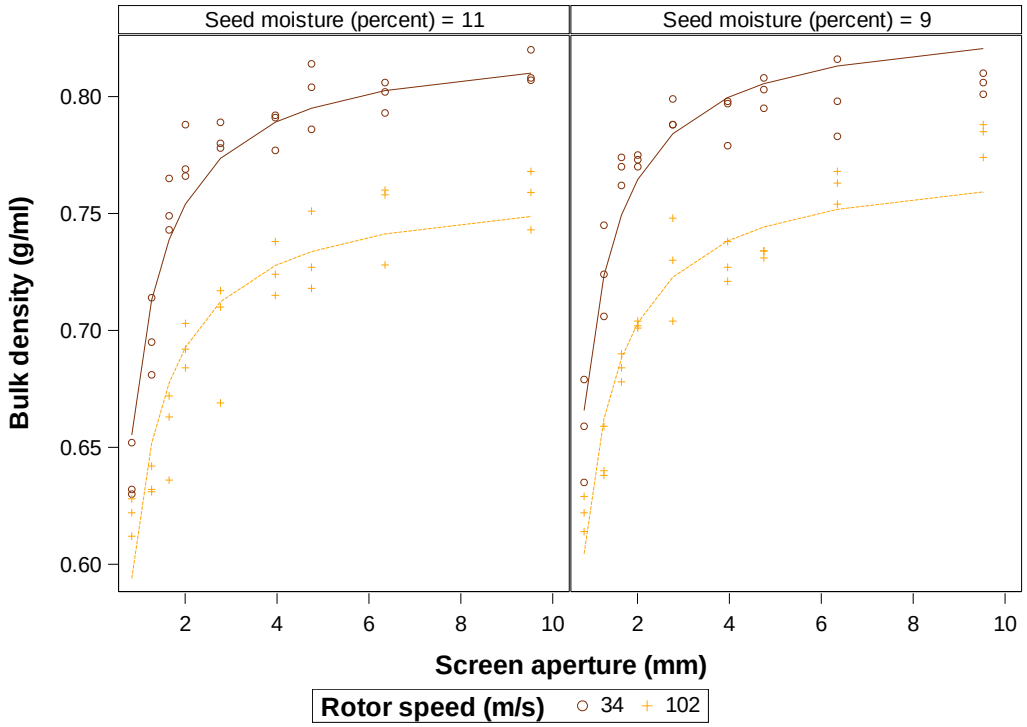

Figure 19. Split pea flour bulk density versus hammer milling variables, with data points representing observed values and lines representing model prediction (R^2_{adj} = 0.924)

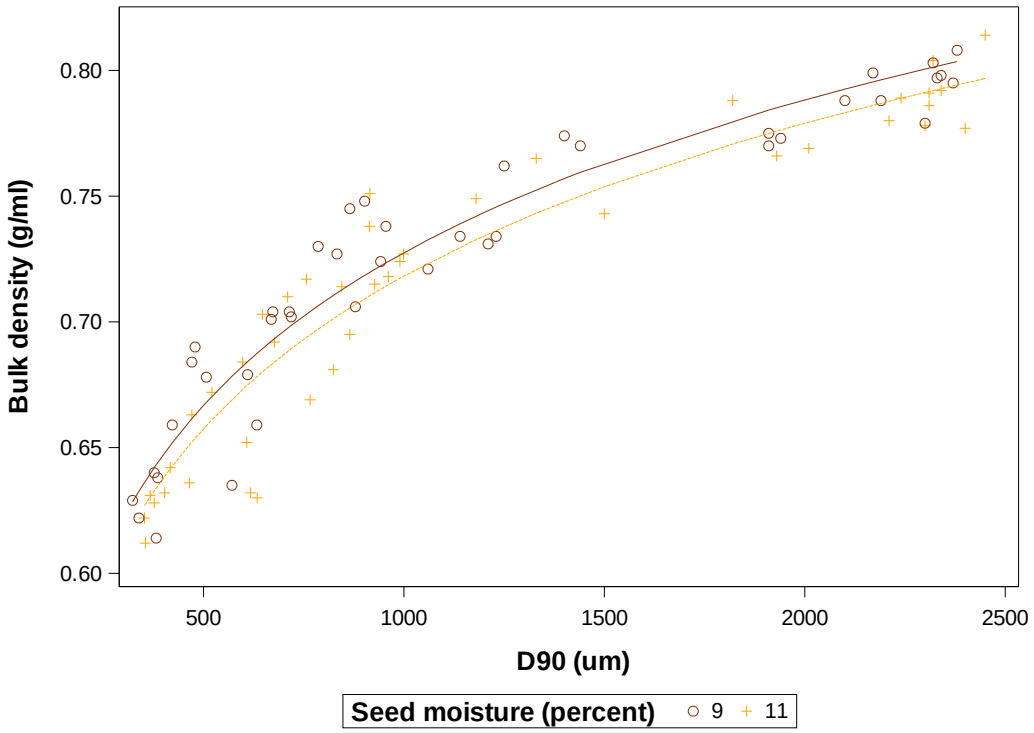

Figure 20. Split pea flour bulk density versus D90 values, with data points representing observed values and lines representing model prediction (R^2_{adj} = 0.913)

Table 2. *F*-test *p*-values from models of hammer-milled yellow split pea flour quality variables vs. seed moisture and particle size parameters

Variable	Moisture	Mean small particle size	Mean large particle size	1/D10	Ln(D50)	Ln(D90)	Square of small:large particle ratio
Brightness	<0.0001		<0.0001				
Redness	<0.0001		<0.0001				
Yellowness	0.0021			<0.0001			
Starch damage	0.0001	<0.0001		<0.0001			
Peak viscosity					<0.0001		
Final viscosity					<0.0001		
Bulk density	0.0156					<0.0001	
Breakdown viscosity							<0.0001

Figure 21. Yellow split pea flour hammer-milled at 9 % seed moisture, 34 m/s (top row) or 102 m/s (bottom row) rotor speed and using the following 9 screen aperture sizes (from left to right): 0.84, 1.27, 1.65, 2.01, 2.77, 3.96, 4.75. 6.35, and 9.53

Color

Color differences were observable among flours produced at different mill settings (Figure 21). Flour brightness (L* value) was significantly affected by seed moisture, rotor speed, screen aperture, and the reciprocal of screen aperture (Table 1). Interaction between seed moisture and rotor speed and between screen aperture reciprocal and rotor speed were also significant. However, the effects of greatest practical significance were screen aperture, rotor speed, and the interaction between screen aperture reciprocal and rotor speed (Figure 22).

As with bulk density, change in flour brightness could be explained in simpler terms by the differences in sample particle sizes due to the various mill settings. Brightness was significantly related to seed moisture and the mean of the large particle size sub-distribution (Figure 23) (Table 2). Brightness was lower at large mean particle size and increased as the large mean particle size decreased. Brightness was also slightly lower when seed moisture was at 9 %.

Flour with higher water content is expected to reflect less light and appear darker than the same flour at lower water content (Sawayama, Adelson & Nishida, 2017). However, lower brightness values were observed at lower moisture content. This result may have been due the heat treatment used to produce the 9 % moisture pea sample. Heating of oat (Sandhu, Godara, Kaur & Punia, 2017) and pearl millet (Siroha & Sandhu 2017) under more intense conditions of 115 °C for 3 h resulted in decreased brightness and increased redness and yellowness, all of which were observed to a lesser extent in the mildly-treated pea samples in this study (Figures 22-27). These color changes during heat processing may be due to polymerization or conversion of native pigments (Yadav, Kaur, Anand & Singh, 2012). The relationship exhibited between brightness and particle size has been previously observed. Brightness increased at smaller particle sizes in corn and lentil flours (Liu, 2009; Ahmed, Taher, Mulla & Al-Hazza, 2016) and was higher for the commercial sample (L* = 88.1) than for any of the hammer-milled samples.

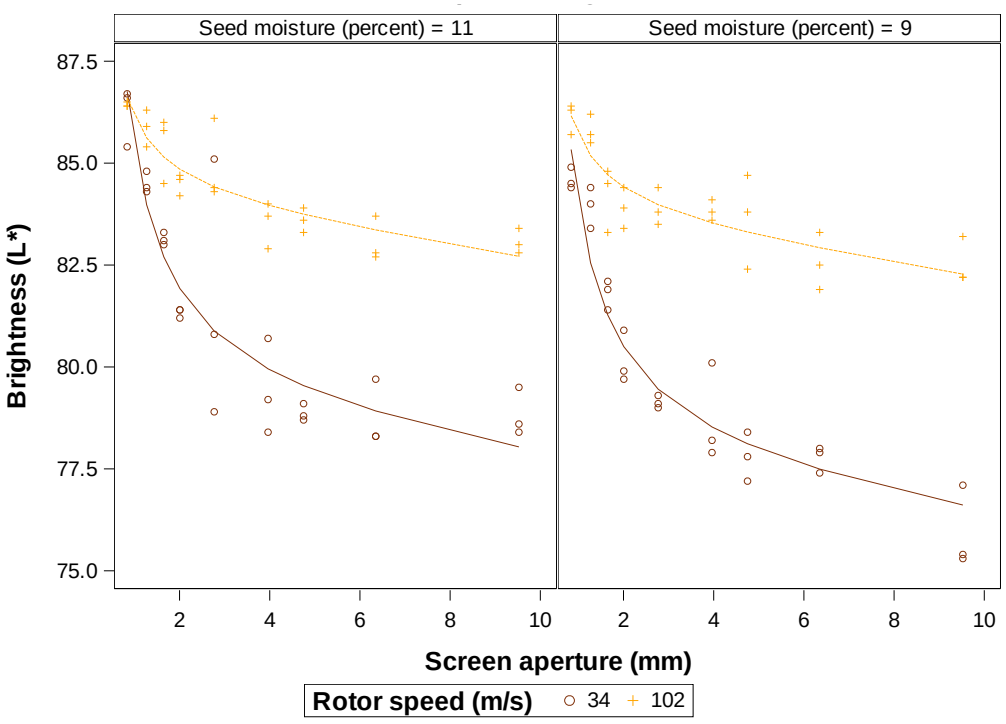

Figure 22. Brightness of yellow split pea flour versus hammer milling variables, with data points representing observed values and lines representing model prediction (R^2_{adj} = 0.912)

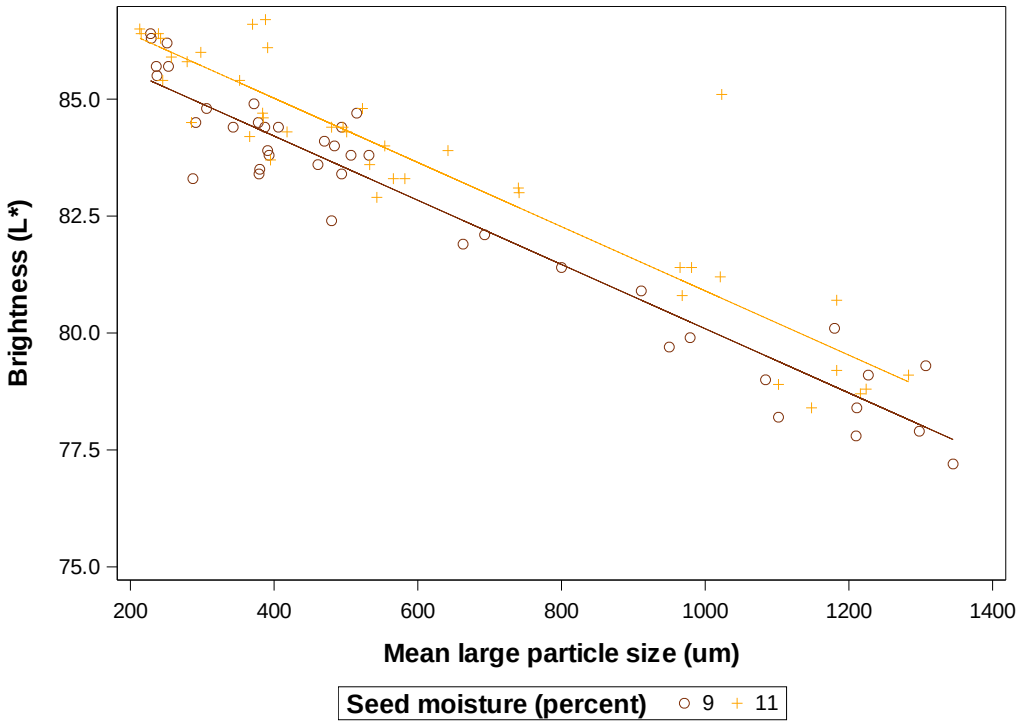

Figure 23. Brightness of yellow split pea flour versus mean large particle size, with data points representing observed values and lines representing model prediction (R^2_{adj} = 0.889)

Flour redness (a* value) was significantly affected by all two-way interactions of seed moisture, rotor speed, and the reciprocal of screen aperture (Table 1). Greater flour redness was observed in flours milled at 9 % seed moisture, 34 m/s hammer speed, and larger screen sizes (Figure 24). Higher redness at 9 % seed moisture may have been due to chemical changes during drying, as noted above for brightness. The relationship between redness and milling parameters could once again be explained more simply by the relationship between redness and particle size. Redness had a positive linear relationship with the mean large particle size (Figure 25) (Table 2). Decreased redness at smaller particle size has also been noted in ground corn and lentil (Liu 2009; Ahmed et al. 2016) and was observed in the commercial sample (a* = -1.0).

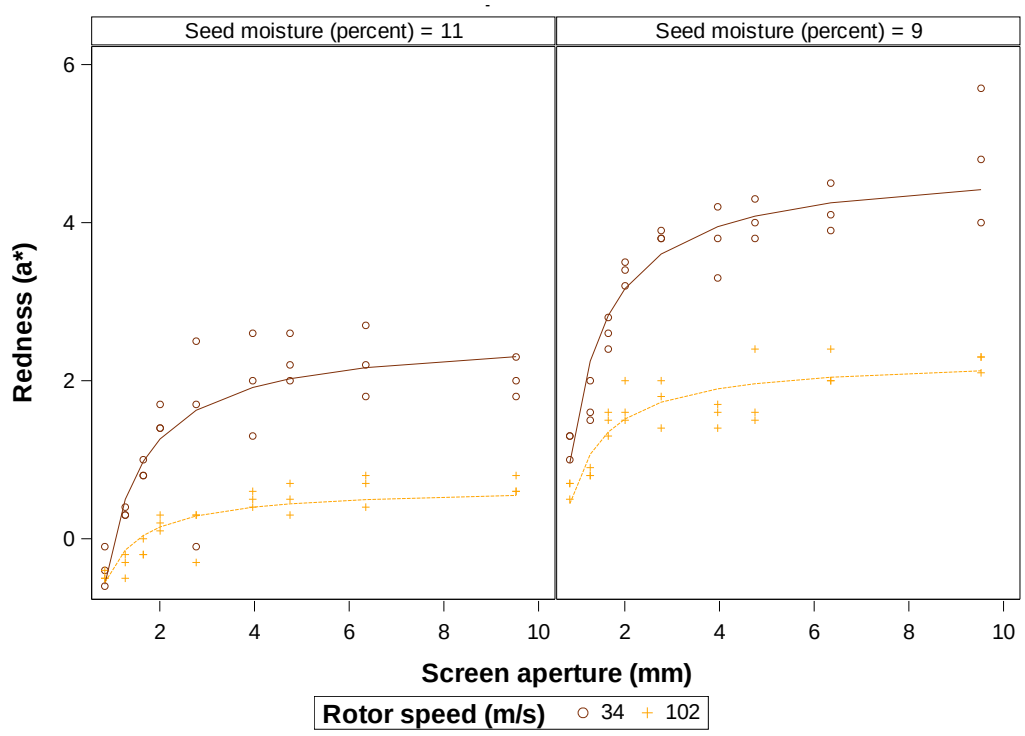

Figure 24. Redness of yellow split pea flour versus hammer milling variables, with data points representing observed values and lines representing model prediction (R^2_{adj} = 0.929)

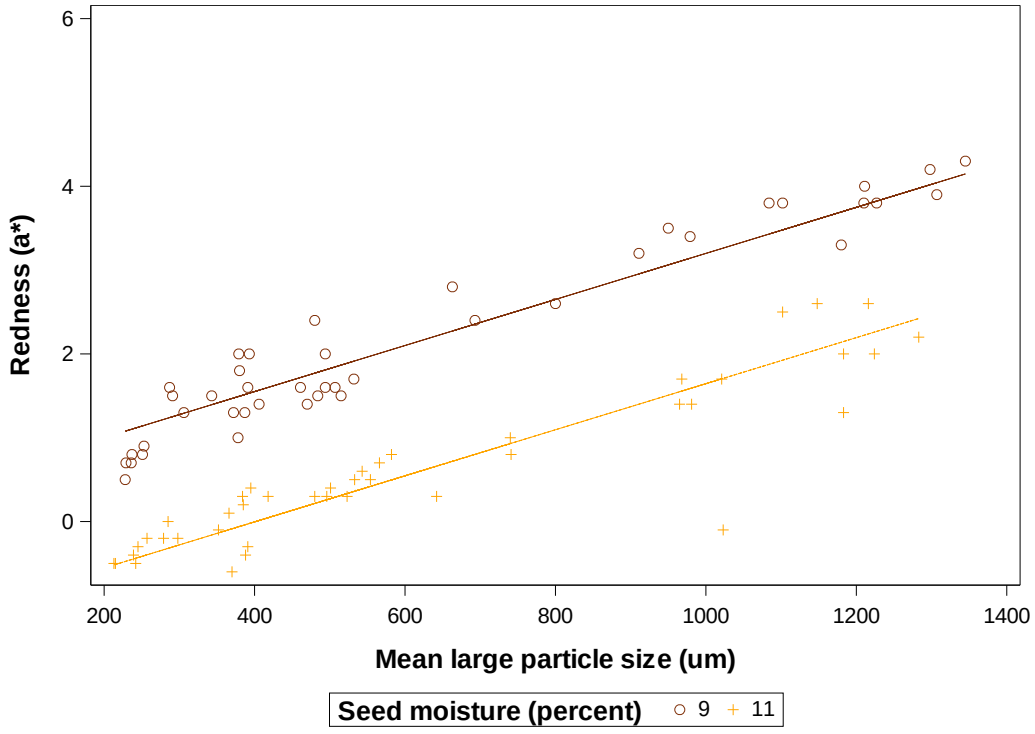

Figure 25. Redness of yellow split pea flour versus mean large particle size, with data points representing observed values and lines representing model prediction (R^2_{adj} = 0.923)

Flour yellowness (b* value) was significantly affected by seed moisture, rotor speed, and the reciprocal of screen aperture and significant interaction was present between seed moisture and rotor speed (Table 1). However, model R^2_{adj} was relatively low, indicating that much of the variation in flour yellowness was not explained by milling parameters (Figure 26). Model adequacy was better when predicting flour yellowness by seed moisture and the reciprocal of the D10 (Figure 27). These results indicated that a sharp increase in small particle volume (indicated by very low values of D10) contributed to a sharper decrease in flour yellowness. Yellowness was also significantly lower at 9 % moisture in both models. Again, the effect of seed moisture on yellowness was probably due to chemical changes in the seeds during drying. Yellowness values also decreased at small particle sizes in ground corn and lentil (Liu 2009; Ahmed et al. 2016) and was lower in the commercial sample (b* = 19.1).

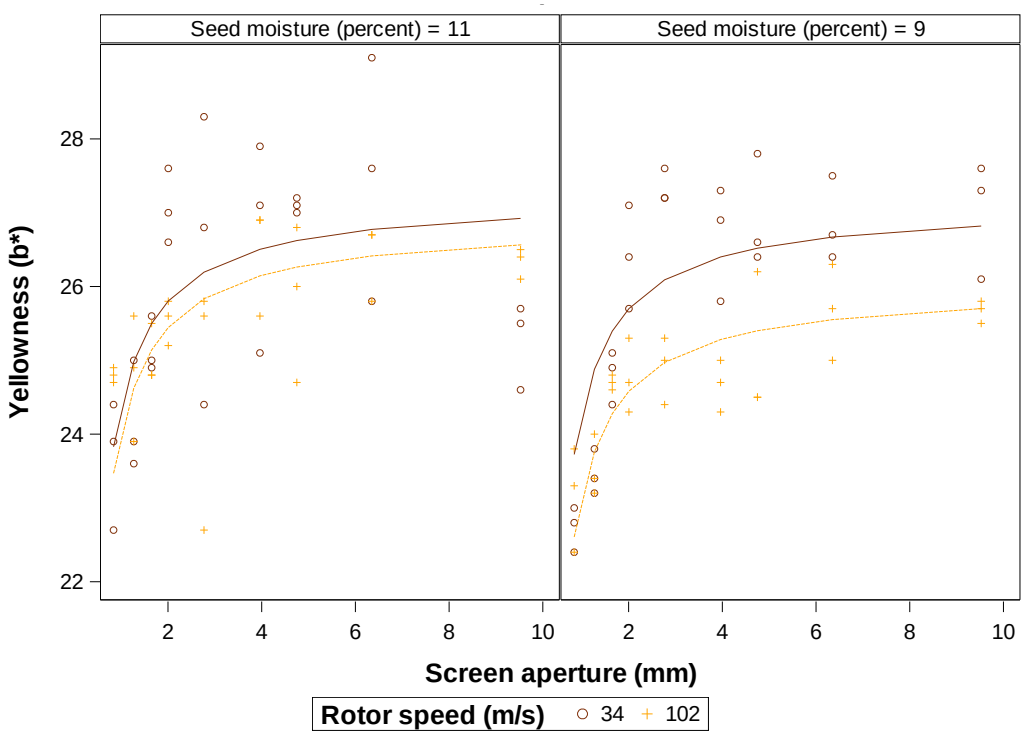

Figure 26. Yellowness of yellow split pea flour versus hammer milling variables, with data points representing observed values and lines representing model prediction (R^2_{adj} = 0.549)

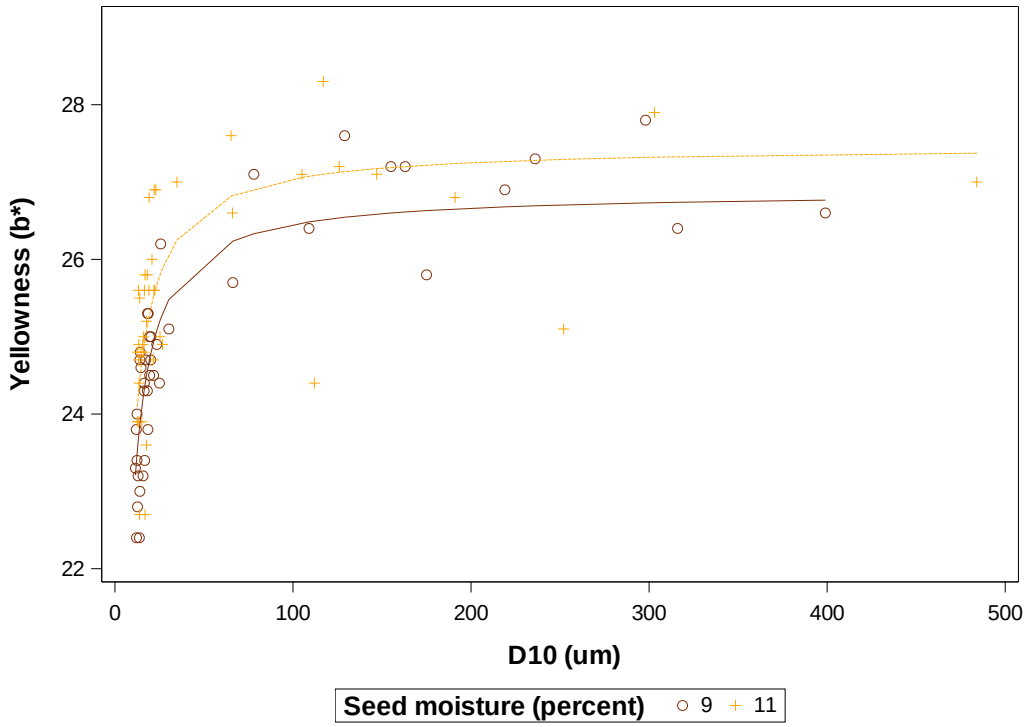

Figure 27. Yellowness of yellow split pea flour versus D10 values, with data points representing observed values and lines representing model prediction (R^2_{adj} = 0.652)

Starch damage

Hammer-milled pea flour starch damage values ranged from 0.1 to 1.4 %, which was comparable to the commercial sample (1.3 %) and previously-reported values for hammer-milled pea flour (1.0 %) and higher than previously-reported values for roller-milled pea flour (2.8 %) (Maskus et al., 2016). Regardless of milling method, pea flour starch damage is lower than that of cereals (e.g. 7.5 to 8.0 % and 6.2 to 12.1 % in roller-milled and ultracentrifugal-milled wheat, respectively) (Khalid et al. 2017; Larson, Baruch & Humphrey-Taylor, 1989). Lower starch damage in milled field pea is probably due to differences in composition. Field pea total starch content (30-49 %) is lower than that of most cereals (60-75 %), while dietary fiber (3-20 %) and protein contents (14-31 %) are higher in field pea than in cereals (2-3 % dietary fiber and 12-14 % protein in wheat) (Delcour & Hoseney, 2010; Hall et al., 2017). Pea starch may be shielded during milling by the other seed constituents, resulting in lower starch damage.

Starch damage was significantly affected by seed moisture, rotor speed, and the reciprocal of screen aperture (Table 1) (Figure 28). Other than bulk density (discussed above) and breakdown viscosity (discussed below), starch damage was the only functional property that had a constant relationship with screen aperture (i.e. no interaction between screen aperture and any other factor). Prediction of starch damage using particle size parameters resulted in a model containing seed moisture, mean of the small particle size sub-distribution, and the reciprocal of the D10 value (Table 2). This model had slightly greater adequacy than the model between starch damage and hammer milling parameters (R^2_{adj} = 0.673). A negative relationship was indicated between starch damage and the volume of small particles present in a sample. This relationship was reasonable since high small particle volume was associated with higher intensity and/or a greater number of collisions during milling, resulting in more opportunities for starch granules to sustain fracture damage. Additionally, increased surface area due to high small particle volume would have increased the exposure of starch granules to starch degrading enzymes. Maskus et al. (2016) reported previously that starch damage increases at smaller particle sizes in yellow pea flours produced by a variety of milling methods (including stone, hammer, roller, and pin milling).

Pasting properties

Pasting properties included the increase in viscosity prior to the first peak of the pasting curve (peak viscosity), the decrease in viscosity immediately following the first peak (breakdown viscosity), viscosity at the end of the procedure (final viscosity), the temperature at the initial rapid increase in viscosity (pasting temperature), and the time to peak viscosity (peak time) (Figure 29). Peak time did not vary significantly across samples and was not included in further analysis.

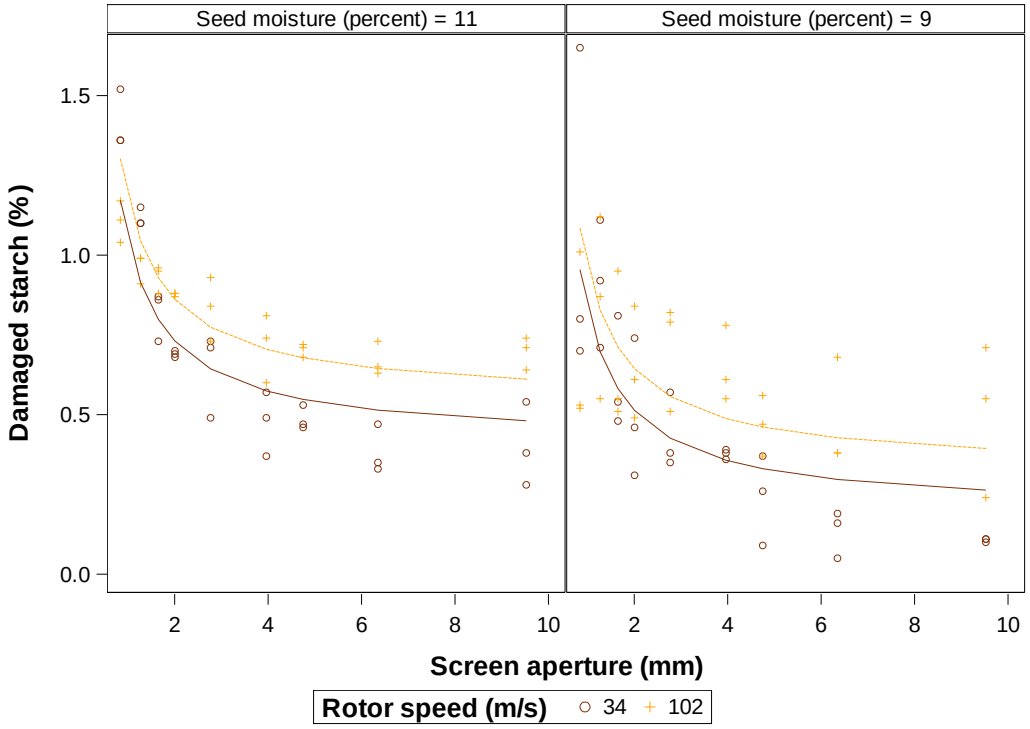

Figure 28. Starch damage of yellow split pea flour versus hammer milling variables, with data points representing observed values and lines representing model prediction (R^2_{adj} = 0.646)

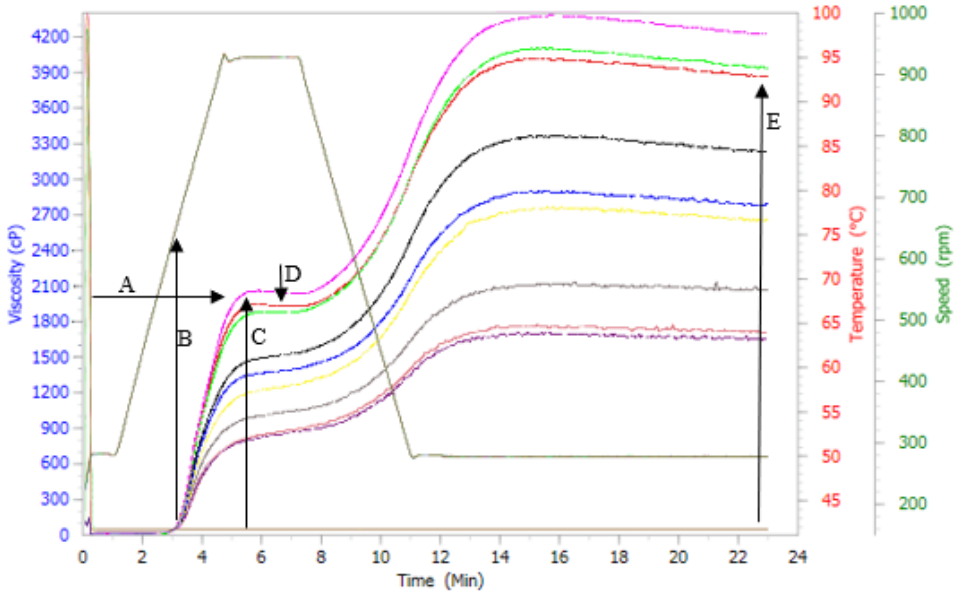

Figure 29. Pasting profiles of yellow split pea milled at 9 % seed moisture, 102 m/s rotor speed, and at screen apertures (top to bottom) of 1.27, 1.65, 0.84, 2.01, 2.77, 3.96, 4.75, 6.35, and 9.53 mm (A=peak time, B=pasting temperature, C=peak viscosity, D=breakdown viscosity, and E=final viscosity)

Peak viscosity was significantly affected by seed moisture, rotor speed, and screen aperture and its reciprocal, and there was significant interaction between rotor speed and both screen aperture and its reciprocal (Table 2). Peak viscosity was slightly higher in samples milled at 11 % moisture (187-2,166 cP) than at 9 % moisture (164-2,049 cP) and was also higher in samples milled at 102 m/s and smaller screen aperture (Figure 30). A model predicting peak viscosity with only the natural log transformation of the D50 fit the data nearly as well as the model containing milling parameters (Figure 31). Peak viscosity increased at an ever-increasing rate as the median particle size became smaller. A negative relationship between particle size and RVA pasting viscosities of yellow split pea flours and rice flours has been reported previously (De la Hera, Martinez, Oliete & Gomez, 2013; Maskus et al., 2016). The peak viscosity at 102 m/s rotor speed and 0.84 mm screen aperture (2,108 cP) was most comparable to the peak viscosity of the commercial sample (2,261 cP).

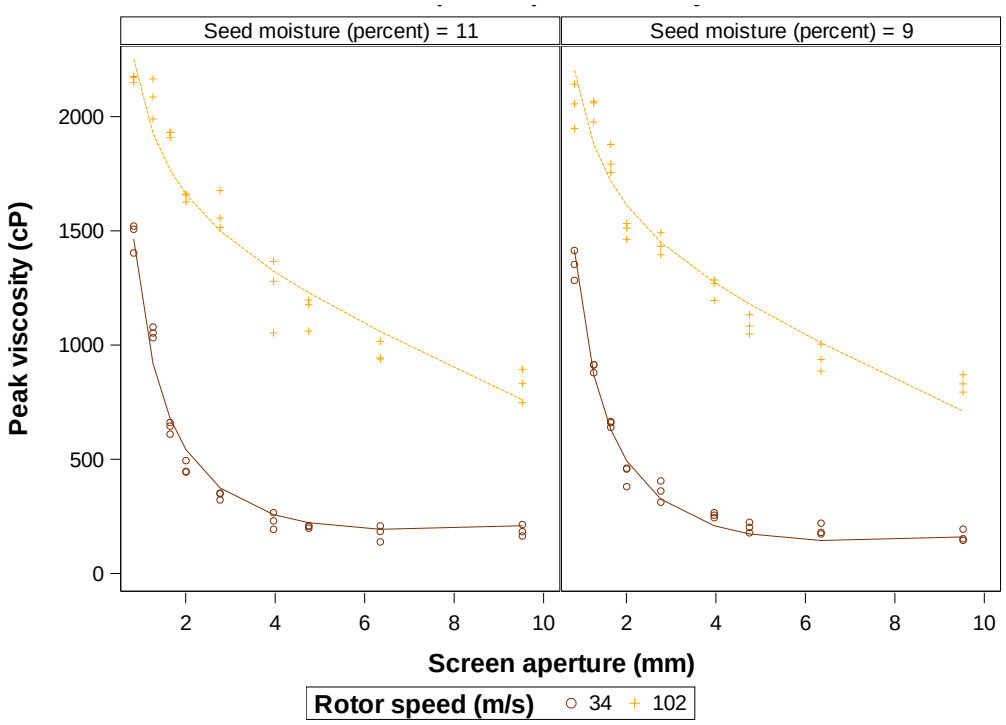

Figure 30. Peak viscosity of yellow split pea flour versus hammer milling variables, with data points representing observed values and lines representing model prediction (R^2_{adj} = 0.979)

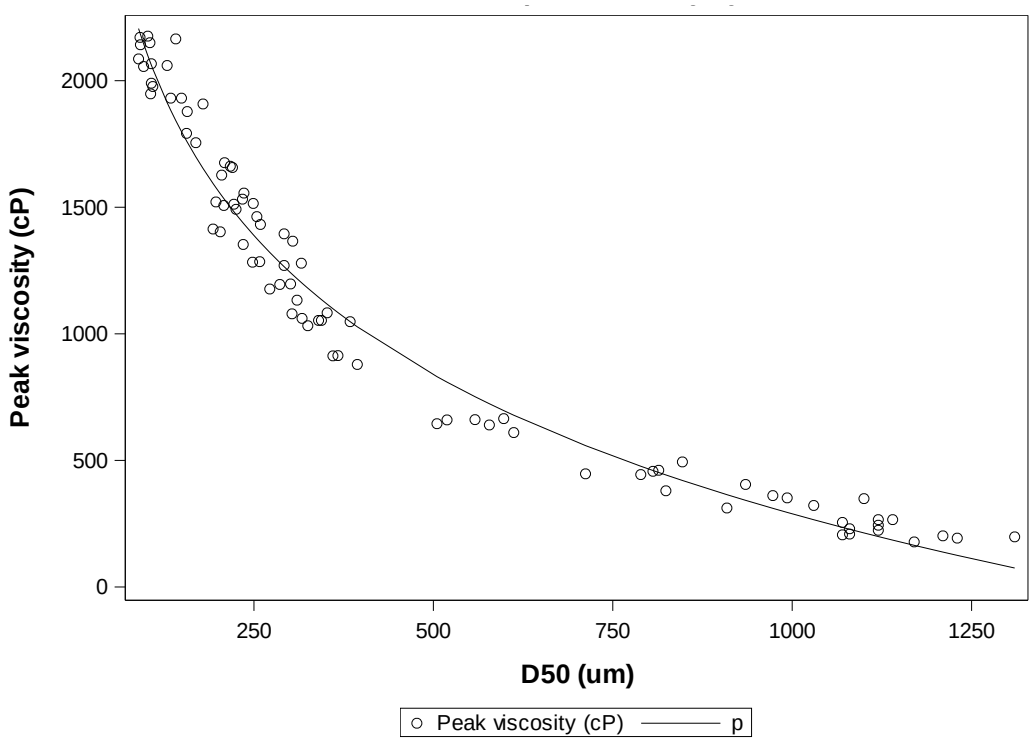

Figure 31. Peak viscosity of yellow split pea flour versus D50 values, with data points representing observed values and lines representing model prediction (R^2_{adj} = 0.973)

Breakdown viscosity was significantly related to rotor speed and the reciprocal of screen aperture (Table 1) and, when modelled separately by particle size variables, to the square of the small to large particle ratio (Table 2). However, modelling of breakdown viscosity was complicated by the absence of a breakdown trough in the pasting curves of all samples except those milled at 102 m/s rotor speed using 0.84- or 1.27-mm screens. As a result, fits for both models were low (R^2_{adj} of 0.206 and 0.295 for models with milling parameters and particle size parameters, respectively). This result was expected since breakdown viscosity is known to be low in pea starch regardless of milling method due to high amylose content and greater resistance of granules to collapse (Hall et al., 2017; U.S. Dry Pea & Lentil Council, 2017).

Final viscosity was significantly impacted by the interaction between rotor speed and screen aperture and between rotor speed and the reciprocal of screen aperture (Table 1) and was

also significantly related to the natural log of the D50 value (Table 2). These significant predictor variables are the same as those for peak viscosity except for the absence of an impact of seed moisture on final viscosity. As with peak viscosity, final viscosity was higher in samples milled at 102 m/s rotor speed and at small screen aperture, and the relationship between final viscosity and screen aperture was more linear at 102 m/s rotor speed than at 34 m/s rotor speed (Figure 32). Final viscosity also increased at an ever-increasing rate with the D50, and the fit for the model of final viscosity versus natural log of the D50 was nearly as good as that for final viscosity versus milling parameters (Figure 33). In general, smaller particle size results in higher pasting viscosities by permitting greater exposure of starch to water during pasting. Indian lentil flour also had higher peak, breakdown, and final viscosities at lower particle size (Ahmed et al. 2016).

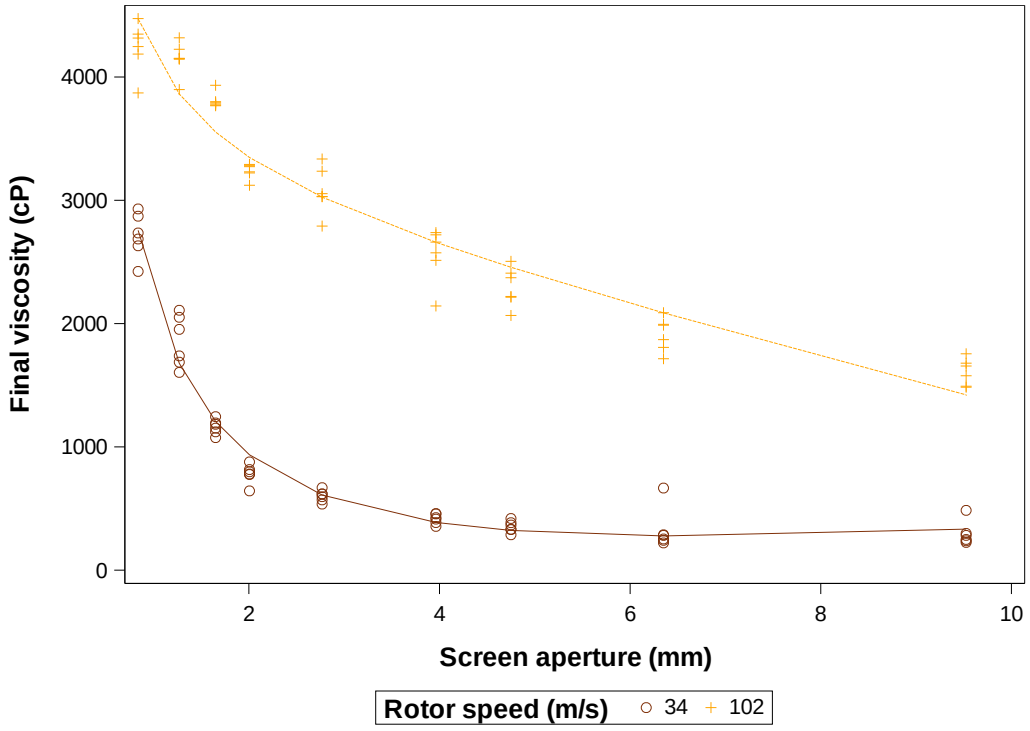

Figure 32. Final viscosity of yellow split pea flour versus hammer milling variables, with data points representing observed values and lines representing model prediction (R^2_{adj} = 0.978)

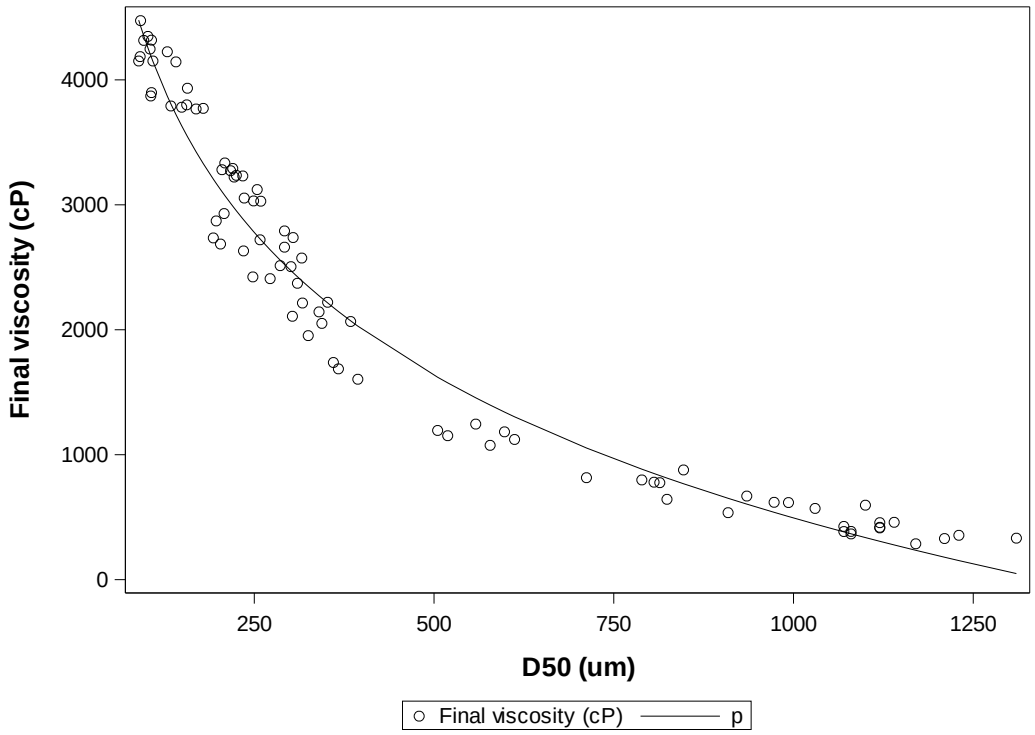

Figure 33. Final viscosity of yellow split pea flour versus D50 values, with data points representing observed values and lines representing model prediction (R^2_{adj} = 0.967)

As with peak viscosity, the final viscosity of sample milled at 102 m/s rotor speed and 0.84 mm screen aperture (4,240 cP) was most comparable to the final viscosity of the commercial sample (4,787 cP). Peak and final viscosities of this treatment and the commercial sample were unexpectedly close considering the differences in particle size distribution (D10, D50, and D90) between the former (13, 99, and 355 µm) and the latter (10, 31, and 132 µm). These results suggest that hammer milling at 102 m/s rotor speed and small screen aperture could produce pea flour appropriate for applications in which high viscosities are appropriate. It should be noted that pasting properties of milled field pea can be impacted greatly by variety and growing location as well as by milling technique (U.S. Dry Pea & Lentil Council, 2017).

Flour pasting temperature was significantly related to seed moisture and the interaction between rotor speed and screen aperture, though the R^2_{adj} indicated low model adequacy (Table

1) (Figure 34). Differences in pasting temperature due to seed moisture were small, as was the effect of screen aperture at 102 m/s rotor speed. However, at low rotor speed, pasting temperature did increase at a rate of 0.7 °C for every 1 mm increase in screen aperture.

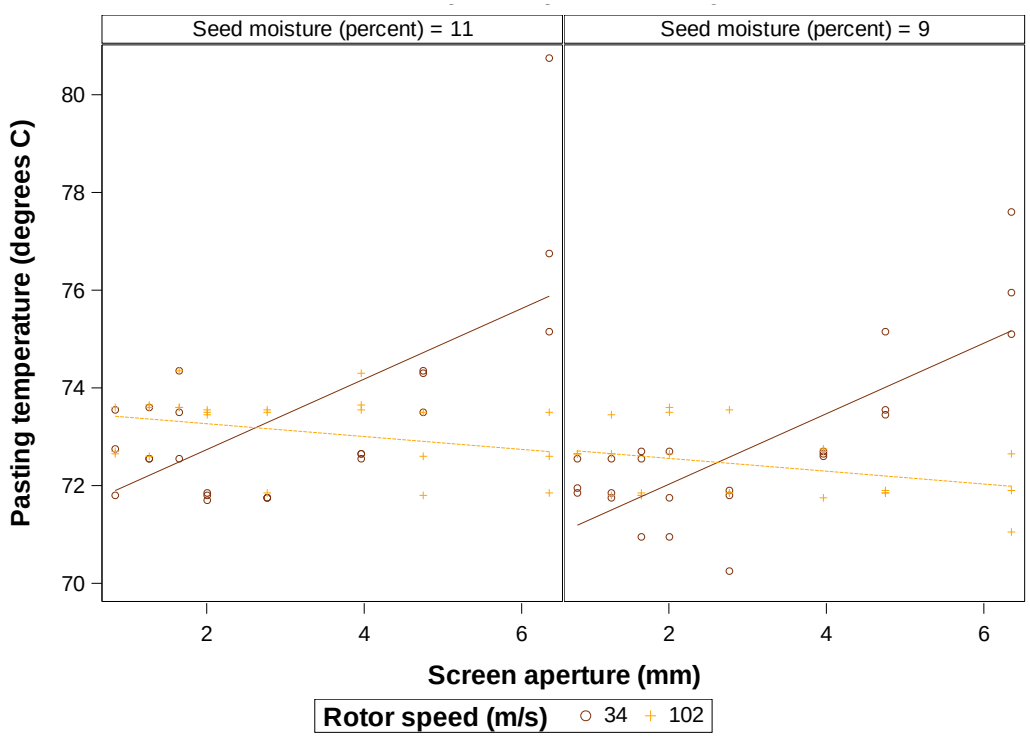

Figure 34. Pasting temperature of yellow split pea flour versus hammer milling variables, with data points representing observed values and lines representing model prediction (R^2_{adj} = 0.473)

Critical water activity (a_w^{crit})

Water activity (a_w) is the ratio of the fugacity (capacity of molecules to escape) of water within a food to that of pure water (Reid and Fennema, 2008). The a_w expresses the strength of the interactions between water and the other components. Moisture content is directly related to a_w, but the relationship between these two variables is sigmoidal rather than linear. The curved relationship between moisture and a_w at a fixed temperature is referred to as a moisture sorption isotherm. Sorption isotherms are dependent upon the history of the product—specifically, whether the product has reached its current moisture content via water adsorption or desorption (a phenomenon known as hysteresis) (Reid and Fennema, 2008). The desorption isotherm tends

to be higher than the resorption isotherm (Figure 35). In other words, at a fixed moisture content a food product tends to have a higher a_w if it is in the process of picking up additional water but tends to have a lower a_w if it is in the process of dehydration. The a_w^{crit} refers to the water activity at which a material transitions from a glassy state (rigid texture with minimal molecular mobility) to a rubbery state (pliable texture with elevated molecular mobility). This transition is important because stability, rheology, and sensory properties change when a food undergoes the transition from a glass to a rubber.

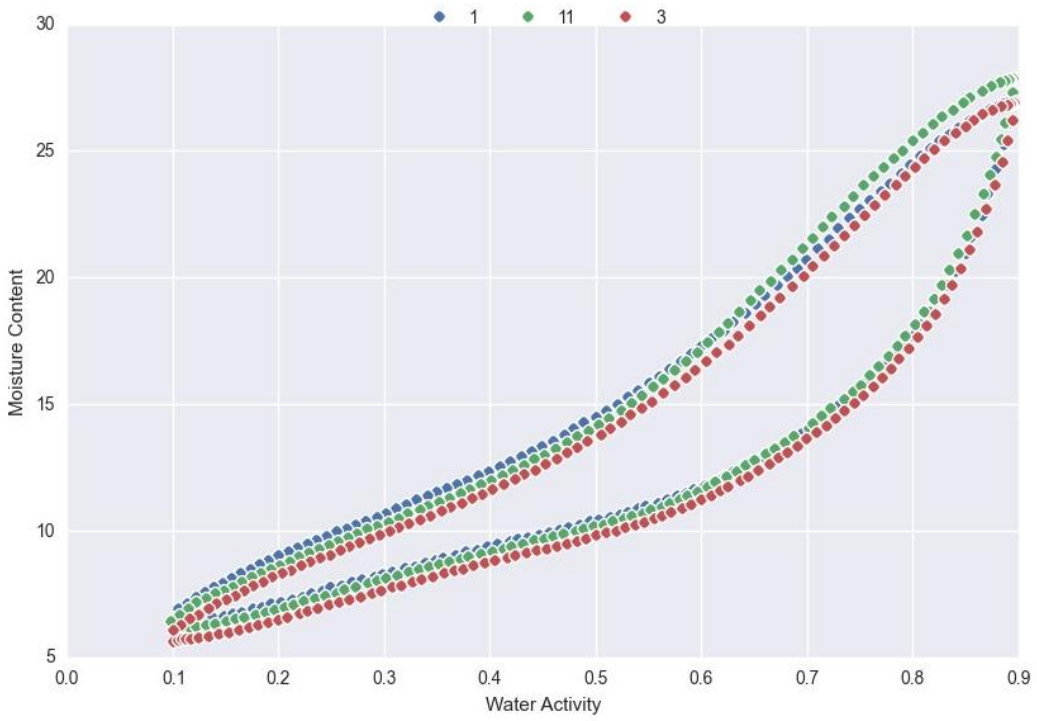

Figure 35. Moisture desorption (upper curves) and resorption (lower curves) isotherms for split pea hammer-milled at 9 % moisture with 34 m/s rotor speed and samples 1 (blue), 3, (red), and 11 (green) corresponding to mill screen apertures of 2.77, 0.84, and 1.65 mm, respectively

Due to the time-consuming nature of the test, isotherm data was collected only on the sample subset mentioned in the methods section. Within this sample subset, only seed moisture was a significant predictor of a_w^{crit} (Figure 36). The lack of significance for either mill rotor speed or screen aperture indicated that particle size was not an important factor within the subset

of samples tested. The a_w^{crit} was lower in samples milled at 9 % moisture than in those milled at 11 % moisture. This result indicated that physical and chemical changes may have occurred during the drying process of the 9 % sample that altered interaction between water and other components of the milled material. Change in grain microstructure due to heat treatment as low at 60 °C has been reported previously (Lang, Lindemann, Ferreira, Pohndorf, Vanier & Oliveira, 2018). However, the difference in a_w^{crit} of 0.02 due to seed moisture is small compared to differences among the a_w^{crit} of various food materials. For example, the a_w^{crit} of cassava starch is 0.58 while that of rice starch is 0.65 (Karrila & Karrila, 2017). Also, the critical moisture content of pea starch is higher than that of pea protein (Pelgrom et al., 2013).

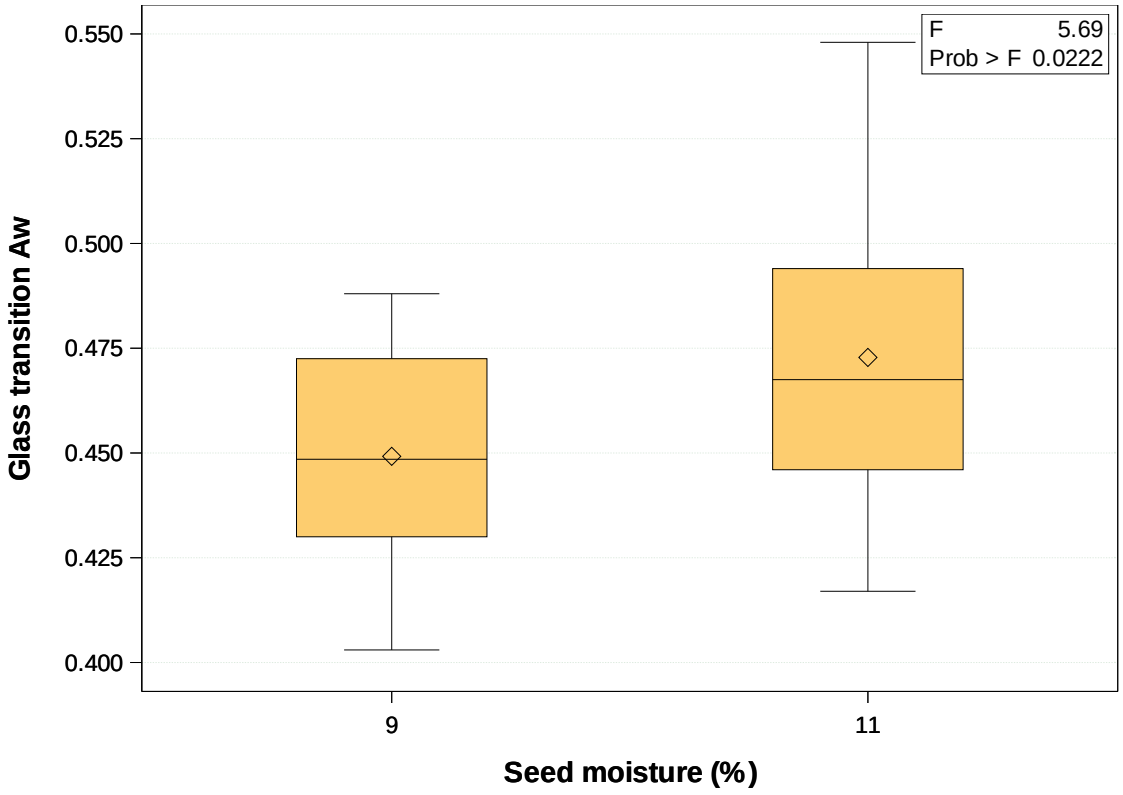

Figure 36. Glass transition a_w (a_w^{crit}) versus seed moisture of hammer-milled split pea (R^2_{adj} = 0.107)

Conclusion

Results indicated that hammer mill parameter selection affected the quality of milled yellow split pea. For color, bulk density, starch damage, and some RVA pasting characteristics, the relationship between mill parameters and flour quality were due mostly to flour particle size, which was controlled by rotor speed and screen aperture. Relationships between flour quality variables and both milling, and particle size parameters were frequently nonlinear, i.e. the rate of change in flour quality due to mill settings or particle size was not constant. High rotor speed (102 m/s) with small screen aperture (0.84 mm) resulted in the narrowest particle size distribution, smallest median particle size, and closest particle size profile to the commercial standard. This treatment also resulted in the brightest color, lowest bulk density, and highest pasting viscosities of all the treatments. Seed moisture content was also important to flour color and starch damage, potentially due to the drying process for the 9 % moisture seed. The interaction of seed moisture, screen aperture size, and hammer rotor speed on pea flour quality indicated that milling process design must consider the combined effects of all milling factors to produce pea flour with desired quality traits.

References

AACC International. *Approved Methods of Analysis*, 11th Ed. Method 08-01.01. Ash—basic method. Approved November 3, 1999. Method 44-15.02. Moisture—air-oven methods. Approved November 3, 1999. Method 46-30.01. Crude protein—combustion method. Approved November 3, 1999. Method 61-02.01. Determination of the pasting properties of rice with the rapid visco analyzer. Approved November 3, 1999. Method 76-31.01. Determination of damaged starch-spectrophotometric method. Approved November 3, 1999. Available online only. St Paul, MN: AACC International, Inc.

Ahmed, J., Taher, A., Mulla, M. Z., Al-Hazza, A., & Luciano, G. (2016). Effect of sieve particle size on functional, thermal, rheological and pasting properties of Indian and Turkish lentil flour. *Journal of Food Engineering*, **186**:34-41. https://doi.org/10.1016/j.jfoodeng.2016.04.008

ASTM International. *Standard Test Methods*. (2009). Method D7481. Standard test methods for determining loose and tapped bulk densities of powders using a graduated cylinder. West Conshohoken, PA: ASTM

Dahl, W. J., Foster, L. M., & Tyler, R. T. (2012). Review of the health benefits of peas (*Pisum sativum* L.). *British Journal of Nutrition*, **108**:S3-S10. https://doi.org/10.1017/S0007114512000852

De la Hera, E., Martinez, M., Oliete, B., & Gomez, M. (2013). Influence of flour particle size on quality of gluten-free rice cakes. *Food and Bioprocess Technology*, **6**:2280-2288. https://doi.org/10.1007/s11947-012-0922-6

Delcour, J. A., & Hoseney, R. C. (2010). *Principles of Cereal Science and Technology*, 3rd ed. St Paul, MN: AACC International, Inc. https://doi.org/10.1094/9781891127632

Efron, B., Hastie, T., Johnstone, I., & Tibshirani, R. (2004). Least angle regression (with discussion). *Annals of Statistics*, **32**:407-499.

FGIS. (2009). *United States Standards for Split Peas*. Washington, DC: USDA.

Hall, C., Hillen, C., & Garden-Robinson, J. (2017). Composition, nutritional value, and health benefits of pulses. *Cereal Chemistry*, **94**:11-31. https://doi.org/10.1094/CCHEM-03-16-0069-FI

Indira, T. N., & Bhattacharya, S. (2006). Grinding characteristics of some legumes. *Journal of Food Engineering*, **76**:113-118. https://doi.org/10.1016/j.jfoodeng.2005.04.040

Kaiser, A. C., Barber, N., Manthey, F., and Hall, C., III. (2019). Physicochemical properties of hammer-milled yellow split pea (*Pisum sativum* L.). *Cereal Chemistry*, **96**:313-323. http:/doi.10.1002/cche.10127

Karrila, T., & Karrila, S. (2017). A switch point model for high-resolution moisture absorption isotherms of raw and pregelatinized starches. *Journal of Food Measurement and Characterization*, **11**:1592-1601. https://doi-org.ezproxy.lib.ndsu.nodak.edu/10.1007/s11694-017-9539-9

Khalid, K. H., Manthey, F., & Simsek, S. (2017). Whole grain wheat flour production using an ultracentrifugal mill. *Cereal Chemistry*, **94**:1001-1007. https://doi.org/10.1094/CCHEM-05-17-0117-R

Lang, G. H., Lindemann, I. da S., Ferreira, C. D., Pohndorf, R. S., Vanier, N. L., & Oliveira, M. de. (2018). Influence of drying temperature on the structural and cooking quality properties of black rice. *Cereal Chemistry*, **95**:564-574. https://doi.org/10.1002/cche.10060

Larsen, N. G., Baruch, D. W., & Humphrey-Taylor, V. J. (1989). The effect of laboratory and commercial milling on lipids and other physicochemical factors affecting the breadmaking quality of wheat flour. *Journal of Cereal Science*, **9**:139-148. https://doi.org/10.1016/S0733-5210(89)80014-1

Le Gall, M., Gueguen, J., Seve, J., & Quillien, L. (2005). Effects of grinding and thermal treatments on hydrolysis susceptibility of pea proteins (*Pisum sativum* L.) *Journal of Agricultural and Food Chemistry*, **53**:3057-3064. https://doi.org/10.1021/jf040314w

Li, E., Dhital, S., & Hasjim, J. (2014). Effects of grain milling on starch structures and flour/starch properties. *Starch/Stärke*, **66**:15-27. https://doi.org/10.1002/star.201200224

Liu, K. (2009). Effects of particle size distribution, compositional and color properties of ground corn on quality of distillers dried grains with solubles (DDGS). *Bioresource Technology*, **100**:4433-4440. https://doi.org/10.1016/j.biortech.2009.02.067

Ma, Z., Boye, J. I., & Hu, X. (2017). *In vitro* digestibility, protein composition and techno-functional properties of Saskatchewan grown yellow field peas (*Pisum sativum* L.) as affected by processing. *Food Research International*, **92**:64-78. https://doi.org/10.1016/j.foodres.2016.12.012

Maskus, H., Bourre, L., Fraser, S., Sarkar, A., & Malcolmson, L. (2016). Effects of grinding method on the compositional, physical and functional properties of whole and split yellow pea flour. *Cereal Foods World*, **61**:59-64. https://doi.org/10.1094/CFW-61-2-0059

Maskus H., Bourre, L., & Malcolmson, L. (2016). The effect of flour milling variables on the functional properties of whole and split yellow pea flour. Winnipeg, MB: Canadian International Grains Institute. Available from: https://cigi.ca/wp-content/uploads/2017/04/The-Effect-of-Flour-Milling-Variables-on-the-Functional-Properties-of-Whole-and-Split-Yellow-Pea-flour_Maskus_11100301.pdf. Accessed 15 September 2017.

Mugabi, R., Eskridge, K. M., & Weller, C. L. (2017). Comparison of experimental designs used to study variables during hammer milling of corn bran. *Transactions of the ASABE*, **60**:537-544. https://doi.org/10.13031/trans.11656

Ngamnikom, P., & Songsermpong, S. (2011). The effects of freeze, dry, and wet grinding processes on rice flour properties and their energy consumption. *Journal of Food Engineering*, **104**:632-638. https://doi.org/10.1016/j.jfoodeng.2011.02.001

Nguyen, G. T., Gidley, M. J., & Sopade, P. A. (2015). Dependence of *in-vitro* starch and protein digestions on particle size of field peas (*Pisum sativum* L.). *LWT – Food Science and Technology*, **63**:541-549. https://doi.org/10.1016/j.lwt.2015.03.037

Pelgrom, P. J. M., Schutyser, M. A. I., & Boom, R. M. (2013). Thermomechanical morphology of peas and its relation to fracture behavior. *Food and Bioprocess Technology*, **6**:3317-3325. https://doi.org/10.1007/s11947-012-1031-2

Posner, E. S., & Hibbs, A. N. (2005). *Wheat flour milling*. St Paul, MN: AACC International, Inc.

Prabhasankar, P., & Rao, P. H. (2001). Effect of different milling methods on chemical composition of whole wheat flour. *European Food Research and Technology*, **213**:465-469. https://doi.org/10.1007/s002170100407

Raigar, R. K., & Mishra, H. N. (2017). Grinding characteristics, physical, and flow specific properties of roasted maize and soybean flour. *Journal of Food Processing and Preservation*, **42**:e13372. https://doi.org/10.1111/jfpp.13372

Raigar, R. K., & Mishra, H. N. (2014). Effect of moisture content and particle sizes on physical and thermal properties of roasted bengal gram flour. *Journal of Food Processing and Preservation*, **39**:1839-1844. https://doi.org/10.1111/jfpp.12419

Reid, D. S., & Fennema, O. R. (2008). Water and Ice. In: S. Damodaran, K. L. Parkin, & O. R. Fennema (eds), *Fennema's Food Chemistry*, 4th ed, pp17-82. CRC Press, Boca Raton, FL.

Sandhu, K. S., Godara, P., Kaur, M., & Punia, S. (2017). Effect of toasting on physical, functional and antioxidant properties of flour from oat (*Avena sativa* L.) cultivars. *Journal of the Saudi Society of Agricultural Sciences*, **16**:197-203. https://doi.org/10.1016/j.jssas.2015.06.004

Sawayama, M., Adelson, E. H., & Nishida, S. (2017). Visual wetness perception based on image color statistics. *Journal of Vision*, **17**:1-24. https://doi.org/10.1167/17.5.7

Siroha, A. K., & Sandhu, K. S. (2017). Effect of heat processing on the antioxidant properties of pearl millet (*Pennisetum glaucum* L.) cultivars. *Journal of Food Measurement and Characterization*, **11**:872-878. https://doi.org/10.1007/s11694-016-9458-1

Tran, T. T. B., Shelat, K. J., Tang, D., Li, E., Gilbert, R. G., & Hasjim, J. (2011). Milling of rice grains. The degradation on three structural levels of starch in rice flour can be independently controlled during grinding. *Journal of Agricultural and Food Chemistry*, **59**:3964-3973. https://doi.org/10.1021/jf105021r

U.S. Dry Pea & Lentil Council. (2017). *2017 U.S. Pulse Quality Survey*. Moscow, ID: U.S. Dry Pea and Lentil Council.

Wang, N., & Daun, J. 2004. Effect of variety and crude protein content on nutrients and certain antinutrients in field peas (*Pisum sativum*). *Journal of the Science of Food and Agriculture*, 84:1021-1029.

Wood, J. A., Knights, E. J., & Choct, M. (2017). Topography of the cotyledon surfaces and adjoining seed coat of chickpea (*Cicer arietinum* L.) genotypes differing in milling performance. *Cereal Chemistry*, **94**:104-109. https://doi.org/10.1094/CCHEM-04-16-0110-FI

Wu, Y. V., & Nichols, N. N. (2005). Fine grinding and air classification of field pea. *Cereal Chemistry*, **82**:341-344. https://doi.org/10.1094/CC-82-0341

Yadav, D. N., Kaur, J., Anand, T., & Singh, A. K. (2012). Storage stability and pasting properties of hydrothermally treated pearly millet flour. *International Journal of Food Science and Technology*, **47**:2532-2537. https://doi.org/10.1111/j.1365-2621.2012.03131.x

PAPER 2. FLOW PROPERTIES OF HAMMER-MILLED YELLOW SPLIT PEA (*PISUM SATIVUM* L.)

Abstract

The flowability of hammer-milled yellow split pea, which is important in the development and scale-up of products containing milled pulses was evaluated. Yellow split pea at 9 and 11 % moisture was hammer-milled at two rotor speeds (34 and 102 m/s) and with 9 mill screen aperture sizes (ranging from 0.84 to 9.53 mm). Particle size distribution, angle of repose (α) and angle of slide (θ) were assessed on 6 surfaces (stainless steel (SS), aluminum (AL), polypropylene (PP), polyvinyl chloride (PVC), high-density polyethylene (HDPE) and polyvinylidene fluoride (PVDF)). Negative quadratic relationships were present between α and particle size parameters, while θ exhibited negative linear relationships with particle size. Moisture had a surface-dependent effect on flow properties. Values of α were lower on AL, PVDF, and HDPE than on PP, PVC, and SS while θ values were lowest on AL and SS at 9 % seed moisture (30 to 32 °), intermediate on SS at 11 % moisture as well as on PP and PVC (33 to 36 °), high on PVDF (38 to 40 °), and very high on HDPE (44 to 45 °). Milled split pea with D50 of 99 μm had higher θ but lower α (40 ° and 32 °, respectively) than those of commercial whole wheat flour (38 ° and 37 °, respectively). This systematic data on milled split pea flow properties could be useful in designing conveying and storage operations.

Introduction

The use of milled pulses in processed food products is on the rise. Between pulse milling and the incorporation of pulse flour into a formulation, the flour generally undergoes multiple transportation, packaging, and storage stages. To avoid wasted time and labor from disrupted powder flow, it is important to design flour handling and storage systems that take the unique

flow properties of all anticipated powdered products into account (Ambrose, Jan & Siliveru, 2015; Abu-Hardan & Hill, 2010; Lee & Yoon, 2015). Flow properties describe the response of a powder to the application of a force (frequently gravity). These properties are affected by flow system configuration such as surface material, angle of flow, flow rate, and temperature, and by powder characteristics, such as shape, size, and composition (Abu-hardan & Hill, 2010), that result in particle friction, interlocking, and stable structure formation (i.e. arching) (Juliano & Barbosa-Canovas, 2010).

Moisture content (total water content) and water activity (an indicator of the energy state of water in a food matrix) can both be important intrinsic characteristics to flow properties. However, the impact of moisture and water activity on flowability is dependent on material composition and particle size. For example, the caking strength of wheat flour at 30 % moisture was 50 times higher than at 12.5 % moisture; however, the caking strength of corn flour did not differ at these same two moisture levels (Abu-hardan & Hill, 2010). In agglomerated food powders, compression characteristics did not differ across a water activity range of 0.15 to 0.56 though they did differ across a particle size range of 106 to 1700 μm (Yan & Barbosa-Canovas, 1997). Additional previous research supports that moisture and water activity are important to flowability of some commodities (such as wheat) but not to others (such as corn and soybean) (Lee & Yoon, 2015; Probst, Ambrose, Pinto, Bali, Krishnakumar & Ileleji, 2013; Siliveru, Ambrose & Vadlani, 2016).

Flow properties can be evaluated with a variety of methods. The industry standard for determining flow properties for silo design is the Jenike shear test; however, this method is difficult to perform and very sensitive to changes in operator technique (Ambrose et al., 2015). Two other common indices of powder flow properties that are easier to obtain are the angle of

repose and the angle of slide, also known as the sliding angle of repose (Ambrose et al., 2015; Chang, Kim, Kim & Jung, 1998; Fitzpatrick, Barringer & Iqbal, 2004; Ileleji & Zhou, 2008). Angle of repose (α) is the slope of a heap of flour on a given storage surface when dropped onto the surface under controlled conditions. This flow property is useful for rapid, simple evaluation of flow properties among samples and can provide results consistent with other flowability tests when conditions of flour pile formation are carefully controlled (Ambrose et al., 2015; Geldart, Abdullah & Verlinden, 2009). However, angle of repose is only indicative of uncompacted flow properties and is a static test that may not be helpful in the design of flour handling systems (Ambrose et al., 2015). It is best used as an indicator of the relative flowability of materials of different particle size or composition. Angle of slide (θ) is the minimum slope (relative to the horizontal) required for a powder to flow under its own weight. This parameter has some similarity to wall friction and is unique to a food contact surface material. Angle of slide is a shear flow property that can be used in the design of bins for grain and flour storage and hoppers for conveyance, since it provides the minimum hopper angle required for unobstructed flow (Ambrose et al., 2015). Methods of determining the angle of slide vary (Chang et al., 1998; Park, Kim, Choung, Han & Yoon, 2015).

Angles of repose and slide of wheat and other common cereals have been evaluated in previous studies (Ambrose et al., 2015; Bian, Sittipod, Garg & Ambrose, 2015; Fitzpatrick et al., 2004; Jan, Karde, Ghoroi & Saxena, 2018; Pordesimo, Onwulata & Carvalho, 2009; Probst et al., 2013; Ricks, Barringer & Fitzpatrick, 2002; Siliveru et al., 2016). However, values of these parameters are not yet widely reported for pulse flours, despite the importance of flow properties in flour handling systems. Angle of slide was evaluated in ground adzuki bean (Park et al., 2015) and black soybean (Lee & Yoon, 2015) as a function of particle size. Beyond these two studies,

little has been reported on the flow properties of pulse flours. The objective of this research was to determine flowability of milled split pea on a variety of common food contact surfaces with the initial hypothesis that the selected contact surface and sample particle size distribution would be important factors in defining flow properties. An additional objective was to determine whether moisture content was a factor in determining the flow properties of milled split pea.

Materials and Methods

Sample preparation

Yellow split pea (11 % moisture) was obtained from AGT Foods USA (Minot, ND). Low-moisture split pea was prepared in a custom-made laboratory-scale pasta dryer (Standard Industry, Fargo, ND) using the 12 h pasta drying cycle. Temperature was brought to 56 °C in the first hour, held at 56 °C for 3 h, brought up to 72 °C in 15 min, held at 72 °C for 6 h, then cooled to 30 °C in 2 h. Moisture of 9 % and 11 % represented typical middle and upper moisture values, respectively, of American-grown field pea (based on 6–11 % annual mean moisture from 2012 to 2017) (U.S. Dry Pea & Lentil Council, 2017). Samples (~1 kg) of both 9 and 11 % moisture samples were ground in a hammer mill (Model DASO6, Fitzpatrick, Elmhurst, IL) at a constant feed rate of 2.3 kg/min with 9 screen aperture sizes (round apertures of 0.84, 1.27, 1.65, 2.01, 2.77, 3.96, 4.75, 6.35, and 9.53 mm diameter) and at two hammer rotor speeds (34 and 102 m/s). Flour temperature immediately after milling was measured with an infrared laser thermometer and ranged from 18-27 °C. Milling combinations were completed in triplicate, resulting in a total of 108 samples. A commercially-available sample of raw split pea flour (AGT, Regina, SK, Canada) was also obtained and evaluated along with the hammer-milled sample.

Flour analysis

Particle size distribution curves and the D10, D50 (median), and D90 were determined with a Mastersizer 3000 laser particle size analyzer with a dry powder dispersion unit. Samples milled at 34 m/s at the two largest screen apertures were too coarse to be evaluated with this system. Small and large mean particle sizes were determined by evaluating the mean particle size above and below 67 µm, and small to large particle size ratio was calculated by dividing the volume of particles below 67 µm by the volume of particles above 67 µm. Bulk density was obtained using the loose bulk density method described in ASTM D7481-09 (ASTM International, 2009). In this method, 250 mL of flour was added, without tapping or shaking, to a graduated cylinder and the weight recorded.

Angle of repose (α) and angle of slide (θ) were determined on aluminum (AL), stainless steel (SS), polyvinyl chloride (PVC), polypropylene (PP), high-density polyethylene (HDPE), and polyvinylidene fluoride (PVDF) using the method of de la Pena (2015). For α, 200 g of sample was poured down a chute to pass through a funnel and into a 7.8 x 12.8 cm metal cup resting on one of the selected surfaces (Figure 37). The metal cup was removed vertically, allowing flour to spread across the surface in a pile. Angle of repose was calculated as the arc tangent of pile height divided by pile radius (calculated as half the mean diameter, from 2 determinations) (Figure 38). For θ, the angle of the surface with respect to horizontal was increased until the majority (> 180 g) of the material had slid down (Figure 39). Angle of slide was measured with a protractor as the surface angle at the end of the experiment.

Figure 37. Flow properties equipment setup

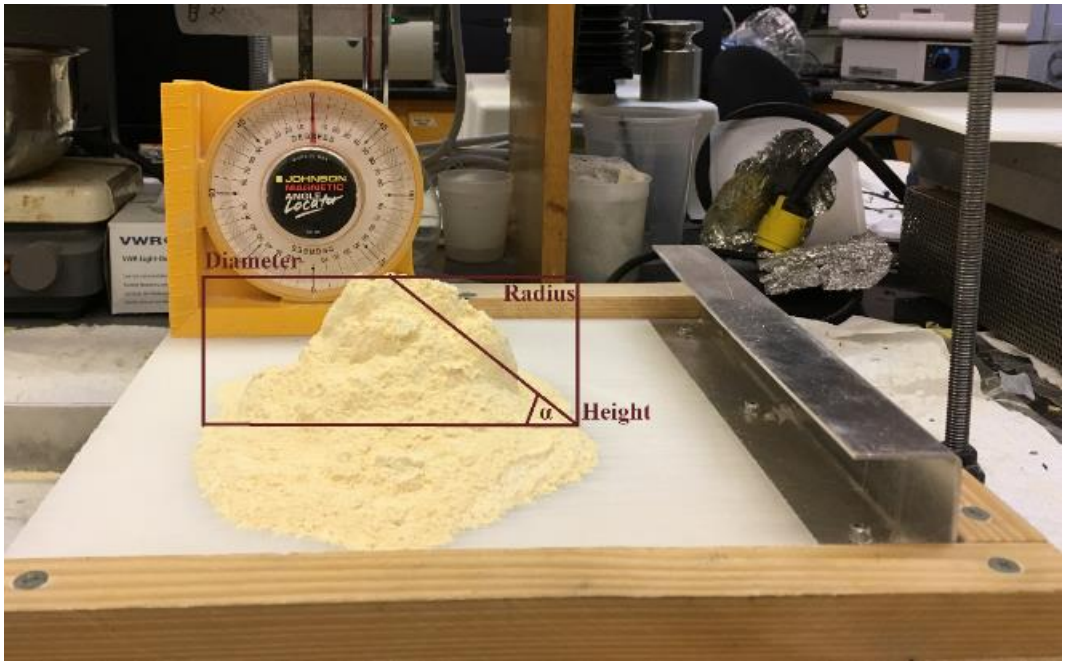

Figure 38. Illustration of angle of repose (α) determination

Figure 39. Illustration of angle of slide (θ) determination

Statistical analysis

Milling treatments were assigned randomly to the sample material and applied in triplicate. Statistical analysis was performed with SAS 9.4 (SAS Institute Inc., Cary, NC) (Appendix A). Since flow properties were related to non-linear transformations of particle size parameters, the GLMSELECT procedure was used to select among the main effects as well as non-linear transformations (reciprocal and square) of the particle size variables and bulk density, in addition to the main effects of surface type and seed moisture level. Due to the presence of multicollinearity among the predictors under consideration, least angle regression was used during model selection (Efron, Hastie, Johnstone & Tibshirani, 2004). Adjusted R^2, Mallow's C_p, and PRESS were used to assess model fits. When fit statistics were close for multiple models, the

most parsimonious model was selected. The GLM procedure was used to perform ANCOVA on flow properties using the factors selected through GLMSELECT. Interaction terms were selected based on models with minimum mean square error and maximum adjusted R^2. *F*-tests were used to test the significance of each factor in each model and only significant factors were retained (except for non-significant main effects when an interaction term was significant). Tukey's adjustment was used for multiple comparisons of means for surface type. A *p*-value of ≤ 0.05 was considered statistically significant for all tests.

Results and Discussion

Angle of repose (α)

Based on Mallow's C_p, R^2_{adj}, and PRESS, step 9 was chosen during model selection as the model that optimized fit and parsimony (Figure 40). Variables included at this step were surface, seed moisture, the square of D50, the square of small to large particle ratio, and the D10. Subsequent removal of the D10 and addition of interaction between surface type and small to large particle size ratio resulted in the model with the best fit and significance for all factors (some linear terms were not significant but were retained due to significance of quadratic terms) (Table 3). Model adequacy was moderately good ($R^2_{adj} = 0.795$).

Table 3. *F*-test *p*-values for the model of yellow split pea flour angle of repose

Predictor variable	*p*-value
Seed moisture	<0.0001
Surface type	<0.0001
D50	0.6542
Square of D50	<0.0001
Small to large particle ratio	0.2277
Square of small to large particle ratio	0.0001
(Surface type)*(small to large particle ratio)	<0.0001
(Surface type)*(square of small to large particle ratio)	<0.0001

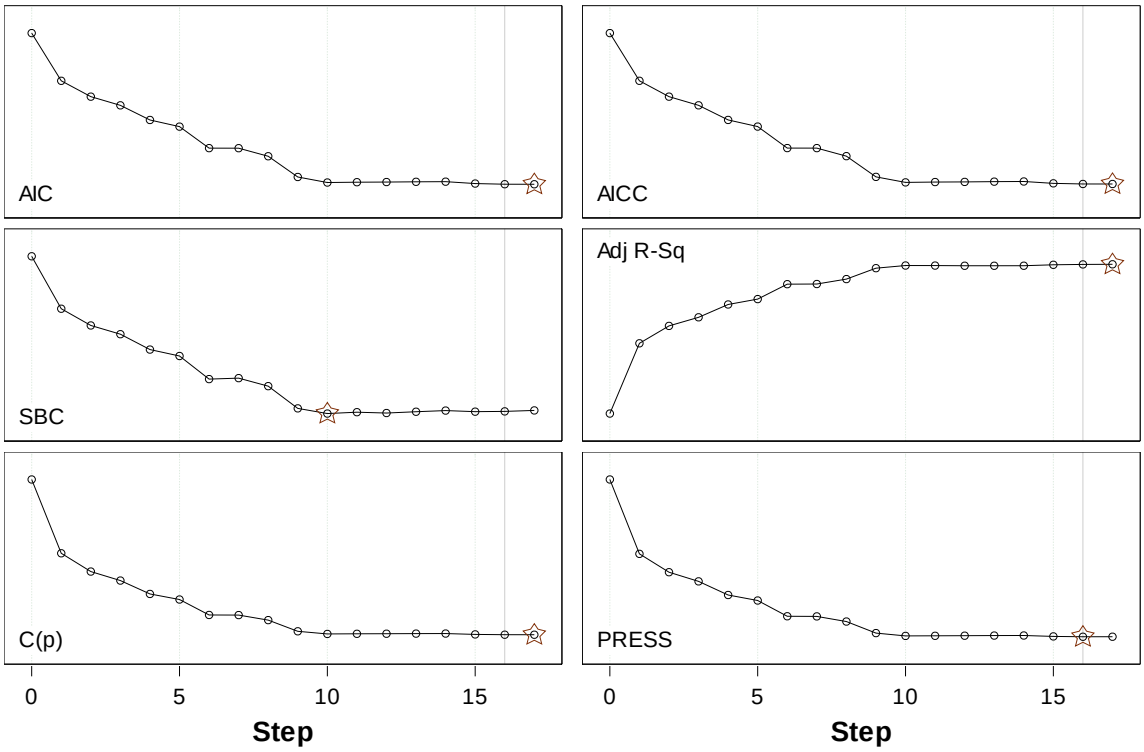

Figure 40. Progression of model selection criteria at each step of model selection for angle of repose of hammer-milled yellow split pea (AIC = Akaike Information Criterion, AIC C = Corrected AIC, SBC = Schwarz Bayesian Criterion, C(p) = Mallow's C_p, and PRESS = Predicted Residual Error Sum of Squares)

When important factors affecting angle of repose were viewed individually, the relationship between repose angle and the D50 followed a rising and falling pattern with lower repose values (higher flowability) at low and high values of the D50 (Figure 41). The same pattern was true in the case of most surface types, although low values of angle of repose at low D50 values were less apparent on polypropylene, polyvinyl chloride, and stainless-steel surfaces. A similar relationship was observed between angle of repose and small to large particle ratio (Figure 42). Samples with a very low ratio (few small particles and many large particles) tended to have a very low angle of repose, particularly on an aluminum surface. The decrease in angle of repose at high ratio values was not striking on polypropylene, polyvinyl chloride, and stainless-steel surfaces.

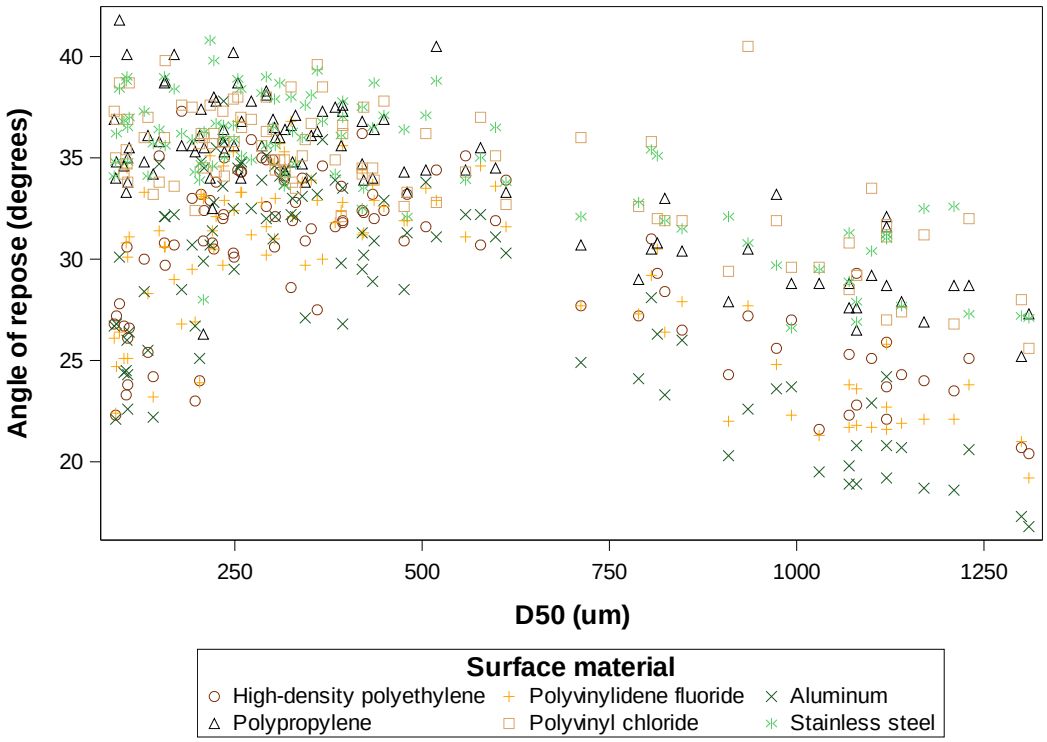

Figure 41. Angle of repose of hammer-milled yellow split pea on six surfaces versus the D50

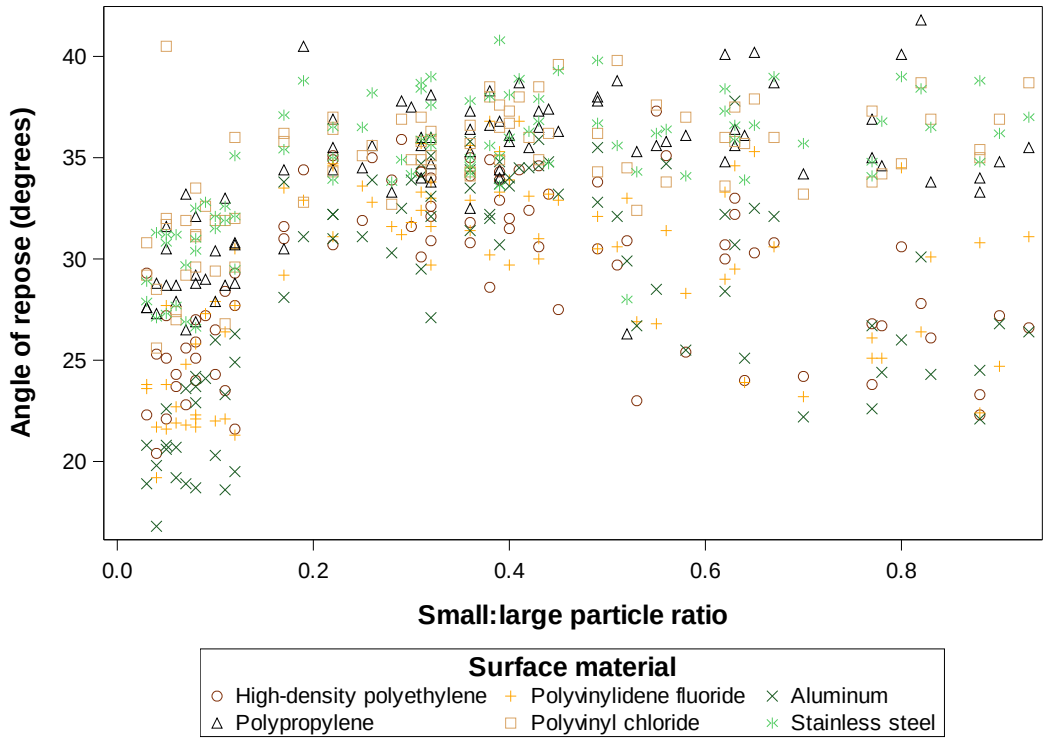

Figure 42. Angle of repose of hammer-milled yellow split pea on six surfaces versus ratio of small to large particles

The tendency of the six surfaces to fall into two groups was supported by the results of tests for differences in the mean repose values for each surface (Figure 43). There were no significant differences among polypropylene, polyvinyl chloride, and stainless-steel surfaces, where mean angle of repose was between 34 and 35 °. There were also no significant differences among high density polyethylene, polyvinylidene fluoride, and aluminum surfaces, where mean angle of repose was between 28 and 30 °. The effect of a 2 % decrease in moisture content was a small increase in angle of repose (31 and 33 ° for 11 % and 9 % seed moisture, respectively) (Figure 44), indicating lower flowability at lower seed moisture. Since there was no significant interaction between surface type and seed moisture, this relationship was constant across the surface types. Small decreases in angle of repose as moisture increases from 10 to 15 % have been reported previously for milled wheat and flax (de la Pena, 2015).

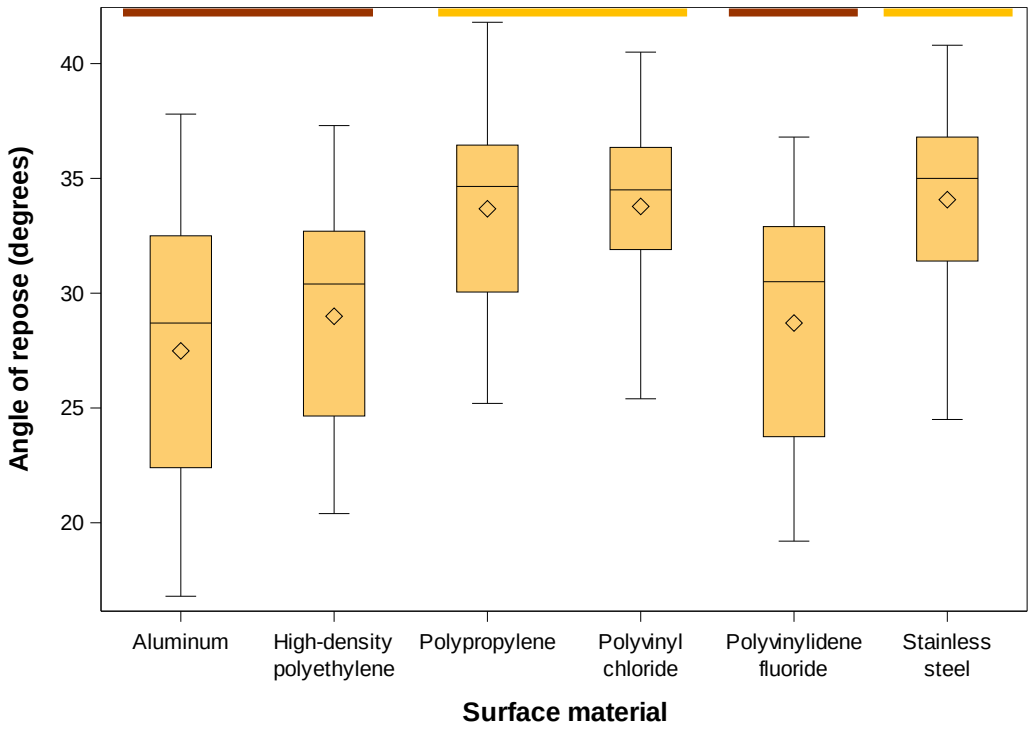

Figure 43. Boxplot of the angle of repose of hammer-milled split pea by surface type (means of treatments covered by the same colored bar were not significantly different)

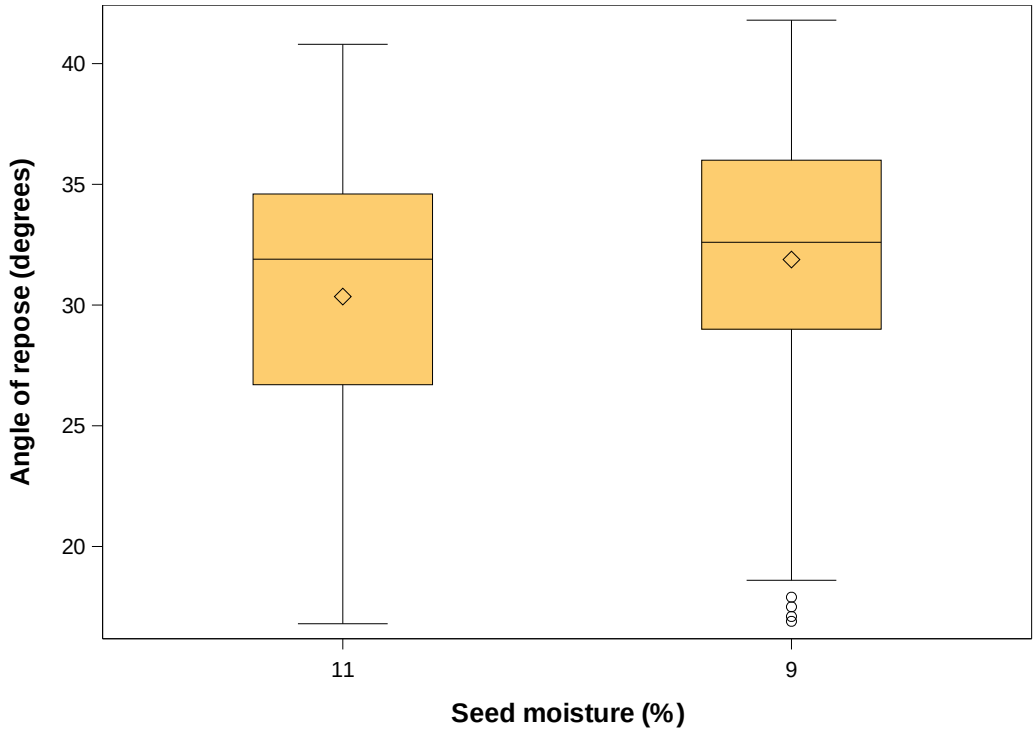

Figure 44. Boxplot of the angle of repose of hammer-milled split pea by seed moisture level

Visualization of the full model involving surface type, D50, and small to large particle ratio all at once was possible with contour plots. Observing the relationship between angle of repose and particle size on each surface was necessary due to the significant interaction between small to large particle ratio and surface type (Table 3). A plot of the observed angle of repose values showed the rising and falling relationship between angle of repose and particle size parameters, particularly the D50, on aluminum (Figure 45). A plot of angle of repose values predicted by the selected model showed that these relationships were approximately represented by the model (Figure 46). On stainless steel, the decrease of angle of repose at low particle size values was less striking than on aluminum for both observed and predicted angle of repose values (Figures 47-48).

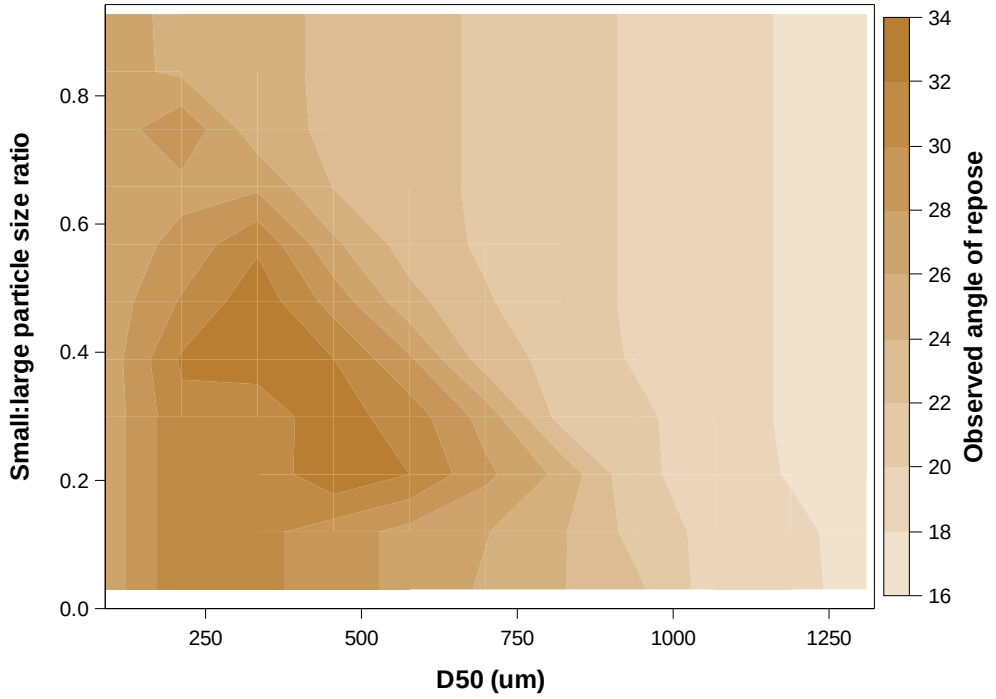

Figure 45. Contour plot of observed angle of repose of hammer-milled split pea on aluminum surface versus the D50 and small to large particle ratio

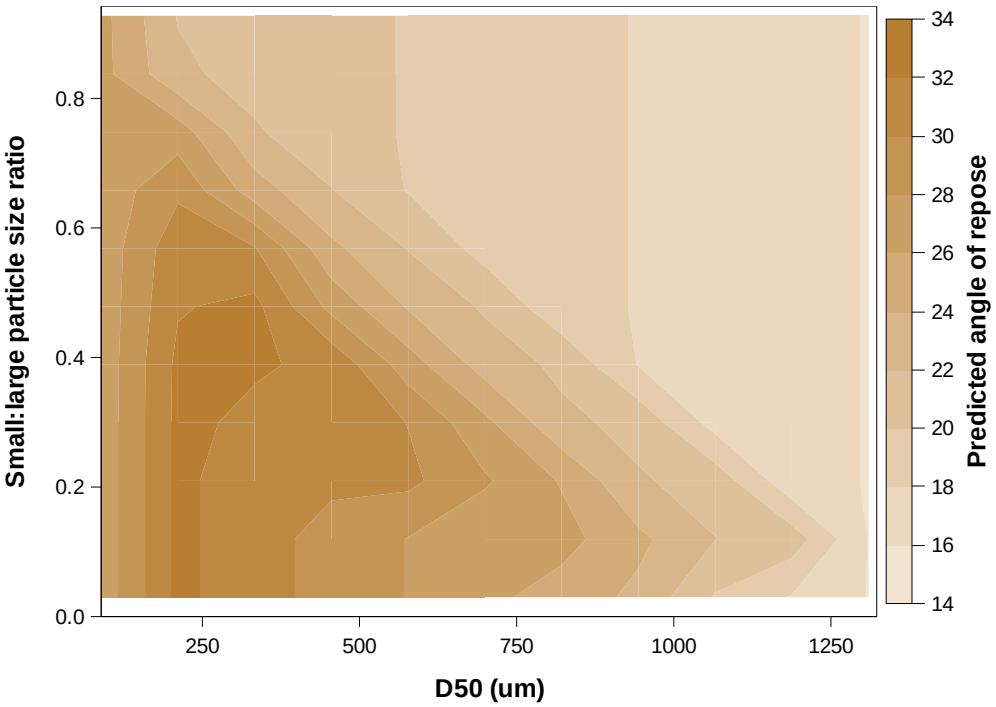

Figure 46. Contour plot of predicted angle of repose of hammer-milled split pea on aluminum surface versus the D50 and small to large particle ratio (based on a model including main and quadratic effects of both continuous variables)

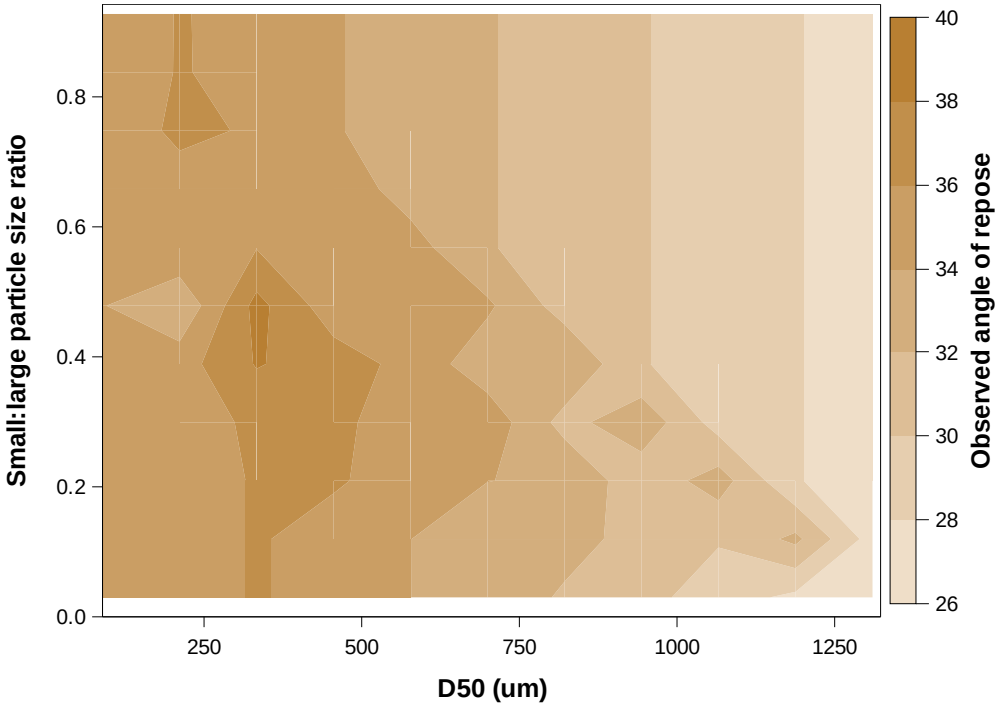

Figure 47. Contour plot of observed angle of repose of hammer-milled split pea on stainless-steel surface versus the D50 and small to large particle ratio

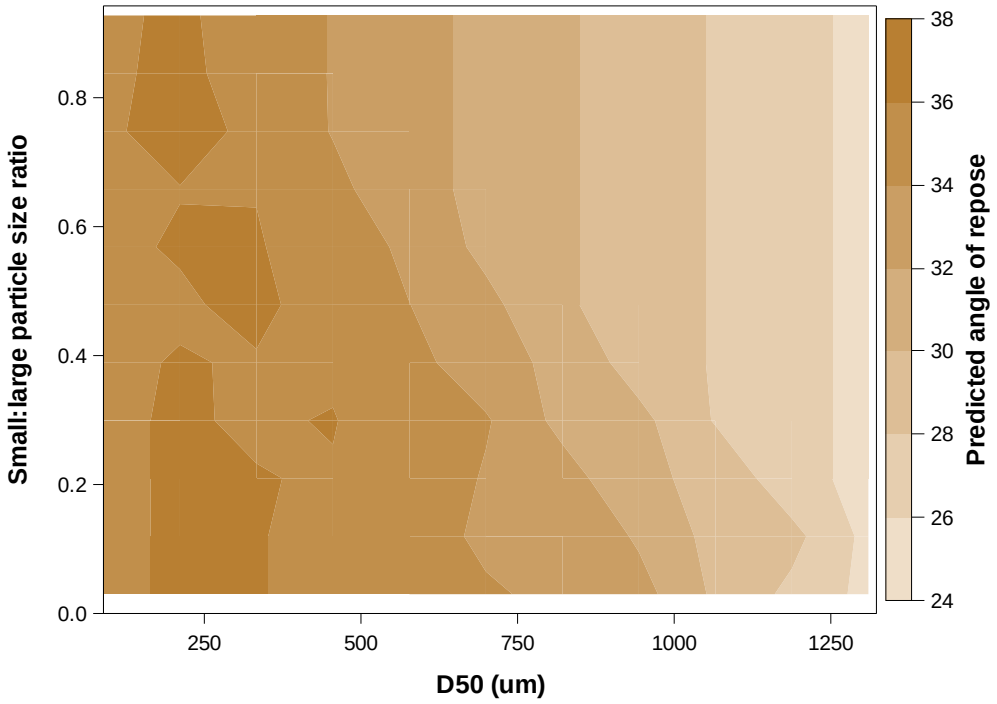

Figure 48. Contour plot of predicted angle of repose of hammer-milled split pea on stainless-steel surface versus the D50 and small to large particle ratio (based on a model including main and quadratic effects of both continuous variables)

The importance of the ratio of small to large particles in predicting angle of repose indicated that small particle volume was important in determining flow properties in milled split pea, a relationship that has been noted previously. Angle of repose has been more associated with the D10 than with any other particle characteristic in previous research (Goh, Heng & Liew, 2018). Larger D10 values and samples with lower volumes of small particles flowed better than those with large volumes of fines (particles < 32 μm). However, data from the current study suggested better flowability of samples with a very large volume of small particles than samples with intermediate volumes of small particles, particularly on aluminum, high density polyethylene, and polyvinylidene fluoride surfaces. Furthermore, median particle size was an important parameter in predicting flowability of milled field pea.

Angle of slide (θ)

Based on Mallow's C_p, R^2_{adj}, and PRESS, step 6 was chosen during model selection as the model that optimized fit and parsimony (Figure 49). Variables included at this step were surface, seed moisture, the reciprocal of D10, and the D90. Subsequent addition of interaction between surface type and moisture and between surface type and the reciprocal of the D10 resulted in the model with the best fit and significance for all factors (Table 4). Model adequacy was again moderately good (R^2_{adj} = 0.843).

Table 4. *F*-test *p*-values for the model of yellow split pea flour angle of slide

Predictor variable	*p*-value
Seed moisture	<0.0001
Surface type	<0.0001
(Seed moisture)*(Surface type)	0.0034
Reciprocal of D10	<0.0001
D90	<0.0001
(Surface type)*(Reciprocal of D10)	<0.0001

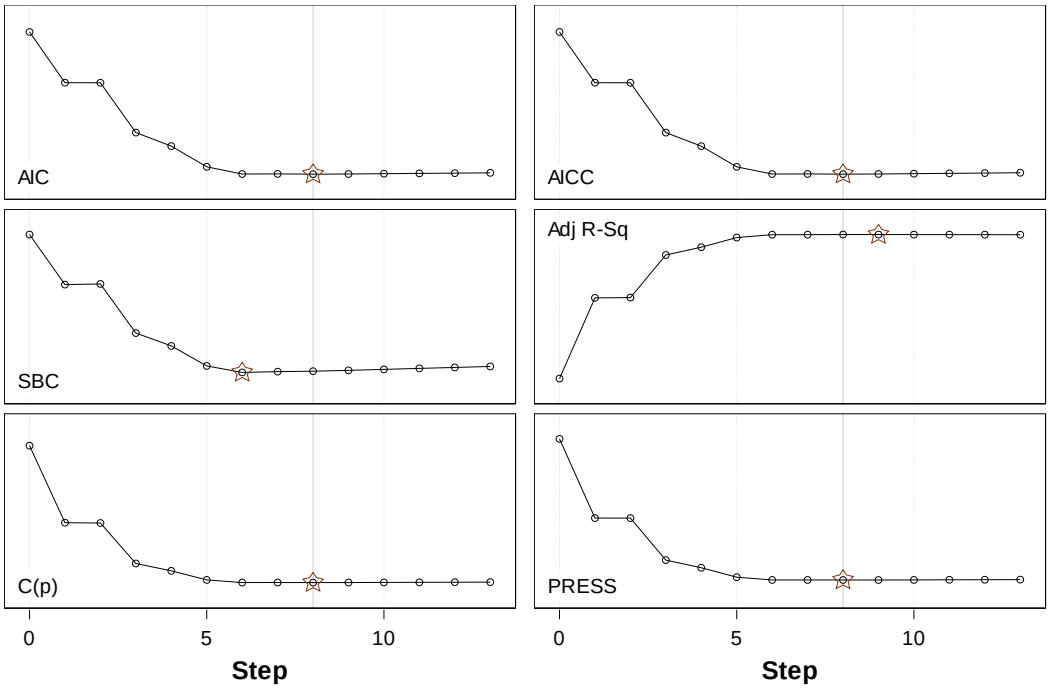

Figure 49. Progression of selection criteria for angle of slide of hammer-milled yellow split pea (AIC = Akaike Information Criterion, AIC C = Corrected AIC, SBC = Schwarz Bayesian Criterion, C(p) = Mallow's C_p, and PRESS = Predicted Residual Error Sum of Squares)

Unlike angle of repose, angle of slide had a linear relationship with some particle size parameters. Although a nonlinear pattern was apparent with the D10 (particularly at low D10 values) (Figure 50), angle of slide tended to decrease linearly with increasing D90 (Figure 51). Due to the interaction between the effect of surface type and that of seed moisture, the effects of both were considered together. Within each surface type, angle of slide differed significantly only on stainless steel and polyvinyl chloride (Figure 52). On these two surfaces, angle of slide was higher (indicating decreased flowability) at 11 % moisture than at 9 % moisture. Angle of slide was highest on high density polyethylene, intermediate on polyvinylidene fluoride, and lowest on aluminum and stainless steel, though only the 9 % moisture treatment on aluminum differed significantly from 9 % moisture treatments on polypropylene and polyvinyl chloride.

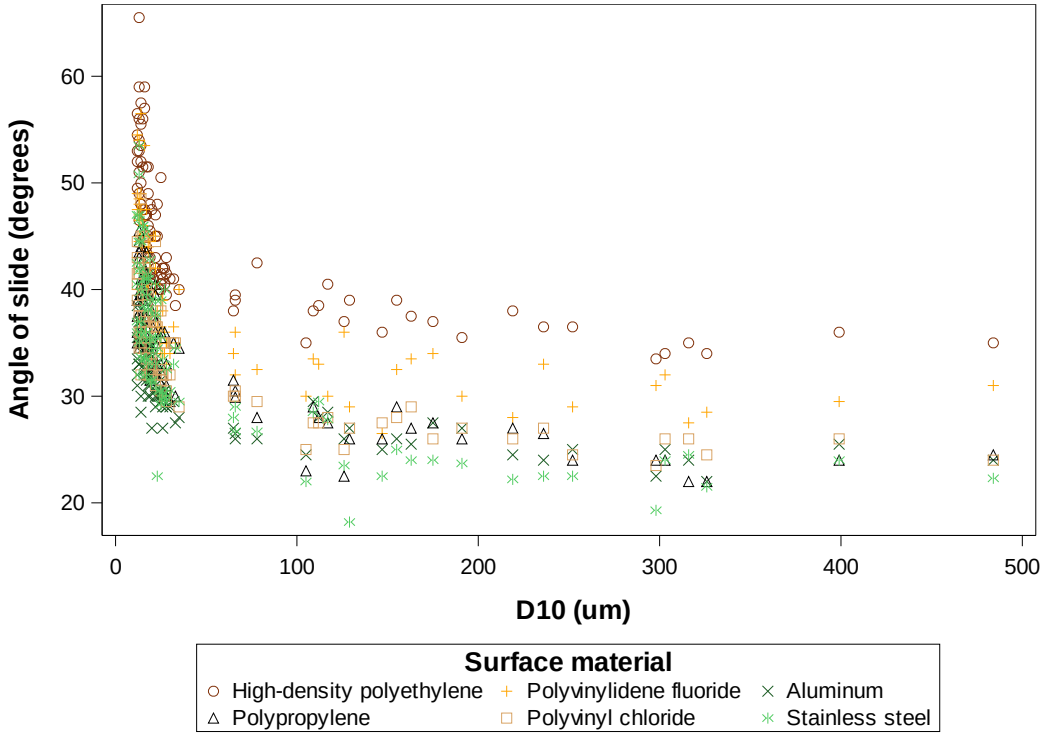

Figure 50. Angle of slide of hammer-milled yellow split pea on six surfaces versus the D10

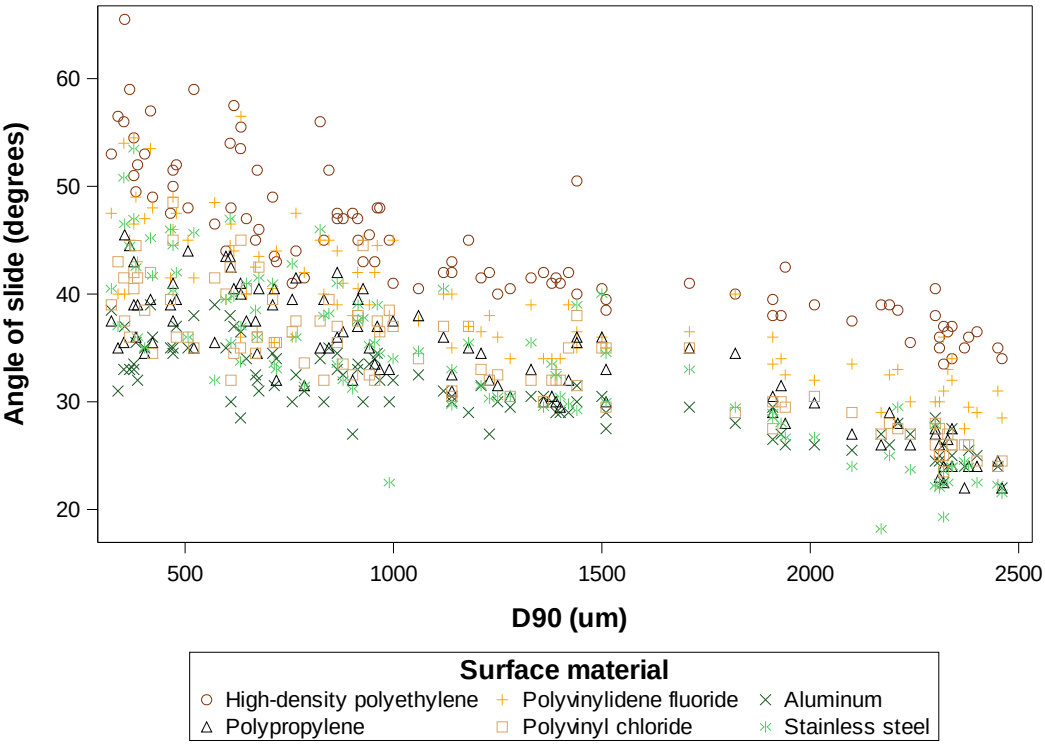

Figure 51. Angle of slide of hammer-milled yellow split pea on six surfaces versus the D90

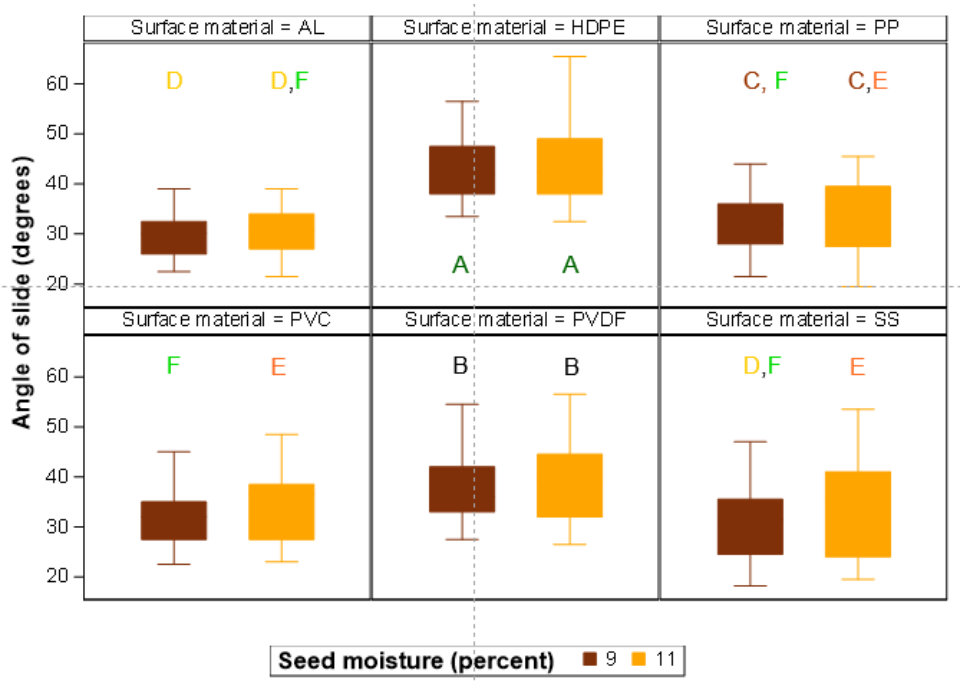

Figure 52. Interaction effect of surface and seed moisture on mean angle of slide of hammer-milled split pea—treatments with the same letter were not significantly different (surface materials: aluminum (AL), stainless steel (SS), polyvinyl chloride (PVC), polypropylene (PP), high-density polyethylene (HDPE), and polyvinylidene fluoride (PVDF))

Contour plots were again used to visualize the full model involving surface type, D10, and D90 all at once. On high density polyethylene, the contour plot showed that angle of slide was highest when both the D10 and the D90 were low (Figure 53). Angle of slide decreased more rapidly as D90 increased when the D10 was around 50 µm than when it was lower or higher than this value. This combined effect of D10 and D90 was less obvious in the contour plot of angle of slide values predicted by the model (Figure 54). A similar, though less striking, pattern was observed in the contour plots of angle of slide on an aluminum surface (Figures 55-56). Association of the angle of slide with the D90 has been noted previously (Goh et al., 2018).

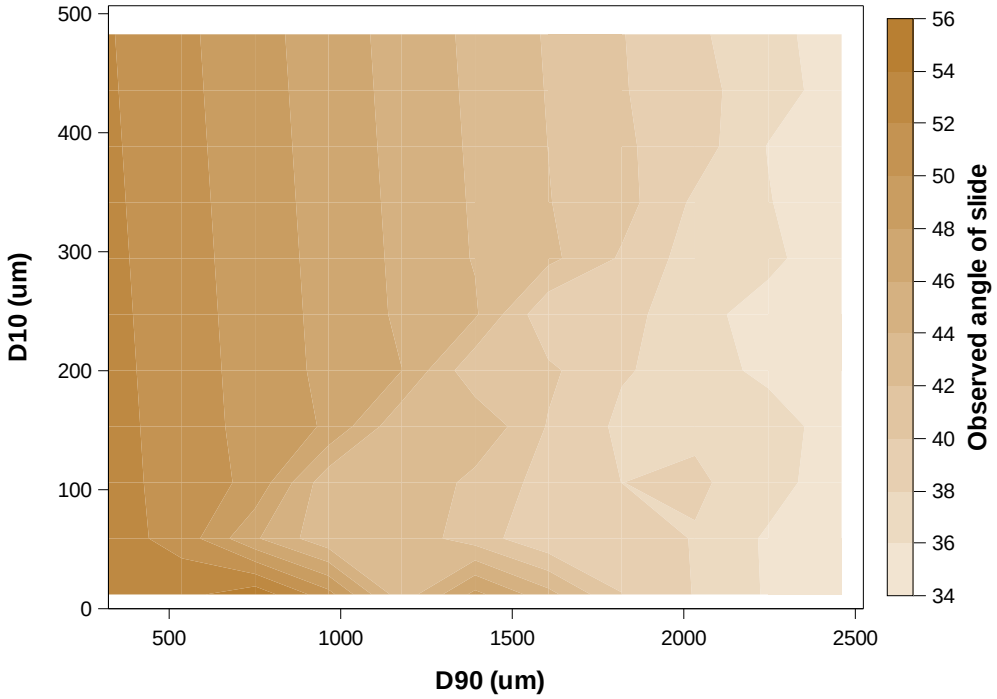

Figure 53. Contour plot of observed angle of slide of hammer-milled split pea on high density polyethylene versus the D10 and D90

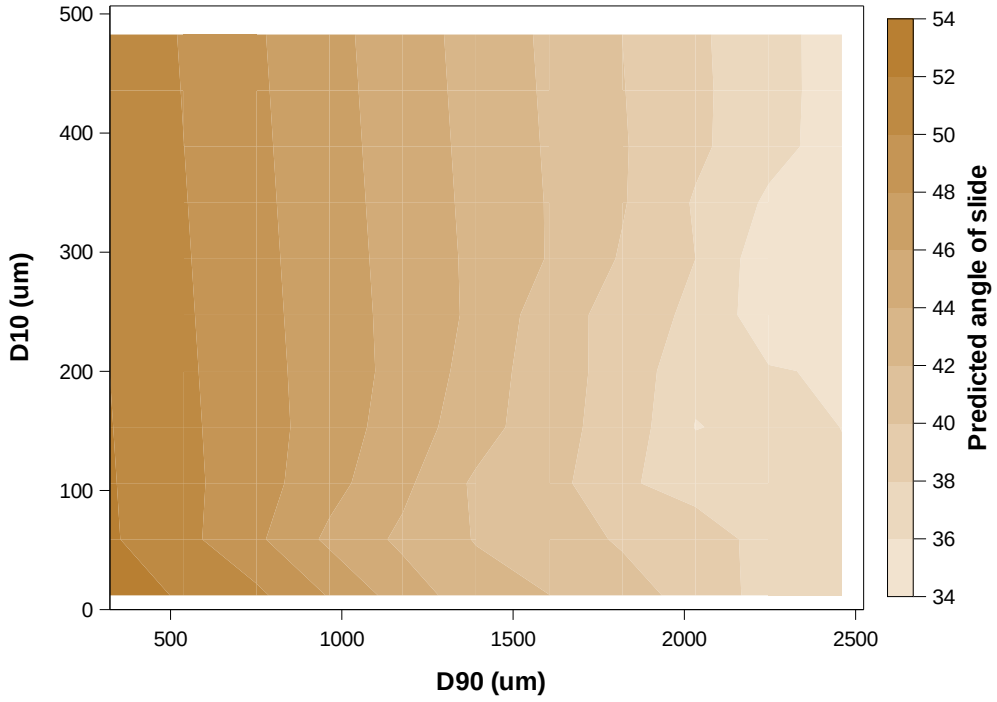

Figure 54. Contour plot of predicted angle of slide of hammer-milled split pea on high density polyethylene versus the D10 and D90 (based on a model including main and quadratic effects of both continuous variables)

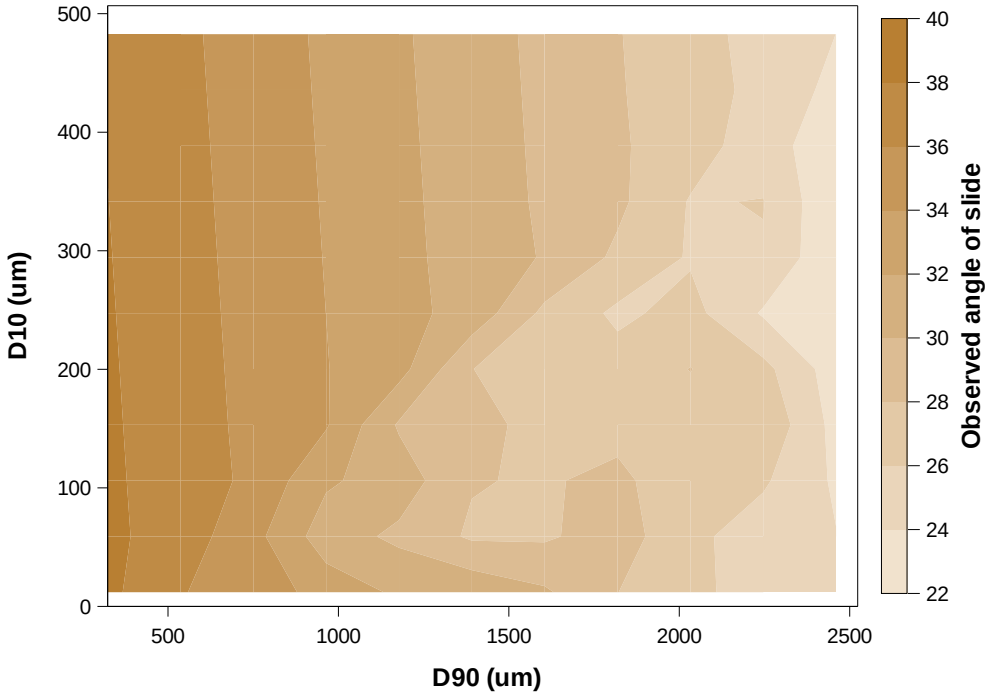

Figure 55. Contour plot of the observed angle of slide of hammer-milled split pea on aluminum versus the D10 and D90

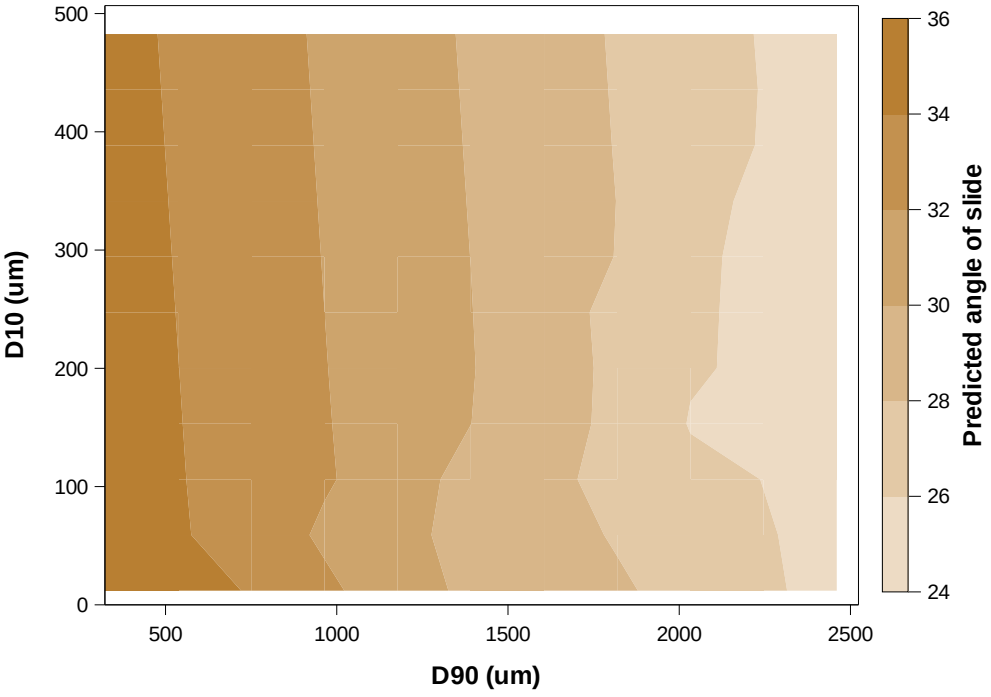

Figure 56. Contour plot of predicted angle of slide of hammer-milled split pea on aluminum versus the D10 and D90 (based on a model including main and quadratic effects of both continuous variables)

Comparing milled split pea flow properties with those of other commodities indicated that commodity-specific factors may have greater impact than particle size. Commercial semolina and yellow split pea with D50 particles sizes of 250 and 1127 µm, respectively, had similar angle of slide values (i.e., 22 and 24 °), while black soybean flour with a more comparable particle size to semolina of 150-250 µm had a higher angle of slide value of 45 ° (Table 5). Likewise, commodity-specific factors impacted values of angle of repose. For example, yellow split pea in this study had a higher angle of repose than commercial semolina despite having a larger D50 (Table 5). Others have noted that composition, which varies by commodity, as well as moisture content, which varies across and within commodities, affect flow properties (Ambrose et al., 2015; Juliano & Barbosa-Canovas, 2010). For example, agglomeration does not occur at low moisture in defatted wheat flours but does occur in non-defatted flours (Neel & Hoseney, 1984). Agglomeration at higher lipid content may be part of the explanation for the higher angle of slide of black soybean flour than that of wheat or yellow split pea of similar particle size (Table 5).

Data from the current study supported an effect of surface type on flow properties in addition to the effects of particle size and commodity. Most previous studies on flow properties have not evaluated flowability of the same commodity on multiple surfaces. Surfaces selected for flow property studies have generally been limited to glass, stainless steel, or aluminum (Table 5). Future research in the flowability of whole and milled grain should consider the impact of different surface types and include information about the coefficient of friction of the surface used, since it is a system-specific property rather than a constant of a material. It is also important to note that the variety of methods for determining angle of slide may also account for some of the variation in values reported.

Table 5. Particle size and flow property data from this study (mean for AL and SS) compared with flow properties of other commodities

Material	Particle size[a]	Surface used[b]	Alpha[c]	Theta	Source
	µm		°	°	
Yellow split pea	99	Mean of AL and SS	32	40	This study
	214		32	36	
	300		35	33	
	1127		25	24	
Adzuki bean	103	SS	nd	40-46	Park, Kim, Choung, Han & Yoon, 2015
	1599		nd	29-33	
Black soybean	150-250	SS	nd	43-47	Leen & Yoon, 2015
	1180-1400		nd	39-42	
Soybean	20**	AL	52	nd	Ricks, Barringer & Fitzpatrick, 2002
HRW wheat	39	NS	31	nd	Pordesimo, Onwulata & Carvalho, 2009
	49**	Glass	41	36-39	Bian, Sittipod, Garg & Ambrose, 2015
SRW wheat	<45	Glass	nd	24-41	Siliveru, Ambrose & Vadlani, 2016
	45-75		nd	28-33	
	75-106		nd	27-33	
	<45		nd	23-37	
	45-75		nd	28-35	
	75-106		nd	30-32	
SWW wheat	48**	Glass	42	54-60	Bian, Sittipod, Garg & Ambrose, 2015
Wheat, unspecified	51**	AL	53	nd	Ricks, Barringer & Fitzpatrick, 2002
	75	NS	31	nd	Pordesimo, Onwulata & Carvalho, 2009
	51**	SS	nd	42	Fitzpatrick, Barringer & Iqbal, 2004
Commercial WW flour	100	Mean of AL and SS	38	37	de la Pena, 2015
Commercial Semolina	250		23	22	

[a] D50, when unspecified; * indicates geometric mean particle size; ** indicates unspecified mean particle size; range indicates fraction isolated via sieving (retaining sieve to passing sieve)
[b] AL: aluminum, SS: stainless steel, NS: not specified
[c] not determined

Conclusion

The angle of repose of hammer-milled split pea flour was most closely associated with median particle size and the ratio of small to large particles. Angle of repose was quadratically, rather than linearly, related to most particle size parameters, an important observation since inappropriate linear modelling can distort or mask strong relationships between variables. Angle of repose increased as seed moisture decreased and was also affected by surface type, being lower on aluminum, high density polyethylene, and polyvinylidene fluoride and higher on stainless steel, polypropylene, and polyvinyl chloride. Angle of slide of milled pea was associated with the D10 and D90. Angle of slide appeared linearly related to most particle size parameters, but not to the D10 with which there was a reciprocal relationship. Angle of slide decreased as seed moisture decreased, but the relationship was not constant across surface types. Angle of slide was highest on high density polyethylene and lowest on aluminum surfaces. These results indicated that particle size parameters were important indicators of the flowability of milled split pea and that surface selection should be considered when assembling flour handling systems. Additionally, small changes in moisture content did affect the flow properties of milled split pea on some surfaces. This result indicated that split pea is a commodity for which moisture content may be important when considering flow properties following milling.

References

Abu-hardan, M., & Hill, S. E. (2010). Handling properties of cereal materials in the presence of moisture and oil. Powder Technology, 198:16-24. https://doi.org/10.1016/j.powtec.2009.10.002

Ambrose, R. P. K., Jan, S., & Siliveru, K. (2015). A review on flow characterization methods for cereal grain-based powders, *Journal of the Science of Food and Agriculture*, **96**:359-364. https://doi.org/ 10.1002/jsfa.7305

ASTM International. *Standard Test Methods*. (2009). Method D7481. Standard test methods for determining loose and tapped bulk densities of powders using a graduated cylinder. West Conshohoken, PA: ASTM

Bian, Q., Sittipod, S., Garg, A., & Ambrose, R. P. K. (2015). Bulk flow properties of hard and soft wheat flours. *Journal of Cereal Science*, **63**:88-94. http://dx.doi.org/10.1016/j.jcs.2015.03.010

Chang, K. S., Kim, D. W., Kim, S. S., & Jung, M. Y. (1998). Bulk flow properties of model food powder at different water activity. *International Journal of Food Properties*, **1**:45-55. https://doi.org/10.1080/10942919809524564

de la Pena, E. (2015). *Manufacturing optimization of non-traditional pasta products* (Doctoral dissertation). Ann Arbor, MI: ProQuest Dissertations and Theses. UMI 3685795.

Efron, B., Hastie, T., Johnstone, I., & Tibshirani, R. (2004). Least angle regression (with discussion). *Annals of Statistics*, **32**:407-499.

Fitzpatrick, J. J., Barringer, S. A., & Iqbal, T. (2004). Flow property measurement of food powders and sensitivity of Jenike's hopper design methodology to the measured values. *Journal of Food Engineering*,**61**:399-405. https://doi.org/10.1016/S0260-8774(03)00147-X

Geldart, D., Abdullah, E. C., & Verlinden, A. (2009). Characterisation of dry powders. *Powder Technology*, **190**:70-74. https://doi.org/10.1016/j.powtec.2008.04.089

Goh, H. P., Heng, P. W. S., & Liew, C. V. (2018). Comparative evaluation of powder flow parameters with reference to particle size and shape. *International Journal of Pharmaceutics*, **547**:133-141. https://doi.org/10.1016/j.ijpharm.2018.05.059

Ileleji, K. E., & Zhou, B. (2008). The angle of repose of bulk corn stover particles. *Powder Technology*, **187**:110-118. https://doi.org/10.1016/j.powtec.2008.01.029

Jan, S., Karde, V., Ghoroi, C., & Saxena, D. C. (2018). Effect of particle and surface properties on flowability of rice flours. *Food Bioscience*, **23**:38-44. https://doi.org/10.1016/j.fbio.2018.03.001

Juliano, P., & Barbosa-Canovas, G. V. (2010). Food powders flowability characterization: theory, methods, and applications. *Annual Reviews in Food Science and Technology*, **1**:211-239. https://doi.org/10.1146/annurev.food.102308.124155

Lee, Y. J., & Yoon, W. B. (2015). Flow behavior and hopper design for black soybean powders by particle size. *Journal of Food Engineering*, **144**:10-19. http://dx.doi.org/10.1016/j.jfoodeng.2014.07.005

Neel, D. V., & Hoseney, R. C. (1984). Factors affecting flowability of hard and soft wheat flours. *Cereal Chemistry*, **61**:262-266.

Park, H. W., Kim, S. T., Choung, M. G., Han W. Y., & Yoon, W. B. (2015). Analysis of grinding kinetics and flow behavior of adzuki bean (*Phaseolus angularis*) flour for hopper design, *Journal of Food Process Engineering*, **39**:366-376. https://doi.org/ 10.1111/jfpe.12229

Pordesimo, L. O., Onwulata, C. I., & Carvalho, C. W. P. (2009). Food powder delivery through a feeder system: effect of physicochemical properties. *International Journal of Food Properties*, **12**:556-570. https://doi.org/10.1080/10942910801947748

Probst, K. V., Ambrose, R. P. K., Pinto, R. L., Bali, R., Krishnakumar, P., & Ileleji, K. E. (2013). The effect of moisture content on the grinding performance of corn and corncobs by hammermilling. *Transactions of the ASABE*, **56**:1025-1033.

Ricks, N. P., Barringer, S. A., & Fitzpatrick J. J. (2002). Food powder characteristics important to nonelectrostatic and electrostatic coating and dustiness. *Journal of Food Science*, **67**:2256-2263. https://doi.org/10.1111/j.1365-2621.2002.tb09537.x

Siliveru, K., Ambrose, R. P. K., & Vadlani, P. V. (2016). Significance of composition and particle size on the shear flow properties of wheat flour. *Journal of the Science of Food and Agriculture*, **97**:2300-2306. https://doi.org/10.1002/jsfa.8038

U.S. Dry Pea & Lentil Council. (2017). *2017 U.S. Pulse Quality Survey*. Moscow, ID: U.S. Dry Pea and Lentil Council.

Yan, H., and Barbosa-Canovas, G. V. 1997. Compression characteristics of agglomerated food powders: Effect of agglomerate size and water activity. *Food Science and Technology International*, **3**:351-359.

PAPER 3. COMPOSITION AND FUNCTIONALITY OF HAMMER- AND ROLLER-MILLED YELLOW SPLIT PEA (*PISUM SATIVUM* L.)

Abstract

Pulse milling continues to be a research focus as consumer interest in cereal-based, pulse-containing convenience foods grows. While roller milling is the standard method for wheat flour production, no standard method exists for producing pulse flour. A hammer mill is a relatively simple and cost-effective method of size reduction that may be available to more food processors than the traditional roller milling system. Yellow split pea milled to a similar particle size via hammer and roller milling systems was compared to determine properties of hammer-milled and roller-milled pea flour. Yellow split pea at 11 % moisture was hammer-milled at 102 m/s through a 0.84 mm screen and roller-milled using a two-pass setup with an intermediate sieving process. Flours from both processes underwent a final sieving through a 150 µm screen. Flour moisture content was lower after hammer milling (10.6 %) than roller milling (11.0 %). Peak and final viscosities were higher for roller-milled flour (2,688 and 5,436 cP, respectively) than for hammer-milled flour (2,478 and 4,806 cP, respectively). Damaged starch content (3.5 % vs. 2.0 %), 10^{th} percentile of particle size (13 µm vs. 10 µm), and oil binding capacity (1.14 vs. 0.91 g/g) were also higher in roller-milled flour than in hammer-milled flour. No significant differences were observed between the two treatments for any of the other compositional or functional parameters evaluated.

Introduction

Protein and fiber content claims continue to be desirable to product formulators, and fortification of cereal-based products with pulses can help achieve these claims in a way that might be positively perceived by the public. The purpose of pulse milling, as with cereal grains,

is to permit such utilization by accomplishing size reduction for ingredient blending, eliciting chemical changes such as starch damage, and facilitating component separation (i.e. starch, protein, and fiber) where desired (Thakur, Scanlon, Tyler, Milani & Paliwal, 2019). Mill type and setup and milled product classification are factors that control the quality of pulse flour, that is, its physical, chemical, and functional attributes.

The milling of cereal grains has been performed for many years and literature on grain milling and flour quality, particularly in the case of wheat, is extensive. However, except for the dehulling process, pulse milling is a relatively new field without extensive peer-reviewed research. The standard for wheat flour production is a well-defined roller-milling and sieving process (Posner & Hibbs, 2005), but standards for milling method and flour quality and even a formal definition for pulse flour have not yet been selected. Such standardization could promote consistency in milled pulse ingredients that would encourage further application in the industry. However, prior to such an outcome, additional information is needed on what constitutes quality for pulse flours and what milling methods are appropriate to produce quality milled pulse products. Some studies have already been completed to investigate the role of milling on pulse quality and functionality (Indira & Bhattacharya, 2006; Kerr, Ward, McWatters & Ressureccion, 2000; Maaroufi, Melcion, De Monredon, Giboulot, Guibert & Le Guen, 2000; Maskus, Bourre, Fraser, Sarkar & Malcolmson, 2016; Pelgrom, Vissers, Boom & Shuteyser, 2013; Singh, Hung, Corredig, Phillips, Chinnan & McWatters, 2005; Vishwanathan & Subramanian, 2014). However, the milling methods for different mill types are not designed to produce comparable particle sizes in these studies. As a result, the effect of mill type on pulse flour quality is confounded with the effect of particle size. The goal of this research was to design hammer- and roller-milling protocols that produced split pea flour with a comparable particle size range to

permit a more direct comparison of the effect of milling method on flour quality. The hypothesis was that the apparent effect of mill type would be much less dramatic once the effect of particle size was removed.

Materials and Methods

Sample preparation

Yellow split pea (11 % moisture) from the 2016 crop was obtained from three different North Dakota sources and was blended in an Eirich FPB-005 blender (Eirich, Hardheim, Germany) for 1 min. Subsamples of 10 kg were taken from the blended raw material. Three replicates were milled on a hammer mill (Model DASO6, Fitzpatrick, Elmhurst, IL) at 2.3 kg/min feed rate, 102 m/s hammer speed, and 0.838 mm diameter screen aperture. Three replicates were milled in two passes on a roller mill (roll stands by Creason, Wichita, KS; rolls by Buhler AG, Uzwil, Switzerland). The first pass was at 0.7 kg/min feed rate with corrugated rolls (8 % spiral, 0.1 mm land, 8.9 flutes per cm, 0.254 mm roll gap) using sharp to sharp action and a front/back roll speed differential of 1:2.5. After the first pass, the milled material was passed through a 707 µm screen using a pilot-sized sieve box (Great Western Manufacturing, Leavenworth, KS). The throughs from this screening step were retained for the second pass, which was at 0.3 kg/min feed rate with smooth rolls (0.038 mm roll gap) and a 1:1.23 front/back roll speed differential. To achieve comparable particle size properties, milled pea flours were sifted with a 150 µm screen. The throughs were retained as the final pea flour samples. Extraction for the hammer-milled samples was approximately 60 %.

Proximate analysis

Moisture, crude protein, total starch, and ash contents were obtained for samples per AACC International Approved methods 44-15.02, 46-30.01, 76-13.01, and 08-01.01,

respectively. Total, soluble, and insoluble dietary fiber content was determined per AACC International Approved method 32-50.01 using an Ankom Technology automated dietary fiber analyzer.

Carotenoid content

Carotenoid content was determined using a modified method of Ashokkumar, Diapari, Jha, Tar'an, Arganosa & Warkentin (2015). Carotenoids were extracted from samples via mixing with a magnetic stir bar for 1 h with 1:1 dichloromethane/methanol at a ratio of 2.5 ml solvent/g sample. After adding an equal volume of acetonitrile, the sample was centrifuged at 5,000 x *g* for 10 min. The supernatant was filtered (0.45 µm nylon), placed in 1 ml amber glass HPLC vials and kept at -20 ° C until analysis. Lutein (97 % min purity from Sigma-Aldrich, St. Louis, MO) was used at four levels to generate the calibration curve. Chromatography was performed using a Waters 2795 separations module (Waters Corporation, Milford, MA) equipped with a Waters 996 photodiode array detector. Separation was done using a YMC C30 carotenoid column (3 µm, 4.6 x 250 mm) (Columnex LLC, Tracy, CA) at 40 ° C with a mobile phase of acetonitrile/methanol/dichloromethane (58:22:20 v/v/v). The solvent flow rate was 0.8 ml/min, injection volume was 20 µl, and total run time was 20 min. Every sample run was followed by a 20-min column wash. Detection was accomplished using a diode-array detector in the range 400-500 nm.

SDS-PAGE

Comparison of protein size profile was determined via SDS-PAGE following a modified method of Ma, Boye & Hu (2017). Proteins were extracted by mixing 100 mg flour with 1 ml Laemmli buffer containing 2% β-mercaptoethanol. Samples were heated at 100 ° C for 5 min, cooled, and centrifuged at 5000 x *g* for 15 min. The supernatant was further diluted 1:4 with

Laemmli buffer/β-mercaptoethanol, and 10 µl of the diluted samples were run on a Bio-Rad (Hercules, CA) pre-cast Mini-PROTEAN TGX 4-20% gradient polyacrylamide gel. Electrophoresis was carried out at 200 V in a Bio-Rad Mini-PROTEAN II cell using 25 mM Tris, 192 mM glycine, 0.1% SDS running buffer. Low-Range and Natural High-Range SDS-PAGE standards from Bio-Rad (Hercules, CA) were used as molecular markers. Gel was stained with 0.25 % Coomassie Brilliant Blue R (Bio-Rad, Hercules, CA) dissolved in 1:5:4 acetic acid/methanol/water and destained in 1:1.5:7.5 acetic acid/methanol/water.

Particle size and bulk density

Particle size distribution curves and the D10, D50, and D90 were determined using a Mastersizer 3000 laser particle size analyzer (Malvern, Worcestershire, UK) with a dry powder dispersion unit. Bulk density was obtained for samples following the loose bulk density method described in ASTM D7481-09 (ASTM International, 2009). In this method, 250 mL of flour was measured without any tapping or shaking using a graduated cylinder and then weighed.

Flow properties

Angle of repose (α) and angle of slide (θ) were determined on aluminum (AL), stainless steel (SS), polyvinyl chloride (PVC), polypropylene (PP), high-density polyethylene (HDPE), and polyvinylidene fluoride (PVDF) using the method of de la Pena (2015). For α, 200 g of sample was poured slowly down a chute to pass through a funnel and into a 7.8 x 12.8 cm metal cup resting on one of the selected surfaces. The metal cup was removed vertically, allowing flour to spread across the surface in a pile. Angle of repose was calculated as the arc tangent of pile height divided by pile radius (calculated as half the mean diameter, from 2 determinations). For θ, the angle of the surface was gradually increased until the majority (> ~180 g) of the material

had slid down. Angle of slide was measured with a protractor as the angle made between the surface at the end of the experiment and the horizontal.

Color

Color was measured with a Miniscan EZ 4500L (Hunter Associates Laboratory, Inc., Reston, VA) and reported in Hunter Lab color space.

Scanning electron microscopy

Flour samples were applied to adhesive carbon tabs on cylindrical aluminum mounts, and the excess blown off gently with a stream of nitrogen gas. They were then sputter coated (Model SCD 030, Balzers, Liechtenstein) with gold-palladium to make them electrically conductive. The samples were viewed, and images were obtained with a JEOL JSM-6490LV scanning electron microscope (JEOL USA, Peabody, Massachusetts) at an accelerating voltage of 15 kV.

Pasting properties and starch damage

Pasting properties were determined with a rapid visco analyzer (RVA 4500, Perten Instruments, Springfield, IL) per AACC International Approved Method 61-02.01 with extension of the final hold time to 12 min. Damaged starch was estimated using the Megazyme starch damage assay kit (Megazyme, Inc., Bray, Ireland) per AACC International Approved Method 76-31.01.

Syneresis and freeze-thaw stability

Syneresis of starch gels prepared with milled pea flour was determined by the method of Ashwar, Gani, Shah & Masoodi (2017) with some modification. Starch suspensions (7.5 %, dry basis) were heated in a 90 ° C water bath for 30 min with intermittent vortexing. Gels were cooled at room temperature for 2 h, then stored at 4 ° C for 0, 24, 48, 72, and 96 h prior to centrifugation at 1000 x *g* for 10 min. Weight of exuded water (removed via pipette from gel

surface) was determined and used to calculate syneresis as the ratio of exuded water weight to original gel weight. Freeze-thaw (F/T) stability of starch gels was determined using a similar method. Starch gels were prepared in the same manner as for syneresis, but were stored at -20 ° C. Every 24 h, gels were thawed at 30 ° C for 2 h and then returned to -20 ° C storage. After the thawing cycle at 0, 48, and 96 h, the gels were centrifuged at 1000 x *g* for 10 min and the weight of the exuded water (removed via pipette from gel surface) was determined and used to calculate F/T stability as the ratio of exuded water weight to original gel weight.

Water and oil absorption capacity

Water and oil absorption capacities (WAC and OAC, respectively) were determined per the method of Maskus et al. (2016). Sample suspensions (10 % in water or safflower oil) were vortexed on high for 30 s and then incubated at room temperature for 30 min. Samples were centrifuged at 2000 x *g* for 30 min, the supernatant was discarded, and tubes were inverted and drained for 10 min. The weight of the remaining gel was determined and WAC and OAC were expressed as g absorbed fluid per g flour on a dry basis.

Foaming and emulsion functionality

Foaming capacity (FC) and stability (FS) were determined using the method of Maskus et al. (2016). Sample suspensions (2 % in water) were homogenized for 1 min at 13,000 rpm using an ULTRA-TURRAX T-25 homogenizer (IKA, Wilmington, NC). Foam was transferred to a graduated cylinder and the total and expelled liquid volumes were measured at 0, 10, 30, and 60 min. The % FC was calculated based on the % change in total volume immediately after homogenization, while the % FS was calculated based on the % change in foam volume (total volume minus expelled liquid volume) at 0, 10, 30, and 60 min after homogenization.

Emulsion capacity (EC) and stability (ES) were determined per the method of Maskus et al. (2016). Sample suspensions (1 % in water) were mixed with an equal volume of safflower oil and homogenized for 1 min by vortexing on high. EC was determined immediately after vortexing by centrifuging the sample at 1100 x g for 5 min, and then recording the height of the emulsion layer and the height of the total tube content in mm. The % EC was calculated using the following equation:

$$\text{Emulsion capacity (\%)} = \frac{height\ of\ emulsified\ layer}{height\ of\ tube\ contents} * 100 * \frac{100}{100 - flour\ moisture}$$

ES was determined by heating emulsions at 80 ° C for 30 min prior to centrifugation, collecting the same height data as for EC, and calculating the % ES using the above equation for % EC.

Statistical analysis

Milling treatments were applied in triplicate. Statistical analysis was performed with SAS 9.4 (SAS Institute Inc., Cary, NC) (Appendix A). Due to the large number of hypothesis tests (47) performed to evaluate the difference between two small samples, raw *p*-values were adjusted to control for the false discovery rate (FDR). The MULTTEST procedure was used to calculate *q*-values for the multiple *t*-tests of difference between means and the CORR procedure was used to obtain Pearson correlation coefficients between selected variables (Storey, 2002; Storey, Taylor & Siegmund, 2004). A *q*-value < 0.05 was considered statistically significant for all tests.

Results and Discussion

With the false discovery rate restrained to 5 % (indicating that no more than 5 % of rejected hypotheses were Type I errors), only six of the forty-seven flour quality parameters differed significantly ($q < 0.05$) between the two milling treatments (Table 6; for raw data from

all 47 quality determinations, see Table 1 in Appendix A). These six quality parameters were water content, D10, oil binding capacity, starch damage, and peak and final viscosities.

Table 6. Raw *p*-values and *q*-values for *t*-tests for differences in quality parameters of roller and hammer milled split pea flour

Variable	Raw *p*-value	FDR *q*-value
Oil binding capacity	0.0005	0.0089
Water content	0.0006	0.0089
Starch damage	0.0010	0.0100
Peak viscosity	0.0019	0.0149
Final viscosity	0.0037	0.0188
D10	0.0031	0.0188
Breakdown viscosity	0.0171	0.0652
Ash content	0.0161	0.0652
Angle of repose, HDPE	0.0215	0.0729
Angle of repose, PP	0.0455	0.0939
Angle of slide, PVC	0.0382	0.0939
D50	0.0437	0.0939
Initial syneresis	0.0364	0.0939
Syneresis after 4 freeze-thaw cycles	0.0414	0.0939
Foaming capacity	0.0460	0.0939

The moisture content of hammer-milled split pea flour was lower than that of roller-milled split pea flour (Figure 57). This small difference of ~0.5 % moisture may be due to increased water loss from slightly more surface area in the hammer-milled samples. The D10, D50, and D90 were 10, 31, and 114 µm for hammer-milled samples and 13, 39, and 127 µm for roller-milled samples, though only the D10 was statistically different between the two samples ($q < 0.05$) (Table 6, Figure 58). Additionally, moisture content had significant positive correlation with the D10 ($p < 0.05$, $r = 0.935$), though not with the D50 or D90, supporting the idea that an

increase in small particle volume resulted in increased sample water loss. In a previous comparison of hammer- and roller-milling of yellow split pea, hammer milling resulted in larger particle sizes than roller milling (15, 142, and 406 as opposed to 14, 49, and 132 µm for the D10, D50, and D90 of hammer- and roller-milled samples, respectively) (Maskus et al., 2016). However, these milling treatments differed from the ones used in this study and did not include a sieving step in hammer-milled sample production.

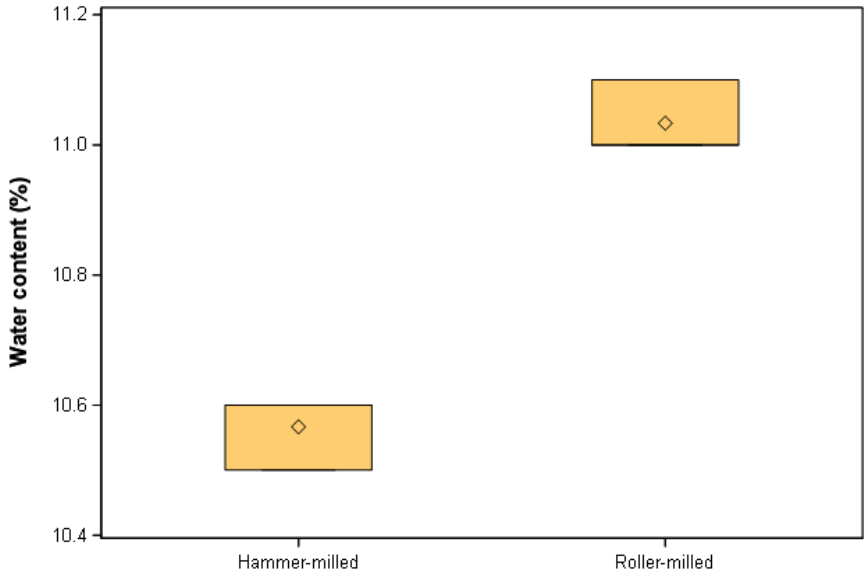

Figure 57. Boxplot of water content in hammer- and roller-milled split pea

Oil binding capacity was significantly lower in hammer-milled (0.91 g/g) than in roller-milled samples (1.14 g/g) ($q < 0.05$) (Figure 59) and in both cases was slightly lower than previously reported values (1.12 and 1.35 g/g for hammer- and roller-milled split pea, respectively) (Maskus et al., 2016). Oil binding capacity was also positively correlated with D10 ($p < 0.05$, $r = 0.979$) and D50 ($p < 0.05$, $r = 0.908$). Previously, oil binding capacity was higher in roller-milled and coarsely pin-milled samples and lower in hammer-milled and finely pin-milled samples (Maskus et al., 2016). The explanation for these results may be that oil binding capacity of high-fiber ingredients such as pulse flours is related to physical entrapment of oil via

a fiber matrix rather than chemical affinity between oil and seed constituents (Masli, Rasco & Ganjyal, 2018). Large particles may reduce fat binding due to low exposure of fiber molecules for fiber matrix formation, as was the case with coarse stone- or hammer-milled split pea with D90 values of 406 and 706 µm, respectively (Maskus et al., 2016). However, very small particles may also reduce fat binding due to disruption of the fiber matrix structure (Zheng & Li, 2018) as was the case with fine pin-milled split pea with D10, D50, and D90 of 6, 25, and 113 µm (Maskus et al., 2016). Therefore, if oil binding capacity is a priority, it may be best to prioritize a milling method that results in a narrow particle size distribution with mostly moderately-small particles. Optimal fat binding at moderately small particle size has also been observed in other powdered high-fiber products (Huang, Dou, Li & Wang, 2018).

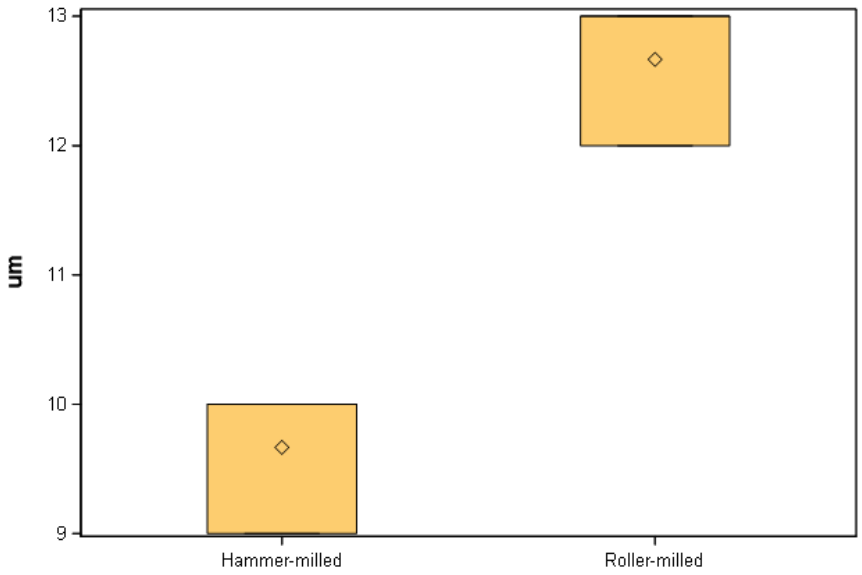

Figure 58. Boxplot of the D10 of hammer- and roller-milled split pea

Starch damage was lower in hammer-milled (2.0 %) than roller-milled (3.5 %) split pea (Figure 60). Higher starch damage in roller-milled split pea (~3.0 %) than in hammer-milled split pea (~1.3 %) has been observed previously (Maskus et al., 2016). While milling procedures in the aforementioned study resulted in wide particle size distribution differences between hammer-

and roller-milled samples, data from this research supported lower starch damage from hammer milling than from roller milling when particle size distributions were comparable.

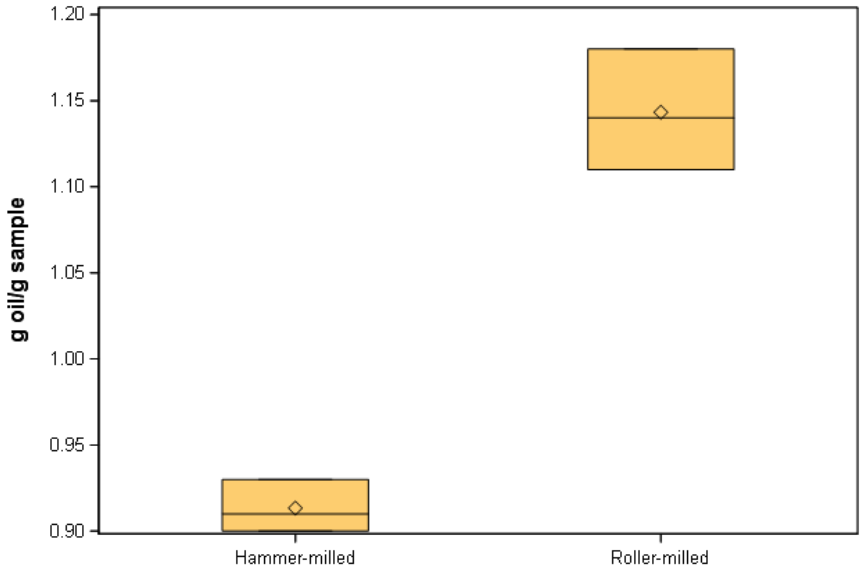

Figure 59. Boxplot of the oil binding capacity of hammer- and roller-milled split pea

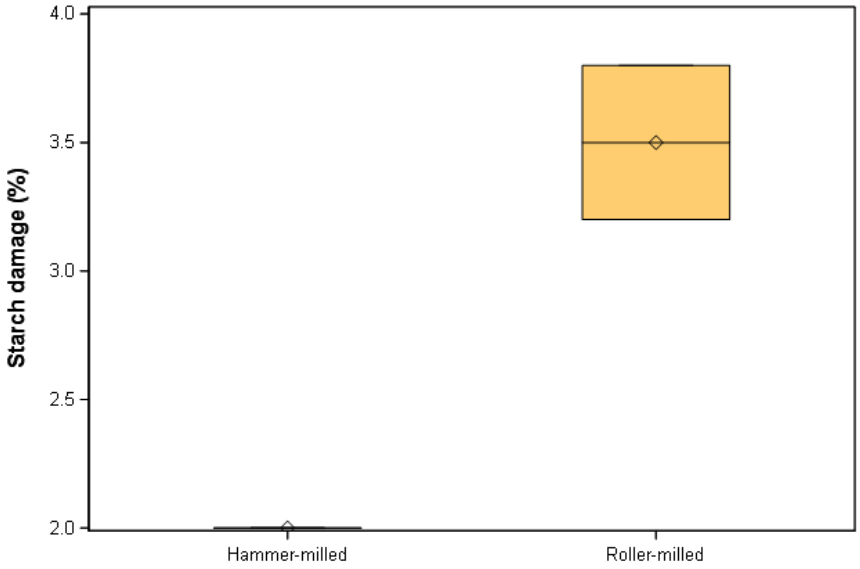

Figure 60. Boxplot of starch damage in hammer- and roller-milled yellow split pea

Starch damage was correlated with both peak ($p < 0.05$, $r = 0.952$) and final viscosities ($p < 0.05$, $r = 0.981$). Starch damage can affect pasting viscosities by impacting granule hydration and the extent of amylose leaching. Both peak and final viscosities were also significantly

different for milling method ($q < 0.05$) (Figures 61 and 62). Hammer-milled split pea had lower peak and final viscosities (2,478 and 4,806 cP) than roller-milled split pea (2,688 and 5,436 cP). These differences equated to a 7.8 % reduction in peak and 13 % reduction in final viscosities in hammer-milled samples, which is much lower than the ~40 % reduction in both peak and final viscosities reported previously for hammer milling rather than roller milling (Maskus et al., 2016). It is possible that part of the difference in pasting functionality between hammer- and roller-milled pea reported previously has been due to large differences in particle size rather than differences due specifically to milling method. Therefore, while the difference in damaged starch was approximately the same as reported previously between the two milling methods, differences in pasting properties were less pronounced at comparable particle size.

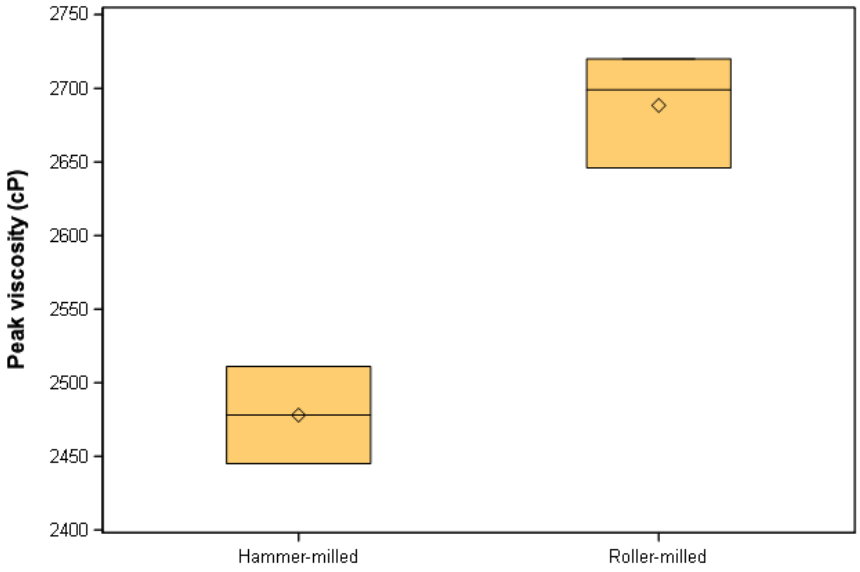

Figure 61. Boxplot of peak viscosity of hammer- and roller-milled yellow split pea

SEM images did not reveal any apparent visual differences between hammer- and roller-milled split pea (Figures 63 and 64). Absence of visually damaged starch granules concurred with the low damaged starch content indicated in the enzyme assay. SDS-PAGE also did not indicate any difference in the proteins present in the two milled samples (Figure 65). Protein size

ranged from < 4 to 97 kDa. Banding patterns concurred with those reported previously for split yellow pea flour, indicating the presence of protease inhibitors and albumins (~8-26 kDa), vicilins and lectins (~30-52 kDa), and legumins, convicilins, and lipoxygenases (~65-98 kDa) (Ma et al., 2017).

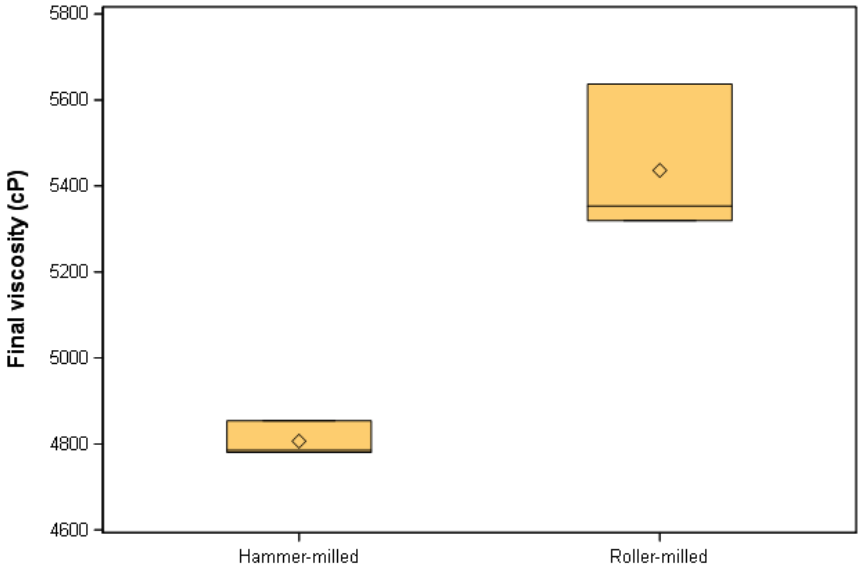

Figure 62. Boxplot of final viscosity of hammer- and roller-milled yellow split pea

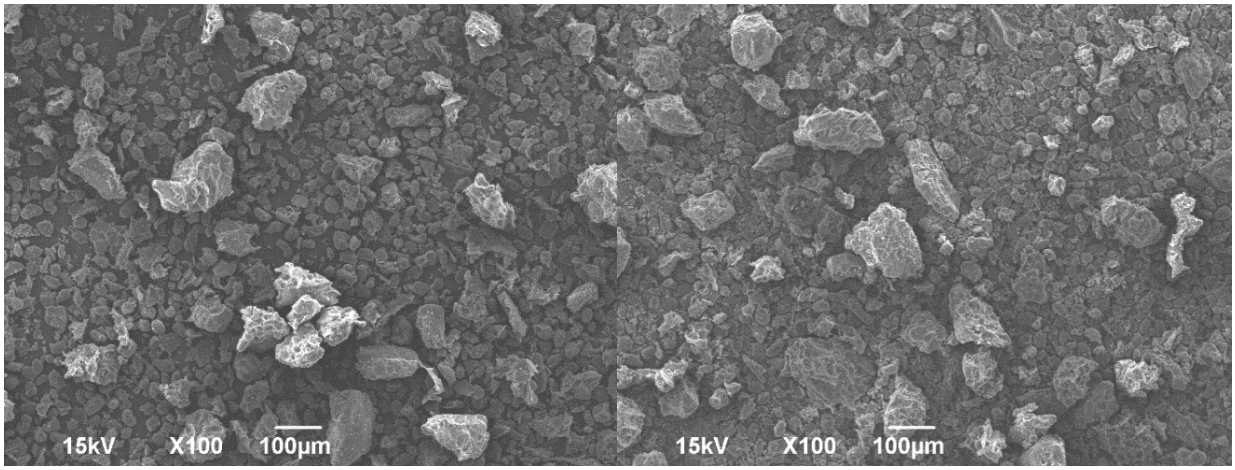

Figure 63. SEM images of roller-milled (left) and hammer-milled (right) split pea

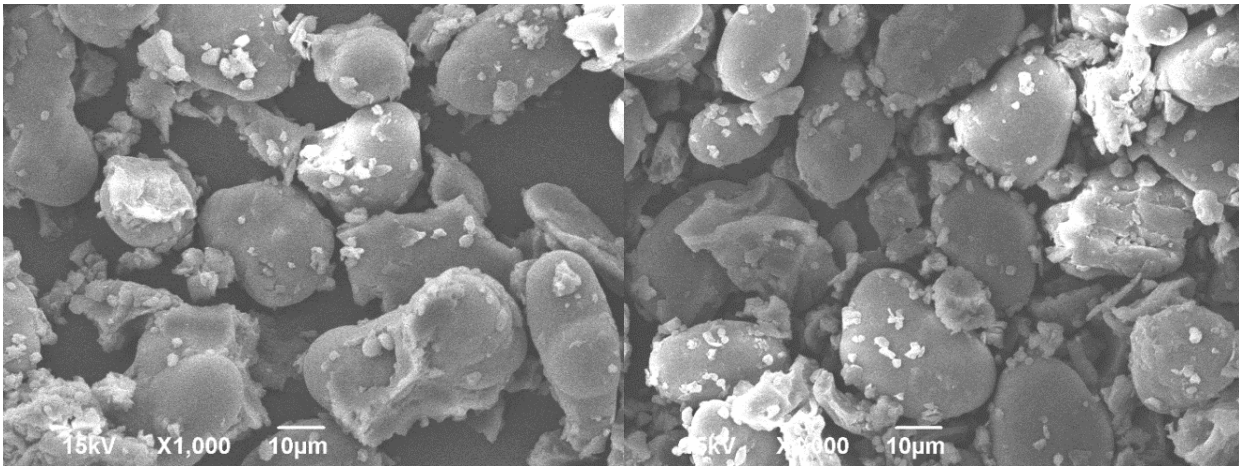

Figure 64. SEM images of roller-milled (left) and hammer-milled (right) split pea

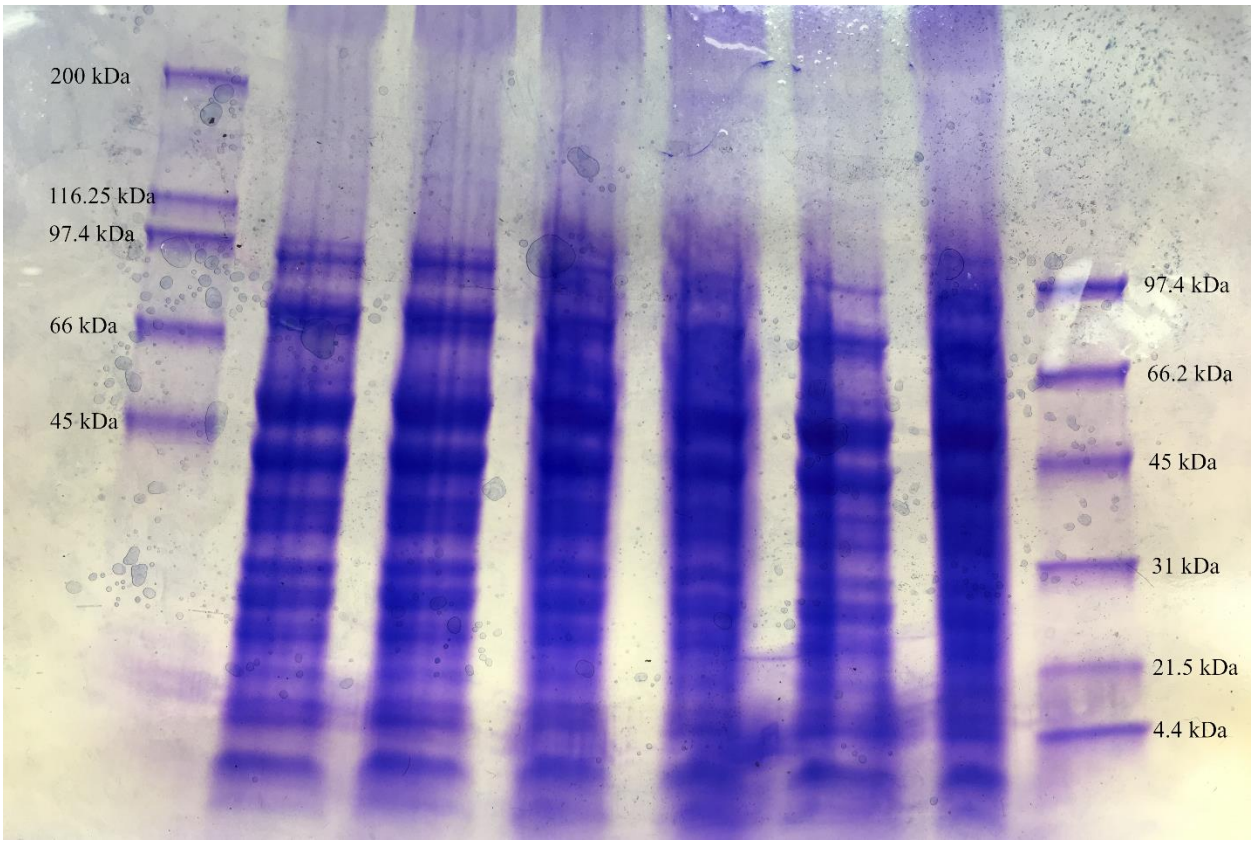

Figure 65. SDS-PAGE of yellow split pea: from left to right, lanes 2-4 and 5-7 are roller- and hammer-milled samples

Conclusion

Significant differences between hammer- and roller-milled split pea flours were few and had relatively small effect sizes. Differences lay chiefly in higher small particle volume and lower starch damage in hammer-milled samples, resulting in slightly lower water content, pasting and final viscosities, and oil binding capacity than those of roller-milled samples. Due to a comparable particle size range, these differences reflect the effect of milling method apart from particle size and demonstrate that comparable quality can be generated in split pea milled using different milling methods. Study results indicated that hammer milling should not be dismissed as a size reduction solution for pulses, particularly when time, skilled labor, and specialized milling equipment are limiting factors.

References

AACC International. Approved Methods of Analysis, 11th Ed. Method 08-01.01. Ash—basic method. Approved November 3, 1999. Method 32-50.01. Insoluble, soluble, and total dietary fiber (codex definition) by an enzymatic-gravimetric method and liquid chromatography. Approved August 2011. Method 44-15.02. Moisture—air-oven methods. Approved November 3, 1999. Method 46-30.01. Crude protein—combustion method. Approved November 3, 1999. Method 61-02.01. Determination of the pasting properties of rice with the rapid visco analyzer. Approved November 3, 1999. Method 76-13.01. Total starch assay procedure (megazyme amyloglucosidase/α-amylase method). Approved November 3, 1999. Method 76-30.02. Determination of damaged starch. Approved November 3, 1999. Available online only. AACCI: St. Paul, MN.

Ashokkumar, K., Diapari, M., Jha, A. B., Tar'an, B., Arganosa, G., & Warkentin, T. D. (2015). Genetic diversity of nutritionally important carotenoids in 94 pea and 121 chickpea accessions. *Journal of Food Composition and Analysis*, **43**:49-60. https://doi.org/10.1016/j.jfca.2015.04.014

Ashwar, B. A., Gani, A., Shah, A., & Masoodi, F. A. (2017). Production of RS4 from rice by acetylation: physico-chemical, thermal, and structural characterization. *Starch/Stärke*, **69**:1600052-1600061. https://doi.org/10.1002/star.201600052

ASTM International. (2009). Standard Test Methods. Method D7481. Standard test methods for determining loose and tapped bulk densities of powders using a graduated cylinder. ASTM, West Conshohoken, PA, U.S.A.

de la Pena, E. (2015). *Manufacturing optimization of non-traditional pasta products* (Doctoral dissertation). Ann Arbor, MI: ProQuest Dissertations and Theses. UMI 3685795.

Huang, X., Dou, J.-Y., Li, D., & Wang, L.-J. (2018). Effects of superfine grinding on properties of sugar beet pulp powders. *LWT – Food Science and Technology*, **87**:203-209. http://dx.doi.org/10.1016/j.lwt.2017.08.067

Indira, T. N., & Bhattacharya, S. (2006). Grinding characteristics of some legumes. *Journal of Food Engineering*, **76**, 113–118. https://doi.org/10.1016/j.jfoodeng.2005.04.040

Kerr, W. L., Ward, C. D. W., McWatters, K. H., & Resurreccion, A. V. A. (2000). Effect of milling and particle size on functionality and physicochemical properties of cowpea flour. *Cereal Chemistry*, **77**, 213–219. https://doi.org/10.1094/CCHEM.2000.77.2.213

Ma, Z., Boye, J. I., & Hu, X. (2017). *In vitro* digestibility, protein composition and techno-functional properties of Saskatchewan grown yellow field peas (*Pisum sativum* L.) as affected by processing. *Food Research International*, **92**:64-78. https://doi.org/10.1016/j.foodres.2016.12.012

Maaroufi, C., Melcion, J. P., De Monredon, F., Giboulot, B., Guibert, D., & Le Guen, M. P. (2000). Fractionation of pea flour with pilot scale sieving. I. Physical and chemical characteristics of pea seed fractions. *Animal Feed Science and Technology*, **85**(1–2), 61–78. https://doi.org/10.1016/S0377-8401(00)00127-9

Maskus, H., Bourre, L., Fraser, S., Sarkar, A., & Malcolmson, L. (2016). Effects of grinding method on the compositional, physical and functional properties of whole and split yellow pea flour. *Cereal Foods World*, **61**:59-64. https://doi.org/10.1094/CFW-61-2-0059

Masli, M. D. P., Rasco, B. A., & Ganjyal, G. M. (2018). Composition and physicochemical characterization of fiber-rich food processing byproducts. *Journal of Food Science*, **83**:956-965. https://doi.org/10.1111/1750-3841.14081

Pelgrom, P. J. M., Vissers, A. M., Boom, R. M., & Schutyser, M. A. I. (2013). Dry fractionation for production of functional pea protein concentrates. *Food Research International*, **53**, 232–239. https://doi.org/10.1016/j.foodres.2013.05.004

Posner, E. S., & Hibbs, A. N. (2005). *Wheat Flour Milling*. St. Paul, Minnesota, USA: American Association of Cereal Chemists, Inc. https://doi.org/10.1016/B978-1-891127-55-7.50012-4

Rao, B. D., Anis, M., Kalpana, K., Sunooj, K. V., & Ganesh, T. (2016). Influence of milling methods and particle size on hydration properties of sorghum flour and quality of sorghum biscuits. *LWT – Food Science and Technology*, **67**:8-13. http://dx.doi.org/10.1016/j.lwt.2015.11.033

Singh, A., Hung, Y.-C., Corredig, M., Phillips, R. D., Chinnan, M. S., & McWatters, K. H. (2005). Effect of milling method on selected physical and functional properties of cowpea (Vigna unguiculata) paste. *International Journal of Food Science and Technology*, **40**, 525–536. https://doi.org/10.1111/j.1365-2621.2005.00964.x

Storey, J. D. (2002). A direct approach to false discovery rates. *Journal of the Royal Statistical Society: Series B*, **64**:479–498.

Storey, J. D., Taylor, J. E., & Siegmund, D. (2004). "Strong control, conservative point estimation, and simultaneous conservative consistency of false discovery rates: a unified approach," *Journal of the Royal Statistical Society: Series B*, **66**:187–205.

Thakur, S., Scanlon, M. G., Tyler, R. T., Milani, A., & Paliwal, J. (2019). A comprehensive review of pulse flour characteristics from a wheat flour miller's perspective. *Comprehensive Reviews in Food Science and Food Safety*, in press.

Vishwanathan, K. H., & Subramanian, R. (2014). Particle size characteristics of ground soy and red gram. *International Journal of Food Properties*, **17**, 1469–1481. https://doi.org/10.1080/10942912.2012.719983

Zheng, Y., & Li, Y. (2018). Physicochemical and functional properties of coconut (*Cocos nucifera* L) cake dietary fibres: effects of cellulase hydrolysis, acid treatment and particle size distribution. *Food Chemistry*, **257**:135-142. https://doi.org/10.1016/j.foodchem.2018.03.012

OVERALL SUMMARY AND CONCLUSION

Conclusions

The selection of milling method (mill type and setup) controlled the particle size distribution characteristics and extent of starch damage in milled split pea. In hammer milling, both rotor speed and screen aperture controlled the particle size distribution. Obtaining a low maximum particle size and narrow particle size distribution that would be appropriate for a pulse flour required both high rotor speed (102 m/s) and small screen aperture (e.g. 0.84 mm). Additionally, starch damage tended to increase with increasing rotor speed and decreasing screen aperture. When hammer and roller milling procedures were designed to produce a comparable maximum particle size, only the small particle volume (D10) was significantly different between the two milling methods. The differences in starch damage between hammer- and roller-milled split pea was greater than that among split pea milled at different hammer mill settings. However, starch damage was much lower in split pea milled by any method than is commonly reported for milled cereals.

Particle size, in turn, strongly impacted many other quality parameters of milled split pea. Particle size parameters, particularly the D50 and D90, impacted color, bulk density, and peak and final viscosities of split pea milled at a variety of hammer mill settings. In some cases, particle size was a better predictor of pea flour quality than the mill parameters. The D50 and ratio of small to large particles were also important predictors of angle of repose, while the D10 and D90 were important predictors of angle of slide. In hammer- and roller-milled split pea flour, the D10 was correlated with flour moisture, pasting properties, and oil binding capacity.

The data from this research supported the potential of both hammer and roller milling as viable alternatives in the production of milled split pea. With appropriate mill settings and a

single sieving step, a one-pass hammer milling process produced split pea flour of comparable quality to that of a three-step roller milling process (two milling passes with intermediate sieving). Extraction of the hammer milling process was, however, considerably lower (60 %) than that reported previously for a 12-step roller milling procedure that resulted in a similar particle size distribution (88 %) (Maskus, Bourre, Fraser, Sarkar & Malcolmson, 2016). Future researchers should evaluate how much the addition of a second mill pass for the oversized particles could improve flour extraction in the hammer milling process, since such a process would still benefit from being simpler that the roller milling process. Small differences were observed in small particle volume, starch damage, and pasting properties between roller- and hammer-milled samples. Depending upon application, these differences may or may not be important.

Future pulse milling research should be geared toward a standard definition of pulse flour, as is the case for wheat flour. Such standardization could promote consistency in the quality of pulse flours available to product formulators. Additionally, pulse flour quality standards could assist in selecting appropriate milling procedures for future studies investigating the link between whole pulse properties and milling quality, which are crucial in the success of pulse breeding programs.

References

Maskus, H., Bourre, L., Fraser, S., Sarkar, A., & Malcolmson, L. (2016). Effects of grinding method on the compositional, physical and functional properties of whole and split yellow pea flour. *Cereal Foods World*, **61**:59-64. https://doi.org/10.1094/CFW-61-2-0059

APPENDIX A. RAW DATA FOR MILLED YELLOW SPLIT PEA SAMPLES (MEAN ± STANDARD DEVIATION)

Variable	Hammer-milled pea	Roller-milled pea
Moisture (% as-is)	10.6 ± 0.1	11 ± 0.1
Ash (% db)	2.7 ± 0.1	2.6 ± 0
Protein (% db)	21.7 ± 0.9	20.2 ± 1.1
Total starch (% db)	52 ± 1.9	53.8 ± 2.2
Insoluble dietary fiber (% as-is)	6.2 ± 0.4	5.9 ± 0.4
Soluble dietary fiber (% as-is)	1.1 ± 0.8	0.9 ± 0.3
Total dietary fiber (% as-is)	7.2 ± 0.8	6.7 ± 0.7
Starch damage (%)	2 ± 0	3.5 ± 0.3
Carotenoid content (ng/g)	34 ± 3	37 ± 2
Brightness (Hunter L)	89 ± 0.1	89.2 ± 0.2
Redness (Hunter a)	2 ± 0.1	2.1 ± 0.2
Yellowness (Hunter b)	19.5 ± 0.3	19.7 ± 0.5
Bulk density (g/ml)	0.53 ± 0.01	0.53 ± 0
Peak viscosity (cP)	2478 ± 33	2688 ± 38
Breakdown viscosity (cP)	340 ± 20	385 ± 3
Final viscosity (cP)	4806 ± 41	5436 ± 175
Peak time (min)	5.3 ± 0	5.3 ± 0
Pasting temperature (° C)	74.3 ± 0	74.3 ± 0
D10 (µm)	10 ± 1	13 ± 1
D50 (µm)	31 ± 2	39 ± 5
D90 (µm)	114 ± 6	127 ± 12
Syneresis – time 0 (% loss)	6.4 ± 0.6	4.4 ± 1
Syneresis – 24 h (% loss)	23.7 ± 3.2	20.4 ± 1.7
Syneresis – 48 h (% loss)	24.1 ± 2.2	24.1 ± 1.1
Syneresis – 72 h (% loss)	2.9 ± 1.3	2.8 ± 1.4
Syneresis – 96 h (% loss)	2.8 ± 0.6	2.1 ± 0.7
Freeze-thaw stability – 2 cycles (% loss)	3.9 ± 1.5	4 ± 0.5
Freeze-thaw stability – 4 cycles (% loss)	4 ± 0.4	3.1 ± 0.3
Foaming capacity (%)	72 ± 12	111 ± 21
Foaming stability – 10 min (%)	92 ± 2	93 ± 1
Foaming stability – 30 min (%)	88 ± 4	89 ± 2
Foaming stability – 60 min (%)	85 ± 6	84 ± 6
Emulsion capacity (%)	62 ± 3	62 ± 3
Emulsion stability (%)	65 ± 3	63 ± 2
Water absorbing capacity (g water/g flour)	1 ± 0	1 ± 0.1
Oil absorbing capacity (g oil/g flour)	0.9 ± 0	1.1 ± 0
Angle of repose – aluminum (°)	23 ± 2	23 ± 1

Variable	Hammer-milled pea	Roller-milled pea
Angle of repose – high density polyethylene (°)	35 ± 6	22 ± 1
Angle of repose – polypropylene (°)	21 ± 1	22 ± 1
Angle of repose – polyvinyl chloride (°)	22 ± 1	22 ± 1
Angle of repose – polyvinylidene fluoride (°)	24 ± 2	21 ± 2
Angle of repose – stainless steel (°)	22 ± 1	22 ± 1
Angle of slide – aluminum (°)	42 ± 3	36 ± 4
Angle of slide – high density polyethylene (°)	53 ± 6	55 ± 6
Angle of slide – polypropylene (°)	48 ± 1	47 ± 4
Angle of slide – polyvinyl chloride (°)	51 ± 3	44 ± 2
Angle of slide – polyvinylidene fluoride (°)	57 ± 5	49 ± 4
Angle of slide – stainless steel (°)	43 ± 5	36 ± 3

APPENDIX B. SAS CODE

Paper 1

```
*******************************************************
*** Pea Milling Chapter 1 - Hammer-milled split pea ***
*******************************************************
Variables
      Group       - Treatment code (speed*screen*seed moisture) (1-36)
      imoist      - Seed water content (%) prior to milling (9 or 11)
      Screen      - Screen aperture size (mm) during milling (9 values)
      Speed       - Head speed of mill hammers (m/s) (34 or 102)
      mmoist      - Milled seed water content (%)
      prot        - Milled seed protein content (%)
      Ash         - Milled seed ash content (%)
      L           - Lightness value (Hunter LAB)
      A           - Redness value (Hunter LAB)
      B           - Yellowness value (Hunter LAB)
      Bdens       - Bulk density (g/ml)
      sdam        - Percent damaged starch
      Peakv       - RVA Peak viscosity (cP)
      Bkdwn       - RVA breakdown viscosity (cP)
      pasteT      - RVA pasting temperature (degrees C)
      Finalv      - RVA final viscosity (cP)
      D10         - 10th percentile of particle size distribution (um)
      D50         - Median particle size (um)
      D90         - 90th percentile of particle size distribution (um)
      sm_mean     - Mean of small particle subpopulation
      lg_mean     - Mean of large particle subpopulation
      S_L         - Ratio of small to large particle subpopulation volume
      Aw          - Glass transition water activity
*************************************************************;

proc template;
      define style styles.pea;
      parent=styles.harvest;
      class GraphColors /
            'gcdata6' = biyg 'gcdata5' = lio
            'gcdata4' = brbl 'gcdata3' = deyg
      'gcdata2' = gold 'gcdata1' = viro
          'gdata6' = biyg 'gdata5' = lio
          'gdata4' = brbl 'gdata3' = deyg
          'gdata2' = gold 'gdata1' = viro;
       style colors /
            'headerfgemph' = cx000000 'headerbgemph' = cxFDCD6F
            'headerfgstrong' = cx000000 'headerbgstrong' = cxFDCD6F
            'headerfg' = cx000000 'headerbg' = cxFDCD6F
            'datafgemph' = cx000000 'databgemph' = cxFFFFFF
            'datafgstrong' = cx000000 'databgstrong' = cxFFFFFF
            'databorder' = cx89562D 'datafg' = cx000000
            'databg' = cxFFFFFF 'batchfg' = cx000000
            'batchbg' = cxFFFFFF 'tableborder' = cx000000
            'tablebg' = cxFFFFFF 'notefg' = cx000000
            'notebg' = cxFFFFFF 'bylinefg' = cx000000
            'bylinebg' = cxFFFFFF 'captionfg' = cx000000
            'captionbg' = cxFFFFFF 'proctitlefg' = cx000000
```

```
            'proctitlebg' = cxFFFFFF 'titlefg' = cx000000
            'titlebg' = cxFFFFFF 'systitlefg' = cx000000
            'systitlebg' = cxFFFFFF 'Conentryfg' = cx000000
            'Confolderfg' = cx000000 'Contitlefg' = cx000000
            'link2' = cx800080 'link1' = cx0000FF
            'contentfg' = cx000000 'contentbg' = cxFFFFFF
            'docfg' = cx000000 'docbg' = cxFFFFFF;
      class GraphFonts /
            'GraphDataFont' = ("<sans-serif>, <MTsans-serif>",10pt)
            'GraphUnicodeFont' = ("<MTsans-serif-unicode>",10pt)
            'GraphFootnoteFont' = ("<sans-serif>, <MTsans-serif>",12pt,bold)
            'GraphTitleFont' = ("<sans-serif>, <MTsans-serif>",12pt,bold)
            'GraphTitle1Font' = ("<sans-serif>, <MTsans-serif>",14pt,bold)
            'GraphValueFont' = ("<sans-serif>, <MTsans-serif>",10pt)
            'GraphLabel2Font' = ("<sans-serif>, <MTsans-serif>",12pt)
            'GraphLabelFont' = ("<sans-serif>, <MTsans-serif>",12pt,bold)
            'GraphAnnoFont' = ("<sans-serif>, <MTsans-serif>",12pt);
      end;
run;

proc template;
      define statgraph ContourPlotParm;
      dynamic _X _Y _Z _TITLE _XLAB _YLAB _ZLAB;
      begingraph;
            entrytitle _TITLE;
            layout overlay / xaxisopts=(label=_XLAB) yaxisopts=(label=_YLAB);
            contourplotparm x=_X y=_Y z=_Z /
            contourtype=fill nhint=12  colormodel=twocolorramp
name="Contour";
            continuouslegend "Contour" / title=_ZLAB;
   endlayout;
endgraph;
end;
run;

data Pea_Ch1;
      infile 'Directory\filename.csv' firstobs=2 dsd;
      input group $ imoist $ screen speed $ mmoist prot ash L a b bdens sdam
peakv bkdwn
            pasteT finalv d10 d50 d90 sm_mean lg_mean S_L;
            lnscreen=log(screen); /*Natural log of screen*/
            screen_1=1/screen; /*Reciprocal of screen*/
            screen2=screen*screen; /*Square of screen*/
            screen3=screen*screen*screen; /*Cube of screen*/
            lnD10=log(D10); /*Natural log of D10*/
            D10_1=1/D10; /*Reciprocal of D10*/
            lnD50=log(D50); /*Natural log of D50*/
            D50_1=1/D50; /*Reciprocal of D50*/
            D502=D50*D50; /*Square of D50*/
            lnD90=log(D90); /*Natural log of D90*/
            D902=D90*D90; /* Square of D90*/
            S_L2=S_L*S_L; /*Square of small:large particle ratio*/
            lg_mean2=lg_mean*lg_mean; /*Square of mean large particle size*/
      label imoist='Seed moisture (percent)' screen="Screen aperture (mm)"
      speed="Rotor speed (m/s)"
      mmoist="Flour moisture (%)" prot="Protein (% db)" ash="Ash (% db)"
      L="Brightness (L*)"
```

```
      a="Redness (a*)" b="Yellowness (b*)" bdens="Bulk density (g/ml)"
      sdam="Damaged starch (%)"
      peakv="Peak viscosity (cP)" bkdwn="Breakdown viscosity (cP)"
      pasteT="Pasting temperature (degrees C)" finalv="Final viscosity (cP)"
      D10="D10 (um)" D50="D50 (um)" D90="D90 (um)" sm_mean="Mean small
      particle size (um)" lg_mean="Mean large particle size (um)"
      S_L="Small:large particle ratio" lnscreen="Natural log of screen
      aperture" screen_1="Reciprocal of screen aperture" screen2="Square of
      screen aperture" screen3="Cube of screen aperture" lnD10="Natural log
      of D10" D10_1="Reciprocal of D10" lnD50="Natural log of D50"
      D50_1="Reciprocal of D50" D502="Square of D50" lnD90="Natural log of
      D90" D902="Square of D90" S_L2="Square of small:large particle ratio"
      lg_mean2="Square of mean large particle size";
run;

data peaGT;
      infile "Directory\filename.csv" firstobs=2 dsd;
      input sample moist $ screen speed $ Aw D10 D50 D90;
      label moist="Seed moisture (%)" Aw="Glass transition Aw";
run;

proc means data=peaGT;
      class moist screen speed;
      var Aw;
      ways 1 2;
      output out=gt_means mean=lvl_mean std=lvl_std;
run;

data gt_graphs;
      set gt_means;
      lower = lvl_mean - lvl_std;
      upper = lvl_mean + lvl_std;
      label moist="Seed moisture (%)" speed="Rotor speed (m/s)"
            screen="Screen aperture (mm)" lvl_mean="Glass transition Aw";
run;

*********************************
*Initial graphics and correlaton*
*********************************;

ods rtf file='Directory\filename.rtf' bodytitle style=styles.pea;

%macro graphmill/parmbuff;
   %let num=1;
   %let dsname=%scan(&syspbuff,&num);
   %do %while(&dsname ne);
            proc sgpanel data=Pea_CH1;
            panelby imoist;
            scatter x=screen y=&dsname /group=speed;
            title "&dsname vs screen aperture, grouped by speed and seed
moisture";
      run;
      %let num=%eval(&num+1);
      %let dsname=%scan(&syspbuff,&num);
   %end;
%mend graphmill;
```

```
%graphmill(mmoist,prot,ash,L,a,b,bdens,sdam,peakv,bkdwn,pasteT,finalv,d10,d50
,d90)

proc corr data=Pea_Ch1;
      var d10 d50 d90;
      with L a b bdens sdam peakv bkdwn finalv;
      title 'Correlation between particle size and functionality';
run;

%macro graphD10/parmbuff;
   %let num=1;
   %let dsname=%scan(&syspbuff,&num);
   %do %while(&dsname ne);
            proc sgplot data=Pea_CH1;
            scatter x=D10 y=&dsname;
            title "&dsname vs D10";
      run;
      %let num=%eval(&num+1);
      %let dsname=%scan(&syspbuff,&num);
   %end;
%mend graphD10;

%graphD10(L,a,b,bdens,sdam,peakv,bkdwn,pasteT,finalv)

%macro graphD50/parmbuff;
   %let num=1;
   %let dsname=%scan(&syspbuff,&num);
   %do %while(&dsname ne);
            proc sgplot data=Pea_CH1;
            scatter x=D50 y=&dsname;
            title "&dsname vs D50";
      run;
      %let num=%eval(&num+1);
      %let dsname=%scan(&syspbuff,&num);
   %end;
%mend graphD50;

%graphD50(L,a,b,bdens,sdam,peakv,bkdwn,pasteT,finalv)

%macro graphD90/parmbuff;
   %let num=1;
   %let dsname=%scan(&syspbuff,&num);
   %do %while(&dsname ne);
            proc sgplot data=Pea_CH1;
            scatter x=D90 y=&dsname;
            title "&dsname vs D90";
      run;
      %let num=%eval(&num+1);
      %let dsname=%scan(&syspbuff,&num);
   %end;
%mend graphD90;

%graphD90(L,a,b,bdens,sdam,peakv,bkdwn,pasteT,finalv)

****************************************
*Modelling response with mill predictors*
****************************************;
```

```
/* STEP 1 - MODEL SELECTION */

proc corr data=Pea_Ch1;
      var screen screen_1 screen2 lnscreen screen3;
      title 'Check for multicollinearity';
run;

proc reg data=Pea_Ch1 plots=all;
      model peakv = screen screen_1 screen2 lnscreen screen3
                  / vif tol collin;
      title 'Check for multicollinearity';
run;

%macro select_mill/parmbuff;
   %let num=1;
   %let dsname=%scan(&syspbuff,&num);
   %do %while(&dsname ne);
            proc glmselect data=Pea_CH1 plots=all;
                  class imoist(ref="11") speed(ref="102");
                  model &dsname = imoist screen speed imoist*screen
imoist*speed screen*speed
                                                screen_1 screen2 lnscreen screen3 /
                                                selection=lar(choose=press
lscoeffs) stats=(adjrsq aicc cp press sbc);
                  title "Model selection for &dsname vs milling variables";
       run;
      %let num=%eval(&num+1);
      %let dsname=%scan(&syspbuff,&num);
   %end;
%mend select_mill;

%select_mill(mmoist prot ash L a b bdens sdam peakv bkdwn
            pasteT finalv d10 lnd10 d50 d90 sm_mean lg_mean S_L);

/* STEP 2 - FINAL MODELS */

*Moisture*;
proc glm data=Pea_Ch1 plots=all;
      class imoist(ref="11") speed(ref="102");
      model mmoist = imoist speed screen / intercept solution;
      output out=moist_mill r=r p=p;
      title 'ANOVA for moisture';
run;
proc sgpanel data=moist_mill;
      panelby imoist;
      scatter x=screen y=mmoist / group=speed;
      series x=screen y=p / group=speed;
      title "Interaction plot for moisture";
run;

*Protein*;
proc glm data=Pea_Ch1 plots=all noprint;
      class imoist(ref="11") speed(ref="102");
      model prot = imoist speed / intercept solution;
      output out=prot_mill r=r p=p;
      title 'ANOVA for protein';
```

```
run;
proc sgplot data=prot_mill;
      scatter x=speed y=prot / group=imoist;
      series x=speed y=p / group=imoist;
      title "Interaction plot for protein";
run;

*Brightness*;
proc glm data=Pea_Ch1 plots=all;
      class imoist(ref="11") speed(ref="102");
      model L = imoist speed screen screen_1 imoist*speed screen_1*speed/
intercept solution;
      output out=bright_mill r=r p=p;
      title 'ANOVA for brightness';
run;
proc sgpanel data=bright_mill;
      panelby imoist;
      scatter x=screen y=L / group=speed;
      series x=screen y=p / group=speed;
      title "Interaction plot for brightness";
run;

*Redness*;
proc glm data=Pea_Ch1 plots=all;
      class imoist(ref="11") speed(ref="102");
      model a = imoist speed screen_1 screen_1*speed imoist*speed
screen_1*imoist / intercept solution;
      output out=red_mill r=r p=p;
      title 'ANOVA for redness';
run;
proc sgpanel data=red_mill;
      panelby imoist;
      scatter x=screen y=a / group=speed;
      series x=screen y=p / group=speed;
      title "Interaction plot for redness";
run;

*Yellowness*;
proc glm data=Pea_Ch1 plots=all;
      class imoist(ref="11") speed(ref="102");
      model b = imoist speed screen_1 imoist*speed / intercept solution;
      output out=yellow_mill r=r p=p;
      title 'ANOVA for yellowness';
run;
proc sgpanel data=yellow_mill;
      panelby imoist;
      scatter x=screen y=b / group=speed;
      series x=screen y=p / group=speed;
      title "Interaction plot for yellowness";
run;

*Bulk density*;
proc glm data=Pea_Ch1 plots=all;
      class imoist(ref="11") speed(ref="102");
      model bdens = imoist screen_1 speed / intercept solution;
      output out=bdens_mill r=r p=p;
      title 'ANOVA for bulk density';
```

```
run;
proc sgpanel data=bdens_mill;
      panelby imoist;
      scatter x=screen y=bdens / group=speed;
      series x=screen y=p / group=speed;
      title "Interaction plot for bulk density";
run;

*Starch damage*;
proc glm data=Pea_Ch1 plots=all;
      class imoist(ref="11") speed(ref="102");
      model sdam = imoist speed screen_1 / intercept solution;
      output out=sdam_mill r=r p=p;
      title 'ANOVA for starch damage';
run;
proc sgpanel data=sdam_mill;
      panelby imoist;
      scatter x=screen y=sdam / group=speed;
      series x=screen y=p / group=speed;
      title "Interaction plot for starch damage";
run;

*Peak viscosity*;
proc glm data=Pea_Ch1 plots=all;
      class imoist(ref="11") speed(ref="102");
      model peakv = imoist screen speed screen_1 screen*speed screen_1*speed/
intercept solution;
      output out=peakv_mill r=r p=p;
      title 'ANOVA for peak viscosity';
run;
proc sgpanel data=peakv_mill;
      panelby imoist;
      scatter x=screen y=peakv / group=speed;
      series x=screen y=p / group=speed;
      title "Interaction plot for peak viscosity";
run;

*Breakdown viscosity*;
proc glm data=Pea_Ch1 plots=all;
      class imoist(ref="11") speed(ref="102");
      model bkdwn = speed screen_1 / intercept solution;
      output out=bkdwn_mill r=r p=p;
      title 'ANOVA  breakdown viscosity';
run;
proc sort data=bkdwn_mill;
      by p;
run;
proc sgplot data=bkdwn_mill;
      scatter x=screen y=bkdwn / group=speed;
      series x=screen y=p / group=speed;
      title "Interaction plot for breakdown viscosity";
run;

*Paste temperature*;
proc glm data=Pea_Ch1(where=(screen<9)) plots=all;
      class imoist(ref="11") speed(ref="102");
      model pasteT = imoist screen speed screen*speed / intercept solution;
```

```
      output out=pasteT_mill r=r p=p;
      title 'ANOVA for paste temperature';
run;
proc sgpanel data=pasteT_mill;
      panelby imoist;
      scatter x=screen y=pasteT / group=speed;
      series x=screen y=p / group=speed;
      title "Interaction plot for peak viscosity";
run;


*Final viscosity*;
proc glm data=Pea_Ch1 plots=all;
      class imoist(ref="11") speed(ref="102");
      model finalv = screen speed screen_1 screen*speed screen_1*speed/
intercept solution;
      output out=finalv_mill r=r p=p;
      title 'ANOVA for final viscosity';
run;
proc sort data=finalv_mill;
      by screen p;
run;
proc sgplot data=finalv_mill;
      scatter x=screen y=finalv / group=speed;
      series x=screen y=p / group=speed;
      title "Interaction plot for final viscosity";
run;

*D10*;
proc glm data=Pea_Ch1 noprint;
      class imoist(ref="11") speed(ref="102");
      model lnD10 = speed lnscreen speed*lnscreen / intercept solution;
      output out=D10_mill r=r p=p;
      title 'ANOVA for D10';
run;
data D10_mill2;
      set D10_mill;
      exp_p=exp(p);
run;
proc sort data=D10_mill2;
      by exp_p;
run;
proc sgplot data=D10_mill2(where=(screen<6));
      scatter x=screen y=D10 / group=speed;
      series x=screen y=exp_p / group=speed;
      title "Interaction plot for D10";
run;

*D50*;
proc glm data=Pea_Ch1 plots=all;
      class imoist(ref="11") speed(ref="102");
      model D50 = screen speed screen_1 screen*speed screen_1*speed/
intercept solution;
      output out=D50_mill r=r p=p;
      title 'ANOVA for D50';
run;
proc sort data=D50_mill;
```

```
      by p;
run;
proc sgplot data=D50_mill(where=(screen<6));
      scatter x=screen y=D50 / group=speed;
      series x=screen y=p / group=speed;
      title "Interaction plot for D50";
run;

*D90*;
proc glm data=Pea_Ch1 plots=all;
      class imoist(ref="11") speed(ref="102");
      model D90 = screen speed screen_1 screen_1*speed/ intercept solution;
      output out=D90_mill r=r p=p;
      title 'ANOVA for D90';
run;
proc sort data=D90_mill;
      by p;
run;
proc sgplot data=D90_mill(where=(screen<6));
      scatter x=screen y=D90 / group=speed;
      series x=screen y=p / group=speed;
      title "Interaction plot for D90";
run;

*Mean small particle size*;
proc glm data=Pea_Ch1 plots=all;
      class imoist(ref="11") speed(ref="102");
      model sm_mean = imoist lnscreen / intercept solution;
      output out=sm_mean_mill r=r p=p;
      title 'ANOVA for mean small PS';
run;
proc sort data=sm_mean_mill;
      by screen p;
run;
proc sgplot data=sm_mean_mill(where=(screen<6));
      scatter x=screen y=sm_mean / group=imoist;
      series x=screen y=p / group=imoist;
      title "Interaction plot for mean small particle size";
run;

*Mean large particle size*;
proc glm data=Pea_Ch1 plots=all;
      class imoist(ref="11") speed(ref="102");
      model lg_mean = screen speed screen_1 screen_1*speed/ intercept
solution;
      output out=lg_mean_mill r=r p=p;
      title 'ANOVA for mean large PS';
run;
proc sort data=lg_mean_mill;
      by p;
run;
proc sgplot data=lg_mean_mill(where=(screen<6));
      scatter x=screen y=lg_mean / group=speed;
      series x=screen y=p / group=speed;
      title "Interaction plot for mean large particle size";
run;
```

```
*Small:large particle ratio*;
proc glm data=Pea_Ch1 plots=all;
      class imoist(ref="11") speed(ref="102");
      model S_L = speed screen_1 / intercept solution;
      output out=S_L_mill r=r p=p;
      title 'ANOVA for small:large particle ratio';
run;
proc sort data=S_L_mill;
      by p;
run;
proc sgplot data=S_L_mill(where=(screen<6));
      scatter x=screen y=S_L / group=speed;
      series x=screen y=p / group=speed;
      title "Interaction plot for small:large particle ratio";
run;

************************************
*Modelling response with PS predictors*
************************************;

ods rtf file='D:\Pea milling dissertation\Chapter 1\CH1_PS.rtf' bodytitle
style=styles.pea;

proc corr data=Pea_Ch1;
      var D10 D50 D90 lg_mean sm_mean S_L;
      title 'Check for multicollinearity';
run;

proc reg data=Pea_Ch1 plots=all;
      model peakv = D10 D50 D90 lg_mean sm_mean S_L
            / vif tol collin;
      title 'Check for multicollinearity';
run;

/* STEP 1 - MODEL SELECTION */

%macro select_ps/parmbuff;
   %let num=1;
   %let dsname=%scan(&syspbuff,&num);
   %do %while(&dsname ne);
            proc glmselect data=Pea_CH1 plots=all;
                  model &dsname = D10 D50 D90 lg_mean sm_mean S_L
                                    lnD10 lnD50 lnD90 D10_1 D50_1 D502 D902
                                    lg_mean2 S_L2 /
                                    selection=lar(choose=press lscoeffs)
                                    stats=(adjrsq aicc cp press sbc);
                  title "Model selection for &dsname vs particle size
variables";
       run;
      %let num=%eval(&num+1);
      %let dsname=%scan(&syspbuff,&num);
   %end;
%mend select_ps;

%select_ps(L a b bdens sdam peakv bkdwn finalv);

/* STEP 2 - FINAL MODELS */
```

```
*Brightness*;
proc glm data=Pea_Ch1 plots=all;
      class imoist(ref="11");
      model L = lg_mean imoist/ intercept solution;
      output out=L_PS r=r p=p;
      title 'ANOVA for brightness based on particle size';
run;
proc sgplot data=L_PS;
      scatter x=lg_mean y=L / group=imoist;
      series x=lg_mean y=p / group=imoist;
      title "Prediction of brightness by mean large particle size";
run;

*Redness*;
proc glm data=Pea_Ch1 plots=all;
      class imoist(ref="11");
      model a = lg_mean imoist/ intercept solution;
      output out=a_PS r=r p=p;
      title 'ANOVA for redness based on particle size';
run;
proc sgplot data=a_PS;
      scatter x=lg_mean y=a / group=imoist;
      series x=lg_mean y=p / group=imoist;
      title "Prediction of redness by mean large particle size";
run;

*Yellowness*;
proc glm data=Pea_Ch1 plots=all;
      class imoist(ref="11");
      model b = D10_1 imoist/ intercept solution;
      output out=b_PS r=r p=p;
      title 'ANOVA for yellowness based on particle size';
run;
proc sort data=b_PS;
      by p;
run;
proc sgplot data=b_PS;
      scatter x=D10 y=b / group=imoist;
      series x=D10 y=p / group=imoist;
      title "Prediction of yellowness by D10";
run;

*Bulk density*;
proc glm data=Pea_Ch1 plots=all;
      class imoist(ref="11");
      model bdens = lnD90 imoist/ intercept solution;
      output out=bdens_PS r=r p=p;
      title 'ANOVA for bulk density based on particle size';
run;
proc sort data=bdens_PS;
      by p;
run;
proc sgplot data=bdens_PS;
      scatter x=D90 y=bdens / group=imoist;
      series x=D90 y=p / group=imoist;
      title "Prediction of bulk density by D90";
```

```
run;


*Starch damage*;
proc glm data=Pea_Ch1 plots=all;
      class imoist(ref="11");
      model sdam = sm_mean D10_1 imoist/ intercept solution;
      output out=sdam_PS r=r p=p;
      title 'ANOVA for starch damage based on particle size';
run;
proc g3grid data=sdam_PS(where=(imoist="9")) out=sdam_9;
      grid sm_mean*D10=sdam / join noscale;
run;
proc g3grid data=sdam_PS(where=(imoist="11")) out=sdam_11;
      grid sm_mean*D10=sdam / join noscale;
run;
proc g3grid data=sdam_PS(where=(imoist="9")) out=sdam_p9;
      grid sm_mean*D10=p / join noscale;
run;
proc g3grid data=sdam_PS(where=(imoist="11")) out=sdam_p11;
      grid sm_mean*D10=p / join noscale;
run;
proc sgrender data=sdam_9 template=ContourPlotParm;
      dynamic _TITLE="Observed starch damage at 9 % seed moisture by D10 and
mean small particle size"
            _X="sm_mean" _Y="D10" _Z="sdam"
            _XLAB="Mean small particle size (um)" _YLAB="D10" _ZLAB="Starch
damage (%)";
run;
proc sgrender data=sdam_11 template=ContourPlotParm;
      dynamic _TITLE="Observed starch damage at 11 % seed moisture by D10 and
mean small particle size"
            _X="sm_mean" _Y="D10" _Z="sdam"
            _XLAB="Mean small particle size (um)" _YLAB="D10" _ZLAB="Starch
damage (%)";
run;
proc sgrender data=sdam_p9 template=ContourPlotParm;
      dynamic _TITLE="Predicted starch damage at 9 % seed moisture by D10 and
mean small particle size"
            _X="sm_mean" _Y="D10" _Z="p"
            _XLAB="Mean small particle size (um)" _YLAB="D10" _ZLAB="Starch
damage (%)";
run;
proc sgrender data=sdam_p11 template=ContourPlotParm;
      dynamic _TITLE="Predicted starch damage at 11 % seed moisture by D10
and mean small particle size"
            _X="sm_mean" _Y="D10" _Z="p"
            _XLAB="Mean small particle size (um)" _YLAB="D10" _ZLAB="Starch
damage (%)";
run;

*Peak viscosity*;
proc glm data=Pea_Ch1 plots=all;
      model peakv = lnD50/ intercept solution;
      output out=peakv_PS r=r p=p;
      title 'ANOVA for peak viscosity based on particle size';
run;
```

```
proc sort data=peakv_PS;
      by p;
run;
proc sgplot data=peakv_PS;
      scatter x=D50 y=peakv;
      series x=D50 y=p;
      title "Prediction of peak viscosity by D50";
run;

*Breakdown viscosity*;
proc glm data=Pea_Ch1 plots=all;
      model lnbkdwn = S_L2/ intercept solution;
      output out=bkdwn_PS r=r p=p;
      title 'ANOVA for breakdown viscosity based on particle size';
run;
proc sort data=bkdwn_PS;
      by p;
run;
proc sgplot data=bkdwn_PS;
      scatter x=S_L y=bkdwn;
      series x=S_L y=p;
      title "Prediction of breakdown viscosity by small:large particle
ratio";
run;

*Final viscosity*;
proc glm data=Pea_Ch1 plots=all;
      model finalv = lnD50/ intercept solution;
      output out=finalv_PS r=r p=p;
      title 'ANOVA for final viscosity based on particle size';
run;
proc sort data=finalv_PS;
      by p;
run;
proc sgplot data=finalv_PS;
      scatter x=D50 y=finalv;
      series x=D50 y=p;
      title "Prediction of final viscosity by D50";
run;

*Correlation coefficients*;
proc corr data=Pea_Ch1;
      var D10 D50 D90 lg_mean sm_mean S_L D10_1 lnD50 lnD90 S_L2;
      with L a b bdens sdam peakv bkdwn finalv;
      title "Correlation between flour quality and particle size";
run;

*****************************
*Visualizing and modelling Aw*
*****************************;

proc sgplot data=gt_graphs(where=(_type_=4));
      scatter x=moist y=lvl_mean / yerrorlower=lower yerrorupper=upper;
      series x=moist y=lvl_mean / lineattrs=(pattern=2);
      title "Moisture - main effect on Tg Aw";
run;
```

```
proc sgplot data=gt_graphs(where=(_type_=5));
      scatter x=speed y=lvl_mean / group=moist yerrorlower=lower
            yerrorupper=upper;
      series x=speed y=lvl_mean / group=moist lineattrs=(pattern=2);
      title "Moisture*speed - interaction effect on Tg Aw";
run;

proc sgplot data=gt_graphs(where=(_type_=6));
      scatter x=screen y=lvl_mean / group=moist yerrorlower=lower
            yerrorupper=upper;
      series x=screen y=lvl_mean / group=moist lineattrs=(pattern=2);
      title "Moisture*screen - interaction effect on Tg Aw";
run;

proc glm data=peagt plots=all;
      class moist(ref="11");
      model Aw = moist / intercept solution;
      lsmeans moist / adjust=tukey;
      title "Inference on Tg Aw";
run;

ods rtf close;
```

```
*******************************************
*** Pea Milling Chapter 2 - Flow Properties ***
*******************************************
Variables
      Moisture    - Seed water content (%) prior to milling (9 or 11)
      Screen      - Screen aperture size (mm) during milling (9 values)
      Speed       - Head speed of mill hammers (m/s) (34 or 102)
      AVG_PS      - D[4,3] (volume moment mean) (um)
      SD_PS       - Span of particle size (D90-D10/D50)(um)
      D10         - 10th percentile of particle size distribution (um)
      D50         - Median particle size (um)
      D90         - 90th percentile of particle size distribution (um)
      Surface     - Surface over which flour was tested (6 surfaces)
      Repose      - Angle of repose
      Slide       - Angle of slide
      Sm_mean     - Mean of small particle size distribution (um)
      Lg_mean     - Mean of large particle size distribution (um)
      S_L         - Ratio of small to large particle subpopulation volume
*************************************************************;

************************
**FORMATS AND TEMPLATES**
************************;

proc format;
      value $Surface    "HDPE"="High-density polyethylene"
                        "PVDF"="Polyvinylidene fluoride"
                        "AL"="Aluminum"
                        "SS"="Stainless steel"
                        "PP"="Polypropylene"
                        "PVC"="Polyvinyl chloride";
run;

proc template;
      define style styles.pea;
      parent=styles.harvest;
      class GraphColors /
            'gcdata6' = biyg 'gcdata5' = lio
            'gcdata4' = brbl 'gcdata3' = deyg
            'gcdata2' = gold 'gcdata1' = viro
            'gdata6' = biyg 'gdata5' = lio
            'gdata4' = brbl 'gdata3' = deyg
            'gdata2' = gold 'gdata1' = viro;
       style colors /
            'headerfgemph' = cx000000 'headerbgemph' = cxFDCD6F
            'headerfgstrong' = cx000000 'headerbgstrong' = cxFDCD6F
            'headerfg' = cx000000 'headerbg' = cxFDCD6F
            'datafgemph' = cx000000 'databgemph' = cxFFFFFF
            'datafgstrong' = cx000000 'databgstrong' = cxFFFFFF
            'databorder' = cx89562D 'datafg' = cx000000
            'databg' = cxFFFFFF 'batchfg' = cx000000
            'batchbg' = cxFFFFFF 'tableborder' = cx000000
            'tablebg' = cxFFFFFF 'notefg' = cx000000
            'notebg' = cxFFFFFF 'bylinefg' = cx000000
```

```
            'bylinebg' = cxFFFFFF 'captionfg' = cx000000
            'captionbg' = cxFFFFFF 'proctitlefg' = cx000000
            'proctitlebg' = cxFFFFFF 'titlefg' = cx000000
            'titlebg' = cxFFFFFF 'systitlefg' = cx000000
            'systitlebg' = cxFFFFFF 'Conentryfg' = cx000000
            'Confolderfg' = cx000000 'Contitlefg' = cx000000
            'link2' = cx800080 'link1' = cx0000FF
            'contentfg' = cx000000 'contentbg' = cxFFFFFF
            'docfg' = cx000000 'docbg' = cxFFFFFF;
      class GraphFonts /
            'GraphDataFont' = ("<sans-serif>, <MTsans-serif>",10pt)
            'GraphUnicodeFont' = ("<MTsans-serif-unicode>",10pt)
            'GraphFootnoteFont' = ("<sans-serif>, <MTsans-serif>",12pt,bold)
            'GraphTitleFont' = ("<sans-serif>, <MTsans-serif>",12pt,bold)
            'GraphTitle1Font' = ("<sans-serif>, <MTsans-serif>",14pt,bold)
            'GraphValueFont' = ("<sans-serif>, <MTsans-serif>",10pt)
            'GraphLabel2Font' = ("<sans-serif>, <MTsans-serif>",12pt)
            'GraphLabelFont' = ("<sans-serif>, <MTsans-serif>",12pt,bold)
            'GraphAnnoFont' = ("<sans-serif>, <MTsans-serif>",12pt);
      end;
run;

proc template;
      define statgraph ContourPlotParm;
      dynamic _X _Y _Z _TITLE _XLAB _YLAB _ZLAB;
      begingraph;
            entrytitle _TITLE;
            layout overlay / xaxisopts=(label=_XLAB) yaxisopts=(label=_YLAB);
            contourplotparm x=_X y=_Y z=_Z /
            contourtype=fill nhint=12  colormodel=twocolorramp
                  name="Contour";
            continuouslegend "Contour" / title=_ZLAB;
   endlayout;
endgraph;
end;
run;

************
**DATASETS**
************;

data flow;
      infile 'Directory\filename.csv' firstobs=2 dsd;
      input moist screen speed AVG_PS SD_PS D10 D50 D90 surface $ repose
            slide rep $ sm_mean lg_mean S_L;
            ln_repose=log(repose);
            sqrt_rep=sqrt(repose);
            lnD10=log(D10);
            D10_1=1/D10;
            D502=D50*D50;
            D902=D90*D90;
            S_L2=S_L*S_L;
            lg_mean2=lg_mean*lg_mean;
            screen_1=1/screen;
            screen2=screen*screen;
            screen3=screen*screen*screen;
      label screen="Screen aperture (mm)" speed="Rotor speed (m/s)"
```

```
            surface="Surface material" D10="D10 (um)" D50="D50 (um)"
            D90="D90 (um)" repose="Angle of repose (degrees)" slide="Angle of
            slide (degrees)" sm_mean="Mean small particle size (um)"
            lg_mean="Mean large particle size (um)" S_L="Small:large particle
            ratio";
run;

ods rtf file='Directory\filename.rtf' bodytitle style=styles.pea;

************************
*ALPHA (ANGLE OF REPOSE*
************************;

/*** Scatter plots ***/

ods graphics on;
proc sgplot data=flow;
      scatter x=D10 y=repose / group=surface;
      format surface $surface.;
      title "Angle of repose vs D10 by surface type";
run;

proc sgplot data=flow;
      scatter x=D50 y=repose / group=surface;
      format surface $surface.;
      title "Angle of repose vs D50 by surface type";
run;

proc sgplot data=flow;
      scatter x=D90 y=repose / group=surface;
      format surface $surface.;
      title "Angle of repose vs D90 by surface type";
run;

proc sgplot data=flow;
      scatter x=sm_mean y=repose / group=surface;
      format surface $surface.;
      title "Angle of repose vs mean small particle size by surface type";
run;

proc sgplot data=flow;
      scatter x=lg_mean y=repose / group=surface;
      format surface $surface.;
      title "Angle of repose vs mean large particle size by surface type";
run;

proc sgplot data=flow;
      scatter x=S_L y=repose / group=surface;
      format surface $surface.;
      title "Angle of repose vs small:large particle ratio by surface type";
run;

/*** Model selection and inference ***/

proc glmselect data=flow plots=all;
      class surface moist;
      model repose = moist surface D10 D10_1 D50 D502 D90 D902
```

```
            sm_mean lg_mean lg_mean2 S_L S_L2 / selection=lasso(choose=press
steps=17 lscoeffs)
            stats=(adjrsq aicc cp press sbc);
      title "Model selection for angle of repose";
run;

proc glm data=flow plots=all;
      class surface moist;
      model repose = moist surface D50 S_L D502 S_L2
                  surface*S_L surface*S_L2 / intercept solution;
      lsmeans surface moist / adjust=Tukey lines;
      output out=out_alpha r=r p=p;
      title "Selected model for angle of repose";
run;

/*** Visualization ***/

/* Boxplot by surface */
ods graphics off;
proc boxplot data=flow;
      plot Repose*Surface;
      format surface $surface.;
      title 'Boxplot of angle of repose by surface type';
run;

/* Boxplot by moisture */
proc sgplot data=flow;
      vbox Repose /category=moist;
      title 'Boxplot of angle of repose by moisture level';
run;

*HDPE*;
ods graphics on;
proc g3grid data=out_alpha(where=(surface="HDPE")) out=r_HDPE_g3;
      grid D50*S_L=repose / join noscale;
run;
proc g3grid data=out_alpha(where=(surface="HDPE")) out=p_HDPE_g3;
      grid D50*S_L=p / join noscale;
run;
proc sgrender data=r_HDPE_g3 template=ContourPlotParm;
      dynamic _TITLE="Observed angle of repose modelled by D50 and
small:large particle ratio for HDPE"
            _X="D50" _Y="S_L" _Z="repose"
            _XLAB="D50 (um)" _YLAB="Small:large particle size ratio"
_ZLAB="Observed angle of repose";
run;
proc sgrender data=p_HDPE_g3 template=ContourPlotParm;
      dynamic _TITLE="Predicted angle of repose modelled by D50 and
small:large particle ratio for HDPE"
            _X="D50" _Y="S_L" _Z="p"
            _XLAB="D50 (um)" _YLAB="Small:large particle size ratio"
_ZLAB="Predicted angle of repose";
run;

*PVDF*;
ods graphics on;
proc g3grid data=out_alpha(where=(surface="PVDF")) out=r_PVDF_g3;
```

```
      grid D50*S_L=repose / join noscale;
run;
proc g3grid data=out_alpha(where=(surface="PVDF")) out=p_PVDF_g3;
      grid D50*S_L=p / join noscale;
run;
proc sgrender data=r_PVDF_g3 template=ContourPlotParm;
      dynamic _TITLE="Observed angle of repose modelled by D50 and
small:large particle ratio for PVDF"
            _X="D50" _Y="S_L" _Z="repose"
            _XLAB="D50 (um)" _YLAB="Small:large particle size ratio"
_ZLAB="Observed angle of repose";
run;
proc sgrender data=p_PVDF_g3 template=ContourPlotParm;
      dynamic _TITLE="Predicted angle of repose modelled by D50 and
small:large particle ratio for PVDF"
            _X="D50" _Y="S_L" _Z="p"
            _XLAB="D50 (um)" _YLAB="Small:large particle size ratio"
_ZLAB="Predicted angle of repose";
run;

*PVC*;
ods graphics on;
proc g3grid data=out_alpha(where=(surface="PVC")) out=r_PVC_g3;
      grid D50*S_L=repose / join noscale;
run;
proc g3grid data=out_alpha(where=(surface="PVC")) out=p_PVC_g3;
      grid D50*S_L=p / join noscale;
run;
proc sgrender data=r_PVC_g3 template=ContourPlotParm;
      dynamic _TITLE="Observed angle of repose modelled by D50 and
small:large particle ratio for PVC"
            _X="D50" _Y="S_L" _Z="repose"
            _XLAB="D50 (um)" _YLAB="Small:large particle size ratio"
_ZLAB="Observed angle of repose";
run;
proc sgrender data=p_PVC_g3 template=ContourPlotParm;
      dynamic _TITLE="Predicted angle of repose modelled by D50 and
small:large particle ratio for PVC"
            _X="D50" _Y="S_L" _Z="p"
            _XLAB="D50 (um)" _YLAB="Small:large particle size ratio"
_ZLAB="Predicted angle of repose";
run;

*PP*;
ods graphics on;
proc g3grid data=out_alpha(where=(surface="PP")) out=r_PP_g3;
      grid D50*S_L=repose / join noscale;
run;
proc g3grid data=out_alpha(where=(surface="PP")) out=p_PP_g3;
      grid D50*S_L=p / join noscale;
run;
proc sgrender data=r_PP_g3 template=ContourPlotParm;
      dynamic _TITLE="Observed angle of repose modelled by D50 and
small:large particle ratio for PP"
            _X="D50" _Y="S_L" _Z="repose"
            _XLAB="D50 (um)" _YLAB="Small:large particle size ratio"
_ZLAB="Observed angle of repose";
```

```
run;
proc sgrender data=p_PP_g3 template=ContourPlotParm;
      dynamic _TITLE="Predicted angle of repose modelled by D50 and
small:large particle ratio for PP"
            _X="D50" _Y="S_L" _Z="p"
            _XLAB="D50 (um)" _YLAB="Small:large particle size ratio"
_ZLAB="Predicted angle of repose";
run;

*AL*;
ods graphics on;
proc g3grid data=out_alpha(where=(surface="AL")) out=r_AL_g3;
      grid D50*S_L=repose / join noscale;
run;
proc g3grid data=out_alpha(where=(surface="AL")) out=p_AL_g3;
      grid D50*S_L=p / join noscale;
run;
proc sgrender data=r_AL_g3 template=ContourPlotParm;
      dynamic _TITLE="Observed angle of repose modelled by D50 and
small:large particle ratio for AL"
            _X="D50" _Y="S_L" _Z="repose"
            _XLAB="D50 (um)" _YLAB="Small:large particle size ratio"
_ZLAB="Observed angle of repose";
run;
proc sgrender data=p_AL_g3 template=ContourPlotParm;
      dynamic _TITLE="Predicted angle of repose modelled by D50 and
small:large particle ratio for AL"
            _X="D50" _Y="S_L" _Z="p"
            _XLAB="D50 (um)" _YLAB="Small:large particle size ratio"
_ZLAB="Predicted angle of repose";
run;

*SS*;
ods graphics on;
proc g3grid data=out_alpha(where=(surface="SS")) out=r_SS_g3;
      grid D50*S_L=repose / join noscale;
run;
proc g3grid data=out_alpha(where=(surface="SS")) out=p_SS_g3;
      grid D50*S_L=p / join noscale;
run;
proc sgrender data=r_SS_g3 template=ContourPlotParm;
      dynamic _TITLE="Observed angle of repose modelled by D50 and
small:large particle ratio for SS"
            _X="D50" _Y="S_L" _Z="repose"
            _XLAB="D50 (um)" _YLAB="Small:large particle size ratio"
_ZLAB="Observed angle of repose";
run;
proc sgrender data=p_SS_g3 template=ContourPlotParm;
      dynamic _TITLE="Predicted angle of repose modelled by D50 and
small:large particle ratio for SS"
            _X="D50" _Y="S_L" _Z="p"
            _XLAB="D50 (um)" _YLAB="Small:large particle size ratio"
_ZLAB="Predicted angle of repose";
run;
```

```
**********************
*THETA (ANGLE OF SLIDE*
**********************;

/*** Scatter plots ***/

ods graphics on;
proc sgplot data=flow;
      scatter x=D10 y=slide / group=surface;
      format surface $surface.;
      title "Angle of slide vs D10 by surface type";
run;

proc sgplot data=flow;
      scatter x=D50 y=slide / group=surface;
      format surface $surface.;
      title "Angle of slide vs D50 by surface type";
run;

proc sgplot data=flow;
      scatter x=D90 y=slide / group=surface;
      format surface $surface.;
      title "Angle of slide vs D90 by surface type";
run;

proc sgplot data=flow;
      scatter x=sm_mean y=slide / group=surface;
      format surface $surface.;
      title "Angle of slide vs mean small particle size by surface type";
run;

proc sgplot data=flow;
      scatter x=lg_mean y=slide / group=surface;
      format surface $surface.;
      title "Angle of slide vs mean large particle size by surface type";
run;

proc sgplot data=flow;
      scatter x=S_L y=slide / group=surface;
      format surface $surface.;
      title "Angle of slide vs small:large particle ratio by surface type";
run;

/*** Model selection and inference ***/

proc glmselect data=flow plots=all;
      class surface moist;
      model slide = moist surface D10 D10_1 D50 D90   sm_mean lg_mean S_L /
            selection=lasso(choose=press steps=13 lscoeffs)
            stats=(adjrsq aicc cp press sbc);
      title "Model selection for angle of slide";
run;

proc glm data=flow plots=all;
      class surface moist;
      model slide = moist surface moist*surface D10_1 D90 D10_1*surface
            / intercept solution;
```

```
      lsmeans surface*moist / adjust=Tukey lines;
      output out=out_theta r=r p=p;
      title "Selected model for angle of slide";
run;

/*** Visualization ***/

/* Boxplot by surface and moisture*/
ods graphics off;
proc sgpanel data=flow;
      panelby surface;
      vbox slide / group=moist;
      title "Angle of slide by moisture and by surface";
run;

*HDPE*;
ods graphics on;
proc g3grid data=out_theta(where=(surface="HDPE")) out=r_HDPE_g3;
      grid D90*D10=slide / join noscale;
run;
proc g3grid data=out_theta(where=(surface="HDPE")) out=p_HDPE_g3;
      grid D90*D10=p / join noscale;
run;
proc sgrender data=r_HDPE_g3 template=ContourPlotParm;
      dynamic _TITLE="Observed angle of slide modelled by D90 and D10 for
HDPE"
            _X="D90" _Y="D10" _Z="slide"
            _XLAB="D90 (um)" _YLAB="D10 (um)" _ZLAB="Observed angle of
slide";
run;
proc sgrender data=p_HDPE_g3 template=ContourPlotParm;
      dynamic _TITLE="Predicted angle of slide modelled by D90 and D10 for
HDPE"
            _X="D90" _Y="D10" _Z="p"
            _XLAB="D90 (um)" _YLAB="D10 (um)" _ZLAB="Predicted angle of
slide";
run;

*PVDF*;
ods graphics on;
proc g3grid data=out_theta(where=(surface="PVDF")) out=r_PVDF_g3;
      grid D90*D10=slide / join noscale;
run;
proc g3grid data=out_theta(where=(surface="PVDF")) out=p_PVDF_g3;
      grid D90*D10=p / join noscale;
run;
proc sgrender data=r_PVDF_g3 template=ContourPlotParm;
      dynamic _TITLE="Observed angle of slide modelled by D90 and D10 for
PVDF"
            _X="D90" _Y="D10" _Z="slide"
            _XLAB="D90 (um)" _YLAB="D10 (um)" _ZLAB="Observed angle of
slide";
run;
proc sgrender data=p_PVDF_g3 template=ContourPlotParm;
      dynamic _TITLE="Predicted angle of slide modelled by D90 and D10 for
PVDF"
            _X="D90" _Y="D10" _Z="p"
```

```
            _XLAB="D90 (um)" _YLAB="D10 (um)" _ZLAB="Predicted angle of
slide";
run;

*PVC*;
ods graphics on;
proc g3grid data=out_theta(where=(surface="PVC")) out=r_PVC_g3;
      grid D90*D10=slide / join noscale;
run;
proc g3grid data=out_theta(where=(surface="PVC")) out=p_PVC_g3;
      grid D90*D10=p / join noscale;
run;
proc sgrender data=r_PVC_g3 template=ContourPlotParm;
      dynamic _TITLE="Observed angle of slide modelled by D90 and D10 for
PVC"
            _X="D90" _Y="D10" _Z="slide"
            _XLAB="D90 (um)" _YLAB="D10 (um)" _ZLAB="Observed angle of
slide";
run;
proc sgrender data=p_PVC_g3 template=ContourPlotParm;
      dynamic _TITLE="Predicted angle of slide modelled by D90 and D10 for
PVC"
            _X="D90" _Y="D10" _Z="p"
            _XLAB="D90 (um)" _YLAB="D10 (um)" _ZLAB="Predicted angle of
slide";
run;

*PP*;
ods graphics on;
proc g3grid data=out_theta(where=(surface="PP")) out=r_PP_g3;
      grid D90*D10=slide / join noscale;
run;
proc g3grid data=out_theta(where=(surface="PP")) out=p_PP_g3;
      grid D90*D10=p / join noscale;
run;
proc sgrender data=r_PP_g3 template=ContourPlotParm;
      dynamic _TITLE="Observed angle of slide modelled by D90 and D10 for PP"
            _X="D90" _Y="D10" _Z="slide"
            _XLAB="D90 (um)" _YLAB="D10 (um)" _ZLAB="Observed angle of
slide";
run;
proc sgrender data=p_PP_g3 template=ContourPlotParm;
      dynamic _TITLE="Predicted angle of slide modelled by D90 and D10 for
PP"
            _X="D90" _Y="D10" _Z="p"
            _XLAB="D90 (um)" _YLAB="D10 (um)" _ZLAB="Predicted angle of
slide";
run;

*AL*;
ods graphics on;
proc g3grid data=out_theta(where=(surface="AL")) out=r_AL_g3;
      grid D90*D10=slide / join noscale;
run;
proc g3grid data=out_theta(where=(surface="AL")) out=p_AL_g3;
      grid D90*D10=p / join noscale;
run;
```

```
proc sgrender data=r_AL_g3 template=ContourPlotParm;
      dynamic _TITLE="Observed angle of slide modelled by D90 and D10 for AL"
            _X="D90" _Y="D10" _Z="slide"
            _XLAB="D90 (um)" _YLAB="D10 (um)" _ZLAB="Observed angle of
slide";
run;
proc sgrender data=p_AL_g3 template=ContourPlotParm;
      dynamic _TITLE="Predicted angle of slide modelled by D90 and D10 for
AL"
            _X="D90" _Y="D10" _Z="p"
            _XLAB="D90 (um)" _YLAB="D10 (um)" _ZLAB="Predicted angle of
slide";
run;

*SS*;
ods graphics on;
proc g3grid data=out_theta(where=(surface="SS")) out=r_SS_g3;
      grid D90*D10=slide / join noscale;
run;
proc g3grid data=out_theta(where=(surface="SS")) out=p_SS_g3;
      grid D90*D10=p / join noscale;
run;
proc sgrender data=r_SS_g3 template=ContourPlotParm;
      dynamic _TITLE="Observed angle of slide modelled by D90 and D10 for SS"
            _X="D90" _Y="D10" _Z="slide"
            _XLAB="D90 (um)" _YLAB="D10 (um)" _ZLAB="Observed angle of
slide";
run;
proc sgrender data=p_SS_g3 template=ContourPlotParm;
      dynamic _TITLE="Predicted angle of slide modelled by D90 and D10 for
SS"
            _X="D90" _Y="D10" _Z="p"
            _XLAB="D90 (um)" _YLAB="D10 (um)" _ZLAB="Predicted angle of
slide";
run;

ods rtf close;
```

Paper 3

```
/*******************************************************
*** Pea Milling Chapter 3 - Roller vs Hammer Milling ***
*******************************************************
Variables
      Rep         - Number of treatment replicate
      Trt         - Treatment (roller vs hammer milling)
      Moist       - Moisture content (%)
      L           - Lightness value (Hunter LAB)
      A           - Redness value (Hunter LAB)
      B           - Yellowness value (Hunter LAB)
      Bdens       - Bulk density (g/ml)
      Peakv       - RVA Peak viscosity (cP)
      Bkdwn       - RVA breakdown viscosity (cP)
      Finalv      - RVA final viscosity (cP)
      Ptime       - RVA peak time (min)
      pasteT      - RVA pasting temperature (degrees C)
      ash         - Percent ash (dry basis)
      prot        - Percent protein (dry basis)
      starch      - Percent total starch (dry basis)
      IDF         - Insoluble dietary fiber content (dry basis)
      SDF         - Soluble dietary fiber content (dry basis)
      TDF         - Total dietary fiber content (dry basis)
      d10         - 10th percentile particle size (um)
      d50         - Median particle size (um)
      d90         - 90th percentile particle size (um)
      sdam        - Percent damaged starch
      carotene    - Carotenoid content (ug/g)
      SFT0        - Syneresis at time 0 (% water loss)
      S1          - Syneresis after 24 h (% water loss)
      S2          - Syneresis after 48 h (% water loss)
      S3          - Syneresis after 72 h (% water loss)
      S4          - Syneresis after 96 h (% water loss)
      F2          - Syneresis after 48 h of freezing (% water loss)
      F4          - Syneresis after 96 h of freezing (% water loss)
      FC          - Foaming capacity (%)
      FS10        - Foaming stability after 10 min (%)
      FS30        - Foaming stability after 30 min (%)
      FS60        - Foaming stability after 60 min (%)
      EC          - Emulsion capacity (%)
      ES          - Emulsion stability (%)
      WAC         - Water absorption capacity (g/g)
      OAC         - Oil absorption capacity (g/g)
      RAL-RSS     - Angle of repose on AL, HDPE, PP, PVC, PVDF, and SS
                  (degrees)
      SAL-SSS     - Angle of slide on AL, HDPE, PP, PVC, PVDF, and SS
                  (degrees)

*******************************************************/

proc template;
      define style styles.pea;
      parent=styles.harvest;
      class GraphColors /
            'gcdata6' = biyg 'gcdata5' = lio
```

```
            'gcdata4' = brbl 'gcdata3' = deyg
            'gcdata2' = gold 'gcdata1' = viro
            'gdata6' = biyg 'gdata5' = lio
            'gdata4' = brbl 'gdata3' = deyg
            'gdata2' = gold 'gdata1' = viro;
      style colors /
            'headerfgemph' = cx000000 'headerbgemph' = cxFDCD6F
            'headerfgstrong' = cx000000 'headerbgstrong' = cxFDCD6F
            'headerfg' = cx000000 'headerbg' = cxFDCD6F
            'datafgemph' = cx000000 'databgemph' = cxFFFFFF
            'datafgstrong' = cx000000 'databgstrong' = cxFFFFFF
            'databorder' = cx89562D 'datafg' = cx000000
            'databg' = cxFFFFFF 'batchfg' = cx000000
            'batchbg' = cxFFFFFF 'tableborder' = cx000000
            'tablebg' = cxFFFFFF 'notefg' = cx000000
            'notebg' = cxFFFFFF 'bylinefg' = cx000000
            'bylinebg' = cxFFFFFF 'captionfg' = cx000000
            'captionbg' = cxFFFFFF 'proctitlefg' = cx000000
            'proctitlebg' = cxFFFFFF 'titlefg' = cx000000
            'titlebg' = cxFFFFFF 'systitlefg' = cx000000
            'systitlebg' = cxFFFFFF 'Conentryfg' = cx000000
            'Confolderfg' = cx000000 'Contitlefg' = cx000000
            'link2' = cx800080 'link1' = cx0000FF
            'contentfg' = cx000000 'contentbg' = cxFFFFFF
            'docfg' = cx000000 'docbg' = cxFFFFFF;
      class GraphFonts /
            'GraphDataFont' = ("<sans-serif>, <MTsans-serif>",10pt)
            'GraphUnicodeFont' = ("<MTsans-serif-unicode>",10pt)
            'GraphFootnoteFont' = ("<sans-serif>, <MTsans-serif>",12pt,bold)
            'GraphTitleFont' = ("<sans-serif>, <MTsans-serif>",12pt,bold)
            'GraphTitle1Font' = ("<sans-serif>, <MTsans-serif>",14pt,bold)
            'GraphValueFont' = ("<sans-serif>, <MTsans-serif>",10pt)
            'GraphLabel2Font' = ("<sans-serif>, <MTsans-serif>",12pt)
            'GraphLabelFont' = ("<sans-serif>, <MTsans-serif>",12pt,bold)
            'GraphAnnoFont' = ("<sans-serif>, <MTsans-serif>",12pt);
      end;
run;

data Pea_CH3;
      infile 'Directory\filename.csv' firstobs=2 dsd;
      input rep trt $ moist L a b bdens peakv bkdwn finalv ptime pasteT ash
            prot starch IDF SDF TDF d10 d50 d90 sdam caroten SFT0 S1 S2 S3 S4
            F2 F4 FC FS10 FS30 FS60 EC ES WAC OAC RAL RHDPE RPP RPVC RPVDF
            RSS SAL SHDPE SPP SPVC SPVDF SSS;
run;

proc format;
      value $Trt  "Hammer"="Hammer-milled"
                  "Roller"="Roller-milled";
run;

ods rtf file='Directory\filename.rtf' bodytitle style=styles.pea;

/* Graphics */

ods graphics on;
proc boxplot data=Pea_CH3;
```

```
      plot (moist)*trt;
      plot (Ash)*trt;
      plot (sdam)*trt;
      label moist="Water content (%)" trt="Milling treatment" Ash="Ash (%
      db)" sdam="Starch damage (%)";
      format trt $Trt.;
      title 'Boxplot of chemical parameters';
run;

proc boxplot data=Pea_CH3;
      plot (d10)*trt;
      plot (d50)*trt;
      label trt="Milling treatment" d10="um" d50="um";
      format trt $Trt.;
      title 'Boxplot of physical parameters';
run;

proc boxplot data=Pea_CH3;
      plot (OAC)*trt;
      plot (peakv)*trt;
      plot (finalv)*trt;
      plot (bkdwn)*trt;
      plot (RHDPE)*trt;
      plot (RPP)*trt;
      plot (SPVC)*trt;
      plot (SFT0)*trt;
      plot (F4)*trt;
      plot (FC)*trt;
      label trt="Milling treatment" OAC="g oil/g sample" peakv="Peak
      viscosity (cP)" finalv="Final viscosity (cP)" bkdwn="Breakdown
      viscosity (cP)" RHDPE="Degrees" RPP="Degrees" SPVC="Degrees" SFT0="g
      water loss/ g starch gel" F4="g water loss/ g starch gel" FC="% volume
      increase";
      format trt $Trt.;
      title 'Boxplot of functional parameters';
run;

/* Descriptive */

ods graphics on;
proc means data=Pea_CH3 mean std;
      class trt;
      var moist L a b bdens peakv bkdwn finalv ptime pasteT ash prot starch
            IDF SDF TDF d10 d50 d90 sdam caroten SFT0 S1 S2 S3 S4 F2 F4 FC
            FS10 FS30 FS60 EC ES WAC OAC RAL RHDPE RPP RPVC RPVDF RSS SAL
            SHDPE SPP SPVC SPVDF SSS;
      title 'Mean and standard deviation for all variables by mill type';
run;

/* ANOVA and correlation*/

ods graphics on;
proc multtest data=Pea_CH3 pfdr plots=all;
      class trt;
      test mean(moist L a b bdens peakv bkdwn finalv ptime pasteT ash prot
            starch IDF SDF TDF d10 d50 d90 sdam caroten SFT0 S1 S2 S3 S4 F2
            F4 FC FS10 FS30 FS60 EC ES WAC OAC RAL RHDPE RPP RPVC RPVDF RSS
```

```
            SAL SHDPE SPP SPVC SPVDF SSS);
      title 't-tests for differences between mean responses';
run;

proc corr data=Pea_Ch3;
      var moist peakv finalv d10 d50 d90 OAC sdam;
      title 'Correlation among significantly different parameters';
run;

ods rtf close;
```